CATALYTIC DEOXYGENATION OF PALMITIC ACID OVER CESIUM FAUJASITE ZEOLITE FOR THE PRODUCTION OF LONG CHAIN HYDROCARBONS

THANASAK SOLOS

A THESIS SUBMITTED IN PARTIAL FULFILLMENT

OF THE REQUIREMENT FOR THE DEGREE OF

MASTER OF SCIENCE IN PETROCHEMICALS AND HYDROCARBON CHEMISTRY

FACULTY OF SCIENCE

KING MONGKUT'S INSTITUTE OF TECHNOLOGY LADKRABANG

2011

KMITL - 2011 - SC - M - 015 - 006

หัวข้อวิทยานิพนธ์	การเร่งปฏิกิริยาการขจัดออกซิเจนของกรดปาล์มิติก บนตัวเร่งปฏิกิริยาซีโอไลต์ซีเซียมฟูจาไซต์ เพื่อผลิตไฮโดรคาร์บอนสายยาว
นักศึกษา	นายธนศักดิ์ โสพส
รหัสประจำตัว	49068001
ปริญญา	วิทยาศาสตรมหาบัณฑิต
สาขาวิชา	ปิโตรเคมีและเคมีของไฮโดรคาร์บอน
พ.ศ.	2554
อาจารย์ที่ปรึกษาวิทยานิพนธ์	รศ.ดร.ตะวัน สุขน้อย

บทคัดย่อ

งานวิจัยนี้ได้ทำการศึกษาปฏิกิริยาการขจัดออกซิเจนของกรดปาล์มิติกเพื่อผลิตเป็นไฮโดรคาร์บอนสายยาว ด้วยตัวเร่งปฏิกิริยาซีโอไลต์ฟูจาไซต์ที่ผ่านการแลกเปลี่ยนไอออนด้วยสารละลายซีเซียมอะซีเตต โดยอาศัยการเกิดปฏิกิริยาเอสเทอริฟิเคชั่นและปฏิกิริยาการกำจัดหมู่คาร์บอกซิลออกในรูปแก๊สคาร์บอนมอนอกไซด์ เมื่อทำการศึกษาในเครื่องปฏิกรณ์แบบเบดนิ่งที่อุณหภูมิ 400-450 องศาเซลเซียส ภายใต้ความดันบรรยากาศ เป็นเวลา 6 ชั่วโมงต่อเนื่องกัน โดยใช้เมทานอลเป็นสารตั้งต้นร่วมกับกรดปาล์มิติกที่อัตราส่วน 2.0-4.5 ต่อ 1.0 โดยน้ำหนัก และทำการเก็บผลิตภัณฑ์ที่เกิดขึ้นเป็นช่วง โดยการควบแน่นให้เป็นของเหลว แล้วนำไปวิเคราะห์ด้วยเทคนิคก๊าซโครมาโตรกราฟี พบว่าผลิตภัณฑ์หลักที่ได้ เป็นแอลฟาโอเลฟินสายยาว และได้ไฮโดรคาร์บอนสายยาวอื่นๆอีกเล็กน้อยเป็นผลิตภัณฑ์ร่วมด้วย ซึ่งปริมาณการเกิดเป็นผลิตภัณฑ์จะเพิ่มขึ้นเมื่อทำการเพิ่มระยะเวลาสัมผัส (space time) อัตราส่วนของเมทานอลในสารตั้งต้นและอุณหภูมิของเครื่องปฏิกรณ์ แต่การเพิ่มระยะเวลาสัมผัสมากจนเกินไป (700 กรัมชั่วโมงต่อโมล) กลับทำให้เกิดการแยกสลาย (cracking) ของกลุ่มไฮโดรคาร์บอนสายยาวไปเป็นไฮโดรคาร์บอนขนาดเล็ก ส่งผลให้ได้ผลิตภัณฑ์ในรูปของเหลวลดลง จากการศึกษาปฏิกิริยาภายใต้บรรยากาศของไฮโดรเจนพบว่า ไม่ส่งผลต่อความสามารถในการเร่งปฏิกิริยาของตัวเร่งปฏิกิริยา แต่จะช่วยป้องกันการเสื่อมสภาพของตัวเร่งปฏิกิริยาได้ เมื่อใช้ตัวเร่งปฏิกิริยาที่มีอัตราส่วนซิลิกอนต่ออะลูมิเนียมต่างกัน พบว่าตัวเร่งปฏิกิริยาทั้งซีโอไลต์ซีเซียมโซเดียมเอกซ์และซีเซียมโซเดียมวาย ต่างมีความสามารถในการเร่งปฏิกิริยาสูง ในกรณีของตัวเร่งปฏิกิริยาซีโอไลต์โซเดียมเอกซ์ให้ผลิตภัณฑ์ที่มีไฮโดรคาร์บอนขนาดเล็กเป็นหลัก เนื่องจากตัวมันมีความเป็นกรด ขณะที่ซีโอไลต์โซเดียมวายกลับให้ความจำเพาะเจาะจงสูงในการเกิดเป็นผลิตภัณฑ์ชนิดแอลฟาโอเลฟินสายยาว ขนาด 15 อะตอม

Thesis Title	Catalytic deoxygenation of palmitic acid over cesium faujasite zeolite for the production of long chain hydrocarbons
Student	Thanasak Solos
Student ID	49068001
Degree	Master of Science
Program	Petrochemicals and Hydrocarbon Chemistry
Year	2011
Thesis Advisor	Assoc.Prof.Dr.Tawan Sooknoi

ABSTRACT

In this thesis, the deoxygenation of palmitic acid to produce the long chain hydrocarbons is studied over a faujasite zeolite catalyst this is modified by ion exchange with cesium acetate aqueous solution. The long chain hydrocarbons can be obtained by selective deoxygenation that involves *in-situ* esterification and subsequent removal of the carboxyl group via carbon monoxide evolution. The catalytic reactions are carried out in a fixed bed flow reactor at 400-450 °C under atmospheric pressure and tested for 6 hours on stream. Methanol is used as a co-reactant with palmitic acid at 2.0-4.5/1.0 weight ratios. The product effluents are condensed, periodically collected and then analyzed by gas chromatography technique. The results showed that linear long chain α-olefins (C_{14} and C_{15}) were major products (13.5 and 24.7% yield) and small amount of linear hydrocarbons (C_9-C_{15}) were also obtained. The increase in yield of products were observed when increase in space time (*W/F* 140-600 g·h/mol), methanol concentration (20-45 %wt.) and reaction temperature (400-450 °C). However, at higher space time (700 g·h/mol), the yield of liquid product was decreased. It is because the pool of hydrocarbon products can consecutively crack to lighter hydrocarbons. The similar activity and product selectivity were observed when using hydrogen and helium as carrier gas. Interestingly, the presence of hydrogen can prevent catalyst deactivation. Both CsNaX and CsNaY catalysts which have different Si/Al ratio, provide the high yield of long chain hydrocarbons. In the case of NaX, the catalyst provides lighter hydrocarbon products due to its acidity, while NaY catalyst offers high selectivity to C_{15} linear long chain α-olefin.

ACKNOWLEDGEMENT

The author wishes to gratefully thank to my advisors, Assoc.Prof.Dr.Tawan Sooknoi for his supports, supervisions, inspiration, suggestions and encouragements throughout this thesis.

I wish also thanks to Asst.Prof.Dr.Vanchat Chuenchom, Dr.Amnat Permsubscul and Asst.Prof.Dr.Siriporn Jongpatiwut for serving as the chairperson and the committee, and valuable comments.

I would like to acknowledge the financial support from PTT public company limited. I also appreciate the supports from the Department of Chemistry, Faculty of Science, King Mongkut's Institute of Technology Ladkrabang for the equipments, chemicals and facilities.

I would like to extend my sincere appreciation to all of my teachers, my friend and my research group for their constant guidance advice, support and encouragement.

Sincere thanks to Dr.Artit Ausavasukhi and Mr.Nipat peamaroon for their advice, suggestion and kindness.

Finally, I deeply appreciate and thank my parents and my family for their constant supports and encouragements.

Thanasak Solos

TABLE OF CONTENTS

TABLE OF CONTENTS (Continued)

TABLE OF CONTENTS (Continued)

TABLE OF CONTENTS (Continued)

LIST OF TABLES

LIST OF FIGURES

Figure Page

LIST OF FIGURES (Continued)

Figure Page

CHAPTER 1

INTRODUCTION

1.1 Motivation

The discovery of crude oil, in the 19th century, created a liquid fuel source that helped industrialize the world and improved standards of living [1]. The demand for fuel and its resources are increasing continuously due to the rapid outgrowth of population and urbanization. However, it is estimated that the fossil sources might be depleted till 2050. In addition, the process of obtaining energy from this source causes atmospheric pollution, resulting in problems as global warming, acid rain, etc. [2]. Hence, research on renewable source that can be used as raw materials for petrochemicals, particularly the long chain olefins, is increasingly important.

In line with this view, animal fats and vegetable oils can be alternative source for the production of long chain hydrocarbons. They have lower limit of availability and give suitable product properties such as negligible sulphur, nitrogen, and metal content [3]. High carbon numbers of the fatty acid (C_{16}-C_{18}) in the palm oils makes them a promising choice for the production of long chain hydrocarbons. This can be achieved by selective deoxygenation that involves *in-situ* esterification and subsequent removal of the carboxyl group via carbon monoxide evolution. For example, Pd/C has been found to be an effective catalyst for decarbonylation of fatty acids [4]. However, carbon monoxide produced from the reaction may competitively adsorb on the metal surface, leading to a reduction or even loss in the catalytic activity as the conversion increases. Hence, hydrogen partial pressure is generally high, in order to keep the surface clean and facilitate the oxygenate–metal surface interaction [5].

An alternative family of catalysts that may overcome some of these limitations is that of solid bases. This is because the fatty acid methyl-ester (FAME) is fairly electrophilic while the decarbonylated by-product, carbon monoxide, is nucleophilic. Thus, while the adsorption of FAME over basic catalyst may be strong and the reaction can be readily promoted at atmospheric pressure, the by-product carbon monoxide should promptly leave the basic surface. In fact, some zeolites have also basic properties. NaX zeolites that have been modified through conventional ion exchange with alkali metal cation, such as cesium (CsNaX), indeed exhibit basic properties useful for catalysis. These catalysts have shown high activity towards reactions involving

deoxygenates, as well as decarbonylation of benzaldehyde and methyl octanoate in inert atmosphere [6, 7].

Accordingly, in this thesis, deoxygenation of the fatty acid to produce the long chain hydrocarbons will be investigated over alkali metal-exchanged faujasite zeolite catalysts. The alkali metal cation is focused on cesium, which is expected to produce the strongest basicity. Palmitic acid will be used as models compound, since it is the major component found in triglyceride from palm oil. Methanol will be used as a co-reactant for *in-situ* esterification. The deoxygenation under atmospheric pressure is the highlight of this work.

1.2 Objectives

1.2.1 To obtain a mixture of long chain hydrocarbons from deoxygenation of palmitic acid.

1.2.2 To understand the role of catalyst in deoxygenation activity and selectivity.

1.2.3 To understand effect of space time, reaction temperature, methanol concentration, exchangeable cations and hydrogen as carrier gas.

1.3 Scope of the study

The scopes of the study on deoxygenation of palmitic acid in a fixed bed flow reactor over faujasite zeolite catalysts are as follow:

1.3.1 Catalyst preparation by ion exchange of NaX and NaY with cesium acetate aqueous solution.

1.3.2 Characterization of NaX, NaY, CsNaX and CsNaY zeolites by X-ray diffractometry (XRD), X-ray fluorescence spectrometry (XRF) and gas adsorption analyzer (Autosorb-1).

1.3.3 Study on effect of space time (*W/F*) from 300-700 $g.h.mol^{-1}$.

1.3.4 Study on effect of temperature ranging from 400 to 450 °C.

1.3.5 Study on effect of methanol concentration in the range of 20 to 45 wt.%.

1.3.6 Study on effect of ion exchanged NaX and NaY zeolites with and without cesium cations.

1.3.7 Study on effect of hydrogen as carrier gas.

1.3.8 Analysis and quantification of products from the reactions by gas chromatography.

1.4 Expected results

It is expected that a new technology for production of long chain hydrocarbons from palmitic acid under atmospheric pressure will be obtained.

CHAPTER 2

THEORY AND LITERATURE REVIEWS

2.1 Fatty acids

Fatty acids or derivatives of fatty acids are used in a wide variety of applications. The demand for fatty acids has been growing by about 4% per year over the past 10 years and has reached about 3,000,000 metric tons per year. Fatty acids are typically present in the raw materials used for the production of biodiesel. The natural fatty acids are obtained from the hydrolysis of hard animal fats (tallow), coconut, palm kernel and soybean oils and from the fractional distillation of crude tall oil (a byproduct of Kraft pulping of pine wood). These acids are almost entirely straight chain, even-numbered mono carboxylic acids containing from 4 to 22 carbons. Most new plants have been built in Southeast Asia which is the major source for coconut, palm and palm kernel oils. The market is dominated by two producers, the Uniquema group and the Henkel group representing about 50% world market share. Other fatty acids are derived from petroleum [8].

Table 2.1 Common saturated fatty acids [9].

Number of Carbon Atoms	Formula	Common Name	Source
4	$CH_3(CH_2)_2COOH$	Butyric acid	Butter
6	$CH_3(CH_2)_4COOH$	Caproic acid	Butter
8	$CH_3(CH_2)_6COOH$	Caprylic acid	Coconut oil
10	$CH_3(CH_2)_8COOH$	Capric acid	Coconut oil
12	$CH_3(CH_2)_{10}COOH$	Lauric acid	Palm kernel oil
14	$CH_3(CH_2)_{12}COOH$	Myristic acid	Oil of nutmeg
16	$CH_3(CH_2)_{14}COOH$	Palmitic acid	Palm oil
18	$CH_3(CH_2)_{16}COOH$	Stearic acid	Beef tallow
22	$CH_3(CH_2)_{20}COOH$	Beheric acid	Sesame oil

Table 2.2 Common unsaturated fatty acids [9].

Number of Carbon Atoms	Formula	Common Name	Source
16	$CH_3(CH_2)_5CH=CH(CH_2)_7COOH$	Palmitoleic acid	Whale oil
18	$CH_3(CH_2)_7CH=CH(CH_2)_7COOH$	Oleic acid	Olive oil
18	$CH_3(CH_2)_4CH=CHCH_2(CH_2)_7COOH$	Linoleic acid	Soybean oil
18	$CH_3CH_2(CH=CHCH_2)_3(CH_2)_6COOH$	Linolenic acid	Fish oils
20	$CH_3(CH_2)_4(CH=CHCH_2)_4(CH_2)_2COOH$	Arachidonic	acid Liver

About 100,000 metric tons of the natural fatty acids are consumed in the preparation of various fatty acid esters. The simple esters with lower chain alcohols (methyl-, ethyl-, n-propyl-, isopropyl- and butyl esters) are used as emollients in cosmetics and other personal care products and as lubricants. Esters of fatty acids with more complex alcohols, such as sorbitol, ethylene glycol, diethylene glycol and polyethylene glycol are consumed in foods, personal care, paper, water treatment, metal working fluids, rolling oils and synthetic lubricants [8].

2.1.1 Palmitic acid

Palmitic acid, $CH_3(CH_2)_{14}COOH$ or hexadecanoic acid in IUPAC nomenclature, is one of the most common saturated fatty acids found in animals and plants [10]. As its name indicates, it is a major component of the oil from palm trees (palm oil and palm kernel oil). Palmitic acid was discovered by Edmond Frémy in 1840, in saponified palm oil [11]. Butter, cheese, milk and meat also contain this fatty acid [10].

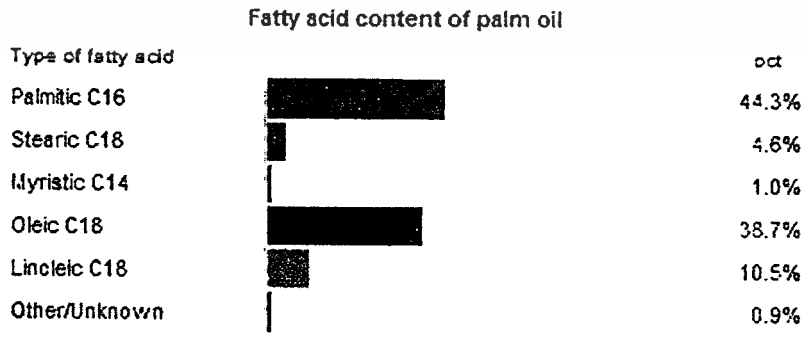

Figure 2.1 The approximate concentration of fatty acids (FAs) in palm oil [12].

2.1.2 Fatty acid reactions

2.1.2.1 Esterification

Esterification is the general name for a chemical reaction in which two reactants (typically an alcohol and an acid) form an ester as the reaction product. The most common esterification processes involve nucleophilic acyl substitution where the carbonyl compound is used as an electrophile and is attacked by a nucleophilic alcohol. However, other processes are possible; esterification by alkylation reverses the roles of "classic" carbonyl chemistry: a carboxylate anion is used as a nucleophile that displaces a halide ion in an SN2 reaction.

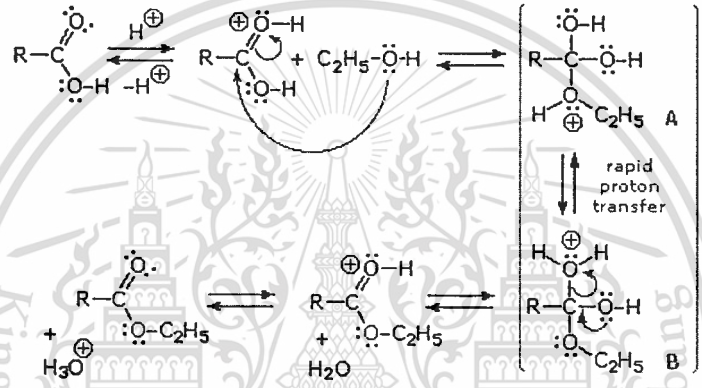

Figure 2.2 Acid-catalyzed esterification of fatty acids.

Currently, there is a great interest in the esterification reaction because of its application to several branches of industry [13]. Organic esters are frequently used in the production of plastic derivatives, in the solvent industry, perfumery, agro-chemistry and other branches of fine chemistry [14]. One of the main products obtained by esterification of long chain fatty acids is biodiesel, whose use has several environmental benefits [15]. Esterifies free fatty acid to alkyl esters in the presence of an acidic catalyst is a route to improving the use of high free fatty acid oils on biodiesel production. Esterification is normally carried out in the homogeneous phase in the presence of acid catalysts such as sulfuric and p-toluene sulfonic acids. This pretreatment step has been successfully demonstrated using sulfuric acid [16]. Unfortunately, use of the homogeneous sulfuric acid catalyst adds neutralization and separation steps as well as the esterification reaction to the process [17]. The use of heterogeneous catalysts in the reaction can be an alternative to reduce cost of biodiesel production.

2.1.2.2 Deoxygenation

Deoxygenation is a chemical reaction involving the removal of molecular oxygen (O_2) from a reaction mixture or the removal of oxygen atoms from a molecule. It is a novel method for production of diesel-like fuel from renewable resources, like vegetable oils and animal fats. This method is being investigated in several laboratories. It has recently been demonstrated that renewable feeds over heterogeneous catalysts in liquid-phase tend to decarboxylate. The production of a deoxygenated fuel involves removal of the carboxyl group in the fatty acid structure via carbon dioxide and/or carbon monoxide release, thus producing a linear hydrocarbon originating from the fatty acid alkyl group [18].

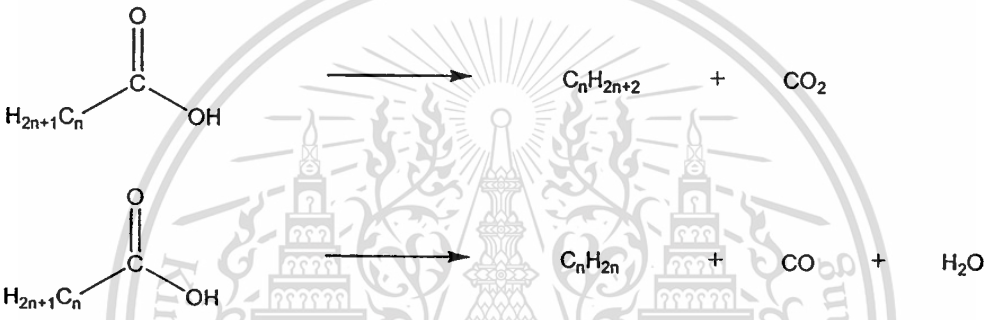

2.2 Zeolites

Zeolites are crystalline aluminosilicate minerals. They have three-dimensional structures arise from a framework of $(SiO_4)^{4-}$ and $(AlO_4)^{5-}$ coordination polyhedral (Figure 2.3) linked by all their corners. The frameworks are generally very open and contain channels and cavities in which are located cations and water molecules (Figure2.4). The cations often have a high degree of mobility giving rise to facile ion exchange and the water molecules are readily lost and regained; this accounts for the well-known desiccant properties of zeolites [19].

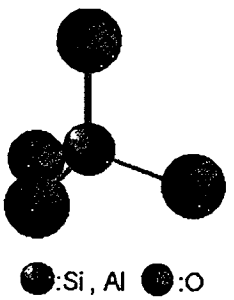

Figure 2.3 Representations of $(SiO_4)^{4-}$ or $(AlO_4)^{5-}$ tetrahedral.

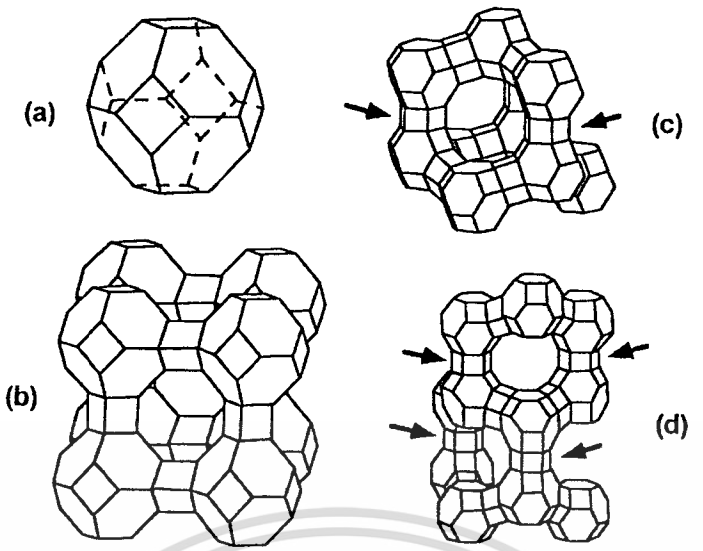

Figure 2.4 The framework structure of faujasite. Each line represents an oxygen atom and each junction represents a silicon or aluminium (Water molecules fill the space in the cages and cations float in the cages in this aqueous environment).

Many of the natural zeolites can be produced synthetically and several crystalline aluminosilicates with framework structures with no known natural counterpart have been made in the laboratory. The best known example of a synthetic zeolite is zeolite A, which can be related structurally to naturally occurring zeolites. It, like other synthetic zeolites, exhibits the definitive zeolitic properties of ion exchange and reversible water loss.

Another characteristic zeolite property arises from their molecular framework structures in that the combining of tetrahedral creating their porous structure happen to create regular arrays of apertures. These apertures are of such a size as to be able to selectively take up some molecules into their porous structure, whilst rejecting others on the basis of their larger effective molecular dimensions. This is the property of 'molecular sieving', which is largely unique to zeolites and responsible for their first commercial success.

2.2.1 The structure of zeolites

As stated earlier all zeolites have framework (three-dimensional) structures constructed by joining together $(SiO_4)^{4-}$ and $(AlO_4)^{5-}$ coordinated polyhedral. By definition these tetrahedral are assembled together such that the oxygen of each tetrahedral corner is shared with that in an identical tetrahedral (Si or Al), as shown in Figure 2.5. This corner (or vertex) sharing creates

infinite lattices comprised of identical building blocks (unit cells) in a manner common to all crystalline materials.

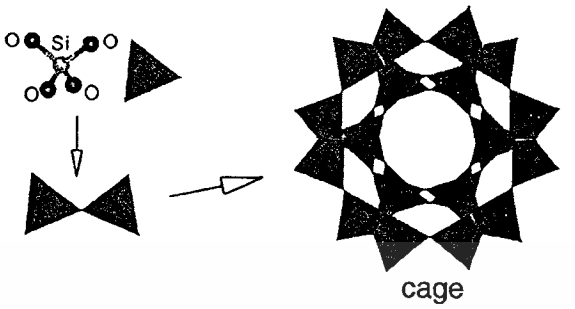

Figure 2.5 Tetrahedral linked together to create a three-dimensional structure.

These recurring units are called 'secondary building units' (sbus) and the simplest, classification described all known zeolite frameworks as arrangements linking eight sbus shown in Figure 2.6. These denote only the aluminosilicate skeleton (i.e. the Si, Al and O positions in space relative to each other) and exclude consideration of the cation and water moieties sited within the cavities and channels of the framework. The cation and water sites are complex and only fully defined in certain zeolites as will become apparent later.

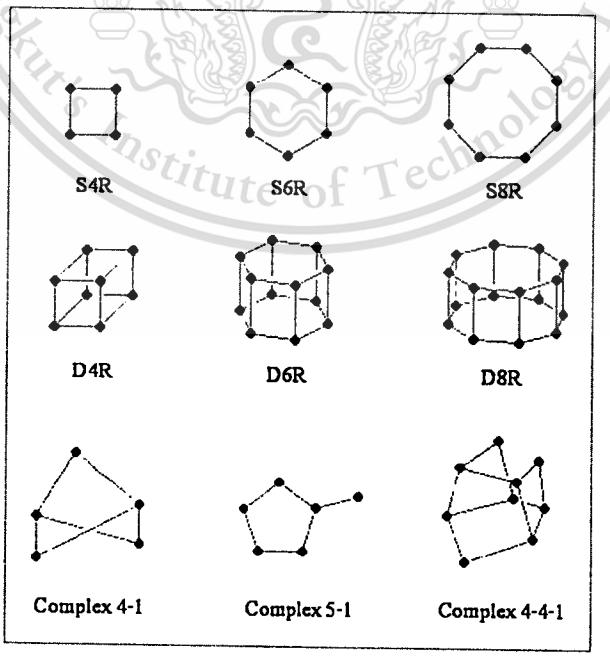

Figure 2.6 Secondary building units (SBUs) in zeolite [20].

For the present it should be noted that the number of cations present within a zeolite structure is determined by the number of $(AlO_4)^{5-}$ tetrahedral included in the framework. This arises from the isomorphous substitution of Al^{3+} for Si^{4+} into the component polyhedral, causing a residual negative charge on the oxygen framework. This negative charge is compensated by those cations present in the synthesis and held in the interstices of the structure on crystallization. The extent and location of water molecular incorporation depends upon (i) the overall architecture of the zeolite molecular structure, i.e. the size and shape of the cavities and channels present, and (ii) the number and nature of the cations in the structure.

The aluminosilicate skeleton can be represented in a number of ways, as for example in the traditional 'ball and stick' model (Figure 2.7). The most favored is the use of tetrahedral arrays; adopted by organic chemists, where the oxygen atoms are drawn as single 'bonds' joining together tetrahedral 'centers' depicting silicon and aluminium. This is the method used in Figure 2.7. Further perusal of Figure 2.6 shows that each sbu contains rings of tetrahedral which are equivalent to rings of oxygen atoms described as 'single six rings' etc. When the sbus are joined to create the infinite lattices they can proscribe larger rings containing 8, 10 or 12 linked tetrahedral (i.e. rings of 8, 10 or 12 oxygen atoms). These rings are obviously important structural features and are often called 'oxygen windows'.

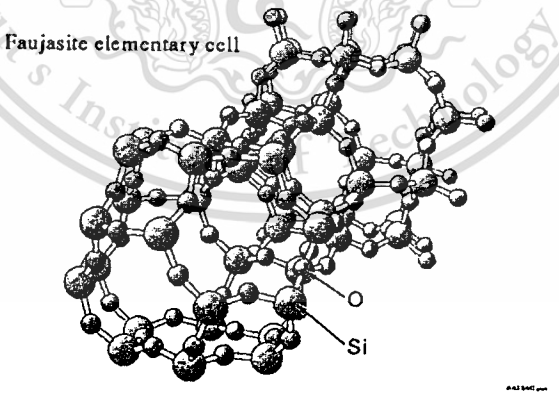

Figure 2.7 A 'ball and stick' representation of the structure of the super cage unit with a framework diagram.

2.2.2 Zeolites X and Y (faujasites) [21]

The zeolites finding more application in the catalysis belong to the family of faujasites, including zeolite X and zeolite Y. Having 0.74-nm apertures (12 membered oxygen rings) and a three-dimension pore structure, they admit even hydrocarbon molecules larger than naphthalene. Their chief application is in catalytic cracking of petroleum molecules (primary in the heavy distillated fraction), giving smaller and gasoline-range molecules.

The framework structure of zeolites X and Y (Figure 2.8) is closely related to that zeolite A. The sodalite cages in faujasites are arranged in an array with greater spacing than in zeolite A. Each sodalite cage is connected to four other sodalite cages; each connecting unit is six bridging oxygen ions linking the hexagonal faces of two sodalite units, as shown in Figure 2.8. The bridging oxygens form what is called a hexagonal prism. The high-resolution electron micrograph of Figure 2.9 shows the regularity if the pores in a crystal of zeolite Y.

Figure 2.8 Structure of faujasite.

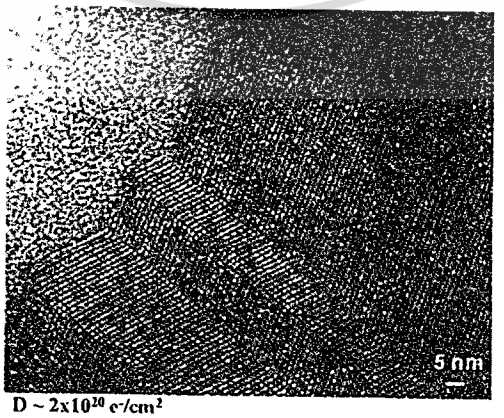

Figure 2.9 High-resolution transmission electron micrograph of crystalline NaY zeolite.

There is a range of faujasite compositions, with a typical unit cell formula being $Na_j[(AlO_2)_j(SiO_2)_{192-j}].zH_2O$, where z is about 260. The value of j is between 48 and 76 for zeolite Y and between 77 and 96 for zeolite X. X-Ray diffraction and NMR data have determined the structures of faujasites, showing, for example, that the unit cell dimension decreases slightly as the Si/Al ratio increases. The X-ray data have also determined the exact positions of cations present to balance the excess negative charge of the AlO_4 tetrahedra. Four cation sites are illustrated in Figure 2.10. Type I sites are located at the centers of the hexagonal prisms, type I' sites are located in the sodalite cages across the hexagonal faces from type I sites, type II sites are located in the supercages near the unjoined hexagonal faces, and type II' sites are located in the supercages, farther from the hexagonal faces than the type II sites.

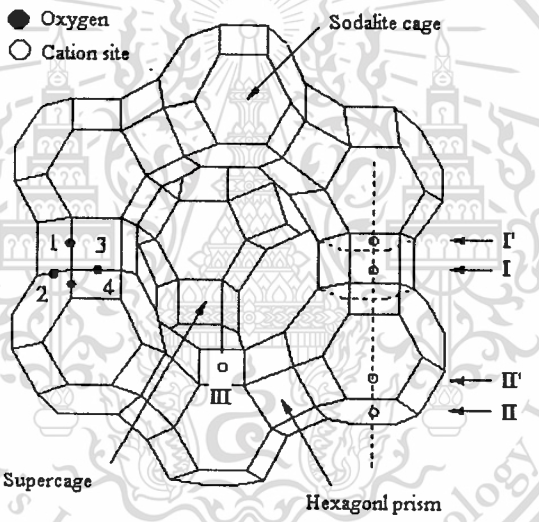

Figure 2.10 Locations of cation sites in X and Y zeolites.

2.2.3 Zeolites application

Because of their unique porous properties, zeolites are used in a variety of applications with a global market of several million tons per annum. In the western world, major uses are in petrochemical cracking, ion-exchange (water softening and purification), and in the separation and removal of gases and solvents. Other applications are in agriculture, animal husbandry and construction. They are often also referred to as molecular sieves.

2.2.3.1 Catalysis

Zeolites have the ability to act as catalysts for chemical reactions which take place within the internal cavities. An important class of reactions is that catalysed by hydrogen-exchanged zeolites, whose framework-bound protons give rise to very high acidity. This is exploited in many organic reactions, including crude oil cracking, isomerisation and fuel synthesis. Zeolites can also serve as oxidation or reduction catalysts, often after metals have been introduced into the framework. Examples are the use of titanium ZSM-5 in the production of caprolactam, and copper zeolites in NOx decomposition.

Underpinning all these types of reaction is the unique microporous nature of zeolites, where the shape and size of a particular pore system exerts a steric influence on the reaction, controlling the access of reactants and products. Thus zeolites are often said to act as shape-selective catalysts. Increasingly, attention has focused on fine-tuning the properties of zeolite catalysts in order to carry out very specific syntheses of high-value chemicals e.g. pharmaceuticals and cosmetics.

2.2.3.2 Adsorption and separation

The shape-selective properties of zeolites are also the basis for their use in molecular adsorption. The ability preferentially to adsorb certain molecules, while excluding others, has opened up a wide range of molecular sieving applications. Sometimes it is simply a matter of the size and shape of pores controlling access into the zeolite. In other cases different types of molecule enter the zeolite, but some diffuse through the channels more quickly, leaving others stuck behind, as in the purification of *para*-xylene by silicalite.

Cation-containing zeolites are extensively used as desiccants due to their high affinity for water, and also find application in gas separation, where molecules are differentiated on the basis of their electrostatic interactions with the metal ions. Conversely, hydrophobic silica zeolites preferentially absorb organic solvents. Zeolites can thus separate molecules based on differences of size, shape and polarity.

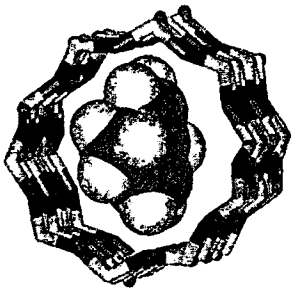

Figure 2.11 The shape of *para*-xylene means that it can diffuse freely in the channel of silicalite.

2.2.3.3 Ion exchange

The loosely-bound nature of extra-framework metal ions (such as in zeolite NaA, right) means that they are often readily exchanged for other types of metal when in aqueous solution. This is exploited in a major way in water softening, where alkali metals such as sodium or potassium prefer to exchange out of the zeolite, being replaced by the "hard" calcium and magnesium ions from the water. Many commercial washing powders thus contain substantial amounts of zeolite. Commercial waste water containing heavy metals and nuclear effluents containing radioactive isotopes can also be cleaned up using such zeolites.

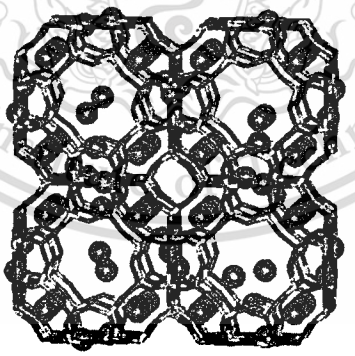

Figure 2.12 Sodium zeolite A used as a water softener in detergent powder.

2.2.3.4 Zeolite and the environment

Zeolites contribute to a cleaner, safer environment in a great number of ways. In fact nearly every application of zeolites has been driven by environmental concerns, or plays a significant role in reducing toxic waste and energy consumption.

In powder detergents, zeolites replaced harmful phosphate builders, now banned in many parts of the world because of water pollution risks. Catalysts, by definition, make a chemical process more efficient, thus saving energy and indirectly reducing pollution. Moreover, processes can be carried out in fewer steps, minimizing unnecessary waste and by-products. As solid acids, zeolites reduce the need for corrosive liquid acids, and as redox catalysts and sorbents, they can remove atmospheric pollutants, such as engine exhaust gases and ozone-depleting CFCs. Zeolites can also be used to separate harmful organics from water, and in removing heavy metal ions, including those produced by nuclear fission, from water.

2.2.4 Basic zeolite catalysts

2.2.4.1 Generation of basic sites in zeolite catalysts

Basicity in zeolites can arise from either the framework oxygen or the incorporated basic species. It has been shown by X-ray photoelectron spectroscopy that, in high aluminium-content zeolites, a decrease in O_{1s} binding energy of the framework oxygen is observed with increase in the size of the exchangeable alkali cations. Since, the electrostatic field strength is reduced when the cations become larger [22], the Lewis acidity of the exchangeable cations is decreased. This means that there is less electron donor interaction of the framework oxygen with the cations. In other words, the large exchangeable cations donate more electrons to the framework oxygen than the smaller cations. Consequently, there should be a concentrated electron density localized on the framework oxygen where Lewis basicity is generated. This is indicated by the highly negative charge of the framework oxygen which can be estimated by the electronegativity equalization method (Sanderson intermediate electronegativity). According to the above discussion and the fact that low binding energy is observed over species with high electron density [23], exchange with large alkali cations results in a lower binding energy of the framework oxygen. This is especially strong in zeolites with high-aluminium content because the adjacent exchangeable cations give an increased interaction to the neighbor oxygens. This leads to in a significant shift in O_{1s} binding energy for cation exchanged zeolite X and zeolite Y but a negligible change for cation exchanged ZSM-5 [24].

2.2.4.2 Basicity in alkali cation-exchanged zeolites [25]

It is generally accepted that the basic sites on the surface of solid catalysts are of the Lewis type, and can, therefore, be defined as sites able to donate an electron pair to an adsorbed

molecule. In zeolites Lewis basicity is associated with the framework oxygen bearing the negative charge of the lattice and consequently the density of negative charge on given oxygen, i.e. its basicity, will depend both on the chemical composition and on the structure of the zeolite. It can generally be said that the lower the average Sanderson electronegativity of the system the higher the basicity of the zeolite.

2.3 Linear alpha olefins

The term 'olefins', also known as alkenes, refers to a large number of compounds that contain carbon and hydrogen and have at least one double bond in their structure. Short-chain olefins, like ethylene, are cracked from naphtha or natural gas. Ethylene is then oligomerised into longer chain linear alpha olefins, ranging from 6 to 30 carbons in length. Alpha olefins are characterized by their high purity, high degree of linearity, and a double bond uniformly positioned between the first and second carbon. For drilling fluid applications, alpha olefins in the C_{14} to C_{18} range are used because they have the right mix of physical properties like viscosity, pour point and flash point. Internal olefins are then produced from linear alpha olefins by catalytically moving the double bond to different locations in the molecule. As a result, the pour point of the fluid decreases significantly, thus enabling these materials to be used successfully in deep-water applications. Internal olefins used as base fluids for drilling mud typically have carbon chain lengths in the C_{15} to C_{18} range [26].

Linear Alpha Olefins (LAO) or Normal Alpha Olefins (NAO) are olefins or alkenes with a chemical formula C_xH_{2x}, distinguished from other mono-olefins with a similar molecular formula by linearity of the hydrocarbon chain and the position of the double bond at the primary or alpha position.

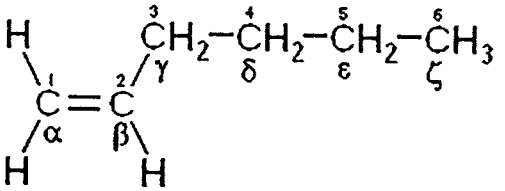

1-hexene, a typical linear alpha-olefin

Linear alpha olefins are a range of industrially important alpha-olefins, including 1-butene, 1-hexene, 1-octene, 1-decene, 1-dodecene, 1-tetradecene, 1-hexadecene, 1-octadecene and higher blends of C_{20}-C_{24}, C_{24}-C_{30}, and C_{20}-C_{30} ranges.

2.3.1 Synthesis

Industrially, linear alpha olefins are commonly manufactured by two main routes: oligomerization of ethylene and by Fischer-Tropsch synthesis followed by purification. Another route to linear alpha olefins which has been used commercially on small scale is dehydration of alcohols. Prior to about 1970's linear alpha olefins were also manufactured by thermal cracking of waxes, whereas linear internal olefins were also manufactured by chlorination/dehydrochlorination of linear paraffin. There are six commercial processes which oligomerize ethylene to linear alpha olefins. Four of these processes produce wide distributions of linear alpha olefins. These are the Ethyl Corporation (Ineos) process, Gulf (Chevron Phillips Chemical Company) process.

2.3.1.1 Ineos (Ethyl) Process

Ethyl linear alpha olefin process is commonly called stoichiometric Ziegler process. It is a two-step process. In the first step, a stoichiometric quantity of triethyl aluminium in olefin diluents is reacted with excess ethylene at high pressure (above 1000 psig) and relatively low temperature (below 400 °F). On the average, nine moles of ethylene are added per mole of triethyl aluminium, resulting in, on average, trioctyl aluminium. The distribution of alkyl chains on the aluminium is determined by statistical bell curve distribution except for some smearing to the light side due to the kinetic phenomena and some smearing to the heavy side due to some incorporation of heavier olefins into the chain. Excess ethylene and olefin diluent are flashed off. The heavy aluminium tri-alkyls are reacted with ethylene again in a displacement or a *tran*-alkylation reaction, but at high temperature (over 400 °F) and at low pressure (less than 1000 psig) to recover triethyl aluminium and a statistical distribution of linear alpha olefins, which serve as the olefin diluents in the chain-growth step [27].

2.3.1.2 CP Chemicals (Gulf) Process

The Gulf linear alpha olefin process is commonly called a catalytic Ziegler process. Triethyl aluminium is used as a catalyst, but in catalytic amounts and the process is a single-step process. Triethyl aluminium and excess ethylene are fed to a plug flow-reactor. The reaction is conducted

at high pressure and high temperature. Excess ethylene is flashed off. The triethyl aluminium catalyst is washed out of the product with caustic and the linear alpha olefins are separated. The product distribution is a Schultz-Flory distribution typical of catalytic processes.

2.3.2 Applications

The terminal double bonds of linear alpha olefins react readily with a wide variety of chemicals. Linear alpha olefins can be used to synthesize any derivative requiring an even-numbered, straight carbon chain.

2.3.2.1 Polymers

Homopolymers & Copolymers Other than Polyethylene

Certain linear alpha olefins can be used to prepare homopolymers and copolymers other than polyethylene. Linear alpha olefin 1-butene can be polymerized to 1-polybutene (PB), a homopolymer that is ideal for many engineering applications because of its excellent long-term mechanical properties.

PB is extremely creep resistant and behaves similarly to a cross-linked plastic. It features a unique combination of unusually high tensile strength and good tear properties. PB shows no signs of cracking, crazing or fracturing when stressed below its short-time failure stress value for long periods of time. In addition, its tear strength increases rapidly as the tear rate escalates. PB's benefits broaden the commercial applications for polymers.

Linear alpha olefins C_6, C_8, C_{10}, C_{16}, C_{18}, C_{20-24} and C_{24-28} are used for the production of copolymers. Using per-esters as initiators, copolymers of maleic anhydride and linear alpha olefins can be formed.

The maleic copolymer made from linear alpha olefin C_{18} is a product known as PA-18, which has been used successfully as a release agent in tapes and paper templates for PVC curtains, and in water-resistant sunscreen formulas.

The copolymers produced from other linear alpha olefin fractions are normally converted to acid amides, half esters or diesters for use as lube-oil additives and pour-point depressants. They are also effective curing agents for epoxy resins and act as unique thermo-set resin compositions in liquid monoepoxides. In addition, linear alpha olefins C_6, C_8 and C_{10} have been co-enter polymerized with vinyl acetate and vinyl chloride.

Polyethylene Copolymers

With the evolution of increasingly sophisticated polyethylene technology, alpha olefins 4, 6 and 8 have become even more valuable co-monomers for the production of a wide range of polyethylene resins.

High-density polyethylene (HDPE) is principally used for the manufacture of high-performance pipe, blow-molded household and industrial bottles, oil bottles, injection-molded food containers, consumer durables and disposable goods and film goods such as grocery sacks and merchandise bags. HDPE possesses high flex stiffness (flexural modulus) but low environmental stress cracking resistance (ESCR). Lowering the melt index (high melt viscosity) can help to alleviate the low ESCR, but the processibility of the polymer suffers, due to lower flow rates. The addition of Chevron Phillips Chemical's alpha olefins 4, 6 or 8 as a co-monomer increases the resulting polymer short chain branching, thereby improving the flow properties while greatly increasing the ESCR.

In addition, HDPE polymers made with alpha olefins 6 or 8 as a co-monomer have much higher ESCR than those made with 1-butene. For a given polymerization process at a polymer density of 0.950 g/cc and melt index ranges of 0.2 to 0.3 g/10 minutes, 1-butene copolymers had ESCR values of 50 to 310 hours, and 1-hexene copolymers exhibited ESCR values of 800 to more than 1,000 hours. Copolymerizing with Chevron Phillips Chemical's alpha olefin 8 rather than 1-hexene produces polymers with even better ESCR values.

Linear low-density polyethylene (LLDPE) is made by incorporating an even higher level of co-monomer (1-butene, 1-hexene or 1-octene) into the product to reduce the density of the resulting polyethylene. Conventional Ziegler-Natta catalysts as well as more recent metallocene technologies are being used today to produce LLDPE. LLDPE provides significantly greater stiffness than low-density polyethylene (LDPE) polymers, which are typically produced in high-pressure processes. Because the melt index of LLDPE can be raised to values much higher than that of LDPE (while maintaining equivalent or superior physical properties), processing cycle times can be reduced. In addition, many products made with LLDPE can be significantly down-gauged to save on raw material costs.

For the greatest possible strength and tear resistance, the density can be reduced even further using emerging metallocene technologies to produce what is referred to as very low-density

polyethylene (VLDPE). Among other benefits, VLDPE has a higher heat-seal temperature than LDPE, yet provides equivalent seal strength.

Regardless of the application, Chevron Phillips Chemical's 1-hexene performs exceptionally well under the most stringent polymerization conditions. This is particularly important with the emergence of sophisticated metallocene technology for the production of LLDPE and VLDPE where high purity co-monomers are critically important to maintain high catalyst activity and resulting product performance.

2.3.2.2 Surfactants

Alpha Olefin Sulfonate (AOS)

Linear alpha olefins are excellent intermediates for producing alpha olefin sulfonate (AOS) surfactants. These surfactants provide outstanding detergency, high compatibility with hard water, and good wetting and foaming properties. AOS is free of skin irritants and sensitizers, and it biodegrades rapidly. It is used in high-quality shampoos, light-duty liquid detergents, bubble baths, and heavy-duty liquid and powder detergents. It is also used in emulsion polymerization. C_{14}-C_{16} AOS blends are frequently used in liquid hand soaps.

To make AOS, linear alpha olefins are first sulfonated in a continuous thin film reactor to produce a mixture of alkene sulfonic acids and sultones (cyclic sulfonate esters). The mixture is neutralized with aqueous sodium hydroxide and then hydrolyzed at elevated temperatures to convert the remaining sultones to alkene sulfonates and hydroxy sulfonates. This results in an aqueous solution of alpha olefin sulfonate. (If a solid anhydrous product is desired, it can be easily obtained by neutralizing and hydrolyzing the solution in isopropanol instead of water).

Detergent Alcohols

Linear alpha olefins are easily converted to primary alcohols via oxo chemistry. By reaction with ethylene oxide, the alcohols form a variety of nonionic ethoxylates, which may themselves serve as surfactants or be further derivatized. Anionic alkyl ether sulfates can be derived from the sulfation of the ethoxylates. These are widely used in the cosmetics and toiletries industries. Alternatively, the alcohols may be directly sulfated to produce alkyl sulfates.

Linear Alkyl Benzene Sulfonates

Linear alpha olefins react with benzene via Lewis acid catalysis to form linear alkyl benzenes (LABs). Sulfonation and subsequent neutralization of LAB result in linear alkyl

benzene sulfonates, which are commonly used in dishwashing liquids, laundry detergents, all-purpose cleaners, and lube-oil additives. Similarly, phenol or naphthalene will react with olefins, producing other types of detergents and wetting agents upon sulfonation/neutralization.

Amine Derivatives

Linear alpha olefins are also suitable for manufacturing alkyl dimethyl amines (ADMAs), which are precursors to a number of surface-active derivatives. Amine oxides produced via hydrogen peroxide oxidation of ADMAs are excellent foam boosters and are typically used in shampoos, bubble baths, and dishwashing detergents.

Quaternary ammonium halides or "Quats," which result from reaction of ADMAs with alkyl or benzyl halides, are highly effective biocides and antistatic agents. Betaines, which are mild amphoteric surfactants, feature good foam boosting and stabilizing properties. They are readily derived from ADMAs by reaction with sodium chloroacetate.

Alkane Sulfonates

Sodium bisulfite will react with linear alpha olefins via a free-radical mechanism to produce alkane sulfonates. Alkane sulfonates with chain lengths of C_{12} or higher have limited water solubility, suggesting their application in synthetic detergent bars. Shorter alkane sulfonates like C_8, however, are hydrotropic.

2.3.2.3 Synthetic Fluids

Polyalphaolefins

Synthetic base fluids for high-performance lubricants and functional fluids can be prepared by oligomerizing Chevron Phillips Chemical's alpha olefins, particularly alpha olefins 10 and 12. The resulting oligomers, consisting of dimers, trimers, tetramers and so on, are typically hydrogenated and then formulated with appropriate additives.

For more than two decades, Chevron Phillips Chemical has been a leader in the development and production of PAOs. Our original products, which are produced from 1-decene, consist of PAOs 2, 4, 6 and 8cSt and C10 dimer. In the mid-1990s, Chevron Phillips Chemical developed unique PAO products, which are synthesized from 1-dodecene. They are PAOs 2.5, 5, 7 and 9cSt as well as the C_{12} dimer.

Now our comprehensive range of PAOs provides our customers with a greater range of physical properties from which to choose, giving them more flexibility and versatility in developing products better suited to their individual applications.

2.3.2.4 Additives

Plasticizer Alcohols

C_8 through C_{10} linear alpha olefins are used to produce primary C_9 through C_{11} plasticizer alcohols via hydroformylation or oxo chemistries. The phthalate plasticizers produced from these alcohols gave superior properties to those made from 2-ethyl 1-hexanol. The same chemistry is used to produce C_{13} to C_{15} synthetic detergent alcohols from C_{12} and C_{14} linear alpha olefins.

Alkenyl Succinic Anhydrides

Alkenyl succinic anhydrides (ASAs) are prepared by heating linear alpha olefins and maleic anhydride to approximately 200°C. Some ASAs are used as dispersants in lube oils and automatic transmission fluids, and as pour-point depressants in lube and crude oils. Others are converted to acid amides, half esters, and diesters. One of the largest applications for ASA is as the paper sizing agent in alkaline media. For this use, linear alpha olefins C_{16} or C_{18} are isomerized to a thermodynamic distribution of internal olefins, which are then reacted with maleic anhydride to produce the desired liquid ASA.

Polyvinylchloride Lubricants & Stabilizers

Heat and pressure are applied during the extrusion of polyvinylchloride (PVC) as it moves through the die. Lubricants (waxes) are compounded into the PVC to ensure proper lubrication in the extruder and to control fusion of the PVC compound. Linear alpha olefin C_{30+} is the preferred lubricant for this application.

During the extrusion process, PVC often begins to decompose. Various materials are used to retard this degradation, including dibutyl or dioctyl tin oxides and/or dioctyl tin mercaptides. These compounds are made using tin (IV) chloride and the corresponding aluminum alkyls, which in turn are derived from linear alpha olefins. The mercaptans used to make the tin mercaptides are usually made from linear alpha olefins.

2.3.2.5 Specialty Chemicals

Epoxides

Treatment of alpha olefins with peracids forms epoxides, which find use as modifiers for epoxy resins. Epoxides may also serve as polyether ingredients in polyurethanes. Almost all carbon number fractions of our alpha olefins find some application in the epoxide market.

Halogenated Linear Alpha Olefins

Chlorinated linear alpha olefin 20-24 (C_{20}-C_{24} alpha olefin) may be used as a secondary plasticizer in PVC formulations. Chlorinated alpha olefin (40 wt. % chlorine) based plasticizer formulations have been evaluated against chlorinated paraffins (42 wt % chlorine) and alkyl-aryl hydrocarbon plasticizer formulations. The evaluation of the mechanical properties of these formulations shows that the chlorinated alpha olefin is equivalent in plasticizing efficiency to the two other secondary plasticizers, while having adequate heat stability and volatility properties. Polychlorinated 1-dodecene, 1-tetradecene, and 1-hexadecene perform well as stable high temperature metalworking fluid additives.

Additional Applications

Chevron Phillips Chemical's alpha olefins are used in many other applications including the production of mercaptans, ketones, ester, pyrazines, alkylphosphines, alkyl silanes, and as a substitute for paraffins and paraffin waxes.

Sulfur-hydrogen bond containing compounds may be added to alpha olefins, under the proper conditions, to form sulfur-containing hydrocarbons. Mercaptans, produced from the reaction between alpha olefin and hydrogen sulfide, are successfully used in rubber additives, ore flotation, and specialty chemical applications.

Alpha olefins may be converted to internal olefins through olefin isomerization or higher carbon number internal olefins by metathesis or dimerization reactions. Chevron Phillips Chemical's blend of isomerized C_{16} and C_{18} alpha olefins is an excellent synthetic fluid for use in offshore drilling muds. The blend has outstanding physical and ecotoxicological properties for this application. In fact, the EPA has selected this product as an ecotox standard for fluids used in offshore drilling muds.

Trialkylphosphine and trialkylphosphine oxides, silylhydrocarbons, alkyl silanes, and some organometallic compounds are produced commercially from linear alpha olefins for a wide variety of end products.

Derivatives of Chevron Phillips Chemical's alpha olefins with carbon numbers above C_{20} find uses in lube oils, transmission fluids, and as pour-point depressants in lube and crude oil. These wax fractions may also be chemically modified to simulate more expensive carnauba or Montan waxes used to make polishes and candles.

The high molecular weight of linear alpha olefins is primary raw material in the chemical industry [28, 29] as shown in table 2.3

Table 2.3 Application of linear alpha olefins.

Linear alpha olefins	Application
1-Decene ($C_{10}H_{20}$)	Detergent alcohols, poly alpha-olefins, alkyl aromatics, plasticizer alcohols, epoxides, di-/poly- halides, personal care, flavors and fragrances
1-Dodecene ($C_{12}H_{24}$)	Detergents, plasticizer alcohols, poly alpha-olefins, alkyl aromatics, ADMA, ASA, epoxides, mercaptans, di-/poly- halides, alkyl silanes, personal care, flavors and fragrances
1-Tetradecene ($C_{14}H_{28}$)	Maleic anhydride copolymers, AOS, alkyl aromatics, ADMA, detergent alcohols, ASA, epoxides, metal working fluids, di-/poly-halides, alkyl silanes, personal care, flavors and fragrances
1-Hexadecene ($C_{16}H_{32}$)	Maleic anhydride copolymers, AOS, alkyl aromatics, ADMA, ASA, lube oil additives, epoxides, metal working fluids, di-/poly- halides, alkyl silanes, personal care, flavors and fragrances
1-Octadecene ($C_{18}H_{36}$)	Maleic anhydride copolymers, AOS, alkyl aromatics, ADMA, ASA, lube oil additives, epoxides, metal working fluids, di-/poly- halides, alkyl silanes, personal care, flavors and fragrances
Alpha Olefin C_{20-24}	Lube oil additives, personal care, epoxides, alkyl aromatics, drilling fluids, maleic anhydride copolymers, pour point depressants
Alpha Olefin C_{24-28}	Epoxides, di-/poly- halides, candles, pour point depressants, personal care

2.4 Literature reviews

In the recent forty years, the catalytic properties of zeolites have been one of the most studied subjects in the field of catalysis. Investigations on the structural nature and catalytic properties of zeolites were especially intense.

In fact, some zeolites have also basic properties. X and Y zeolites that have been modified through conventional ion exchange with alkali metal cation solutions indeed exhibit basic properties useful for catalysis, as shown by their effectiveness for various test reactions which include transesterification of soybean oil with methanol (methanolysis) [30,31] and decarbonylation of benzaldehyde and methyl octanoate in inert atmosphere [6,7].

Also known as methanolysis, the transesterification reaction of vegetable oils with methanol is commonly carried out in the presence of homogeneous base or acid catalysts. Acid-catalyzed process often uses sulfonic acid and hydrochloric acid as catalysts; however the reaction time is very long (48–96 h) even at reflux of methanol, and a high molar ratio of methanol to oil is needed (30–150:1,by mol) [32]. Potassium hydroxide, sodium hydroxide, their carbonates as well as potassium and sodium alkoxides such as $NaOCH_3$, are usually used as base catalysts for this reaction [33]. As the catalytic activity of a base is higher than that of an acid and acid catalysts are more corrosive, the base catalyzed process is preferred to acid catalyzed one, and is thus most often used commercially. However, in the conventional homogeneous manner, removal of these base catalysts is technically difficult and a large amount of wastewater is produced to separate and clean the catalyst and the product. Therefore, conventional homogeneous catalysts are expected to be replaced in the near future by environmentally friendly heterogeneous catalysts mainly due to environmental constraints and simplifications in the existing processes.

Many different heterogeneous catalysts have been developed to catalyze the trans-esterification of vegetable oils to prepare fatty acid methyl esters. For example, CsX zeolites, anionic clays (hydrotalcite-like), calcium carbonate rock, EST-10, Li/CaO and Na/NaOH/c–Al_2O_3 have been found to be efficient heterogeneous catalysts for the transesterification of vegetable oils [30, 34]. However, they are quite expensive or complicated to prepare, which limits their industrial application.

Fatty acid methyl ester biofuels (FAME) exhibit high cetane number and are considered to burn cleanly; however, there is growing concern about the fungibility of these fuels with conventional petroleum-derived diesel due to the oxidative and thermal instability [35-39].

Reduction of the oxygen content in the fuel would readily improve the stability of the fuel and therefore its utilization potential. Various processes including hydrogenolysis [40.41], decarbonylation [42], and decarboxylation of FAME have been proposed to transform the biodiesel into the hydrocarbon base fuel [4].

The decarbonylation and decarboxylation have advantages over hydrogenolysis because, while the hydrocarbons thus produced may contain less carbon than its fatty acid counterpart, the former reactions require much less hydrogen than the latter. Moreover, the properties of the fuel obtained by decarbonylation and decarboxylation are not significantly different from those obtained from hydrogenolysis [4]. Typically, decarbonylation takes place over supported noble metal catalysts at relatively high temperature (>350 $^{\circ}$C). For example, Pd/C has been found to be an effective catalyst for decarbonylation and decarboxylation [4]. However, carbon monoxide produced from the reaction may competitively adsorb on the metal surface, leading to a reduction or even loss in the catalytic activity as conversion increases. Hence, the required hydrogen partial pressure is generally high, in order to keep the surface clean and facilitate the oxygenate–metal surface interaction.

An alternative family of catalysts that may overcome some of these limitations is that of solid bases. This is because FAME is fairly electrophilic while the decarbonylated by-product, carbon monoxide, is nucleophilic. Among possible solid base catalysts, low-silica zeolites containing highly polarizable cations, such as cesium, may be good candidates. These catalysts have been found to exhibit relatively high activity towards reactions involving oxygenates, as well as hydrogenation and hydrogenolysis of acrylonitrile and propionitrile [43]. It has been suggested that, in addition to the need for strong basicity, an active catalyst requires the co-existence of acid and basic sites for reactions such as hydrogenation and hydrogenolysis. In fact, an alkali-exchanged zeolite such as the CsNaX contains conjugate acid–base pairs, in which the exchangeable alkali cation has Lewis acidity and the oxygen that bridges Si and Al near the exchangeable cation has basicity.

In previous work, Sooknoi *et al.* studied the deoxygenation of methyl octanoate over a CsNaX zeolite catalyst as a model reaction for the production of deoxygenated liquid hydrocarbons from biodiesel. Heptenes and hexenes were major products. Octenes and other hydrogenated products were formed in lower amounts via hydrogenation by hydrogen produced on the surface by methanol decomposition.

CHAPTER 3

EXPERIMENTAL DETAILS

3.1 Reagents

Chemicals	Grade of purity	Manufactures
1. Air zero	High purity	Praxair
2. Ammonia in Helium gas	1%	TIG
3. Cesium acetate	≥ 95%	Fluka
4. Distilled water	-	-
5. Helium gas	High purity	Praxair
6. Hydrogen gas	High purity	Praxair
7. Methanol	HPLC	Fisher Scientific
8. Molecular sieve, 13X, powder	-	Aldrich
9. Palmitic acid	≥ 98%	Fluka
10. Standard hydrocarbon	GC	PTT
11. Tetrahydrofuran	HPLC	LAB-SCAN
12. Zeolite Y,powder	-	Tosoh

3.2 Apparatus

1. Bubble flow meter
2. Buchner flask
3. Circulator with cooling unit (002-4288, Haake)
4. Clamp
5. Gas adsorption analyzer (Autosorb-1C, Quantachrome)
6. Gas Chromatograph with thermal conductivity detector (TCD) (CP-3800, Varian)
7. Gas chromatograph with flame ionization detector (FID)(5890 series II, Hewlett Packard)
8. Gas Chromatograph/Mass spectrometer (6890N/5973N, Agilent)
9. Glass tube reactor with glass rod and glass wool
10. HPLC Pump (307, Gilson)
11. Laboratory glassware

12. Magnetic stirrer hot plate with temperature controller system (RCT basic, IKA)
13. Mass flow controllers (GFC17, Aalborg)
14. Oven (500, Memmert)
15. Scanning electron microscope (LEO 1455VP, LEO Electron Microscopy)
16. Septum
17. Sieve (USA standard sieve, AASHO N-92)
18. Stainless steel tubes, connectors, valves and fittings
19. Teflon tubes and fittings
20. Thermogravimetric analyzer (Pyris 1 TG, Perkin Elmer)
21. Tube furnace with temperature-controller (MTF 12/25/250, Carbolite)
22. Vials
23. X-ray diffractometer (D8 Advance, Bruker AG)
24. X-ray fluorescence spectrometer (SRS 3400, Bruker AG)

3.3 Experiment procedure

3.3.1 Preparation of basic zeolite catalysts

3.3.1.1 Cesium cation exchanged zeolite X and zeolite Y

3.3.1.2 Preparation of pelleted zeolite catalysts

3.3.2 Characterization of zeolites catalysts

3.3.2.1 Crystal morphology using scanning electron microscope (SEM)

3.3.2.2 Zeolite structure using X-ray power diffractrometer (XRD)

3.3.2.3 Chemical composition of the zeolite using X-ray fluorescense spectrometer (XRF)

3.3.2.4 Surface area using gas adsorption analyzer

3.3.2.5 Carbon dioxide adsorption

3.3.3 Catalytic activity testing

3.3.3.1 Effect of contact time

3.3.3.2 Effect of temperature

3.3.3.3 Effect of feed concentration

3.3.3.4 Effect of exchangeable cations

3.3.3.5 Effect of carrier gas

3.3.4 Analysis of products

Qualitatively and quantitatively analysis of products by FID-gas chromatograph

3.4 Experimental details

3.4.1 Preparation of basic zeolite catalysts

3.4.1.1 Cesium cation exchanged zeolite X and zeolite Y

Cesium exchanged zeolite X and zeolite Y incorporated with cesium cation will be prepared by ion exchange of NaX and NaY with cesium acetate aqueous solution (1gram of zeolite in 100 ml, 0.1 M $C_2H_3CsO_2$) at 80 ^{0}C for 24 hours. After that, the sample will be filtrated without washing and dried at 105 ^{0}C overnight. These samples are designated as CsNaX and CsNaY.

3.4.1.2 Preparation of pelleted zeolite catalysts

All zeolite catalysts will be calcined in dry air at 450 ^{0}C (heating rate at 2 ^{0}C/min) for an hour. After that, these catalysts are pressed into a disc at 3 tons then crushed and sieved into 600-850 micron (20-30 meshes) of USA standard sieve (AASHO N-92). The zeolite pellets are kept in dried plastic containers at room temperature.

3.4.2 Characterization of zeolites catalyst

3.4.2.1 Crystal morphology of zeolites

The crystal morphology and crystallite size can be determined by scanning electron microscopy (SEM). This technique is done according to the following procedure: the sample is finely dispersed on a SEM stub. The sample surface is then coated with gold thin film. After that the sample holder is transferred to sample chamber, and evacuated from ambient pressure to below 10^{-4} Torr. Then, the holding sample can be adjusted, tilted and moved in the X, Y and Z directions. As a consequence, sample surface can be viewed from almost any perspective.

3.4.2.2 Zeolites structure

The zeolites structure can be determined by X-ray diffractometry (XRD). The sample is prepared by packing the zeolite powder in the sample holder. Cu-Kα X-ray beam is used for analysis at 45 kV, 30 mA. The sample is scanned over the angle ranged from 2-theta: 5 to 60

degrees, with 0.040 degrees/step, and detection time 1 second/step. X-ray diffraction pattern of sample is compared with the X-ray diffraction pattern of standard zeolite for determining the structure.

3.4.2.3 Chemical composition of the zeolite samples

The chemical composition of zeolite catalysts can be determined by X-ray fluorescence spectrometry (XRF). The sample is prepared by mixing 4.5 grams of boric acid and 0.5 grams of zeolites and sent to a grinder. The mixer is packed onto sample holder and then compressed at 150 kN. The sample is placed in the sample chamber. Rhodium is used as X-ray source for measuring at 50 kV, 60 mA.

3.4.2.4 Surface area

Surface area of zeolites can be determined by Gas Adsorption Analyzer (Autosorb-1C, Quantachrome). The sample is prepared by weighing approximately 50 mg of zeolites into a cleaned and dried sample cell. The sample cell is attached to the out gassing station. Heating mantle is installed and the temperature is raised to 350^{0}C. The sample cell is then removed from the out gassing station after the nitrogen is filled and attached to the analysis station. The equilibration time is set to 3 minutes and the adsorption is tested at the partial pressure (P/P_0) range of 10^{-6} to 1.0.

3.4.2.5 Carbon dioxide adsorption

Carbon dioxide adsorption is the technique using for determination of the basicity and basic strength of the catalyst. This technique is done according to the following procedure: the zeolite sample is weighed accurately about 50 mg and transferred to a cleaned and dried sample cell. The sample cell is attached to the outgassing station. Then, a heating mantle is installed with the sample cell and the temperature is raised to 350°C. After the residual adsorbed gas was removed by temperature and reduced pressure, the carbon dioxide adsorbate is filled by open the gas inlet valve. The sample cell is attached to the sample station. At the initiate adsorption, an ice bath is placed around the sample cell and the measurement of carbon dioxide adsorption is set with 3 minutes equilibration time. When the adsorption is complete, the sample cell is removed from the sample station and dried thoroughly.

3.4.3 Catalytic activity testing

The zeolite pellets are packed into the glass reactor (6 mm of inside diameter) and covered by glass wool and glass rod, as shown in Figure 3.1 (enlargement of reactor).

The catalytic testing rig is also illustrated in Figure 3.1. The reactor is positioned at the center of a vertical tube furnace. Helium is used as a carrier gas. The gas flow rate is controlled by a mass flow controller and checked by bubble flow meter. Before activity testing, the catalyst is activated by heating at 2°C/min to 450°C and held at that temperature for an hour under the stream of air zero (30 ml/min). The reactor is cooled to the reaction temperature (400-450°C) and purged with carrier gas (30 ml/min) for an hour. After that, the reactant (10 wt.% palmitic and 20-45 wt.% methanol in tetrahydrofuran) is fed into the reactor by a HPLC pump at 0.025 ml/min. The reaction is operated for 6 hours on stream. The product effluents are trapped at 20°C and collected hourly.

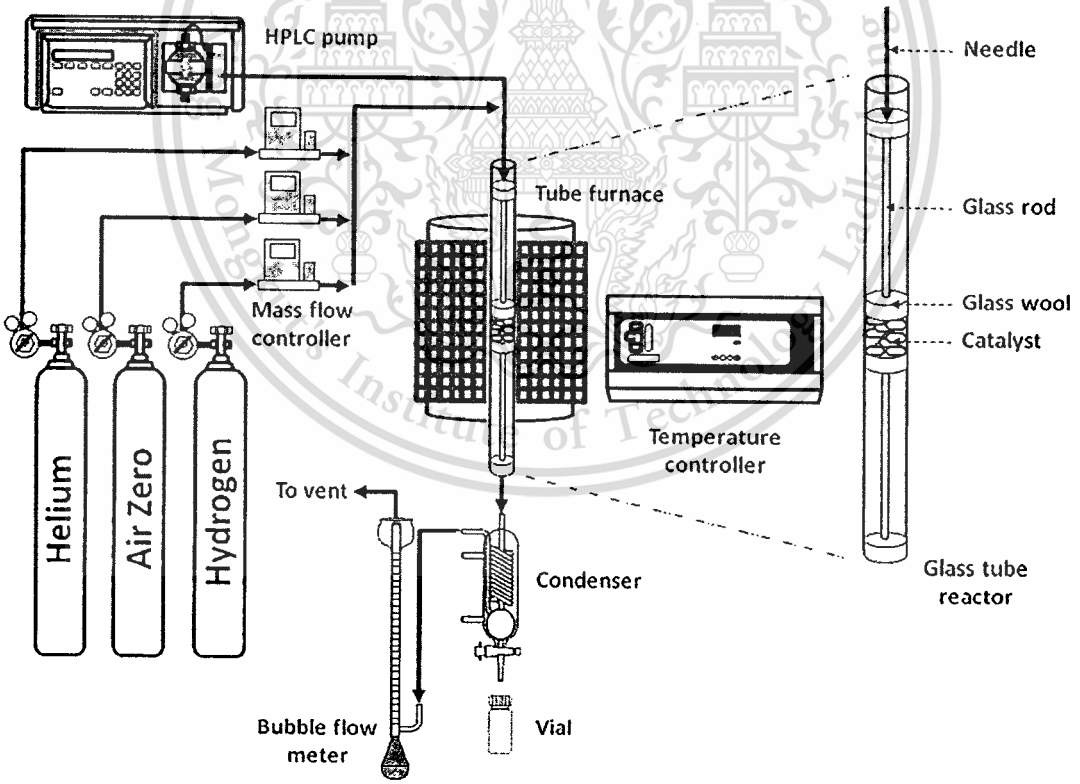

Figure 3.1 Schematic of catalytic testing unit

3.4.4 Analysis of products

The reaction products are qualitatively analyzed by gas chromatograph equipped with mass detector (GC-MS Agilent 6890) with HP-5 (0.25 mm X 30 m) as a separating column.

The liquid products are quantitatively determined by a gas chromatograph equipped with a flame ionized detector (GC-FID HP 5890 series II) using DB-5 (0.25 mm X 30 m) as a separating column.

The gas products are quantitatively determined by a gas chromatograph equipped with a thermal conductivity detector (GC-TCD Varian CP-3800) using MoleSieve 13X 45/60 (2.3 mm X 1.83 m) as a separating column.

The details of GC conditions and separating columns are summarized in Table 3.1.

Table 3.1 GC conditions.

	Agilent 6890	HP 5890 series II	Varian CP-3800
Column	HP-5	DB-5	MoleSieve13X 45/60
Diameter (mm)	0.25	0.25	2.3
Length (m)	30	30	1.83
Carrier gas	He	He	He
Detector	FID	FID	TCD
Detector temperature (°C)	290	290	120
Injector temperature (°C)	265	265	120
Detector gases			
Hydrogen (psi)	15	15	-
Air-zero	35	35	-
Column head pressure (psi)	15	15	25
Linear velocity (cm/s)	88	88	12
Oven temperature			
Initial temperature (°C)	40	40	50
Initial time (min)	10	10	20
Rate 1 (°C)	15	15	-
Final temperature (°C)	280	280	-
Final time (min)	19	19	-
Total time (min)	45	45	20

CHAPTER 4

RESULTS AND DISCUSSION

4.1 Catalyst characterization

4.1.1 Catalyst structure

X-ray diffraction patterns of catalyst were obtained from Bruker X-ray powder diffractometer using Cu-Kα radiation. X-ray diffraction patterns of zeolite CsNaX and NaX were shown in Figure 4.1.

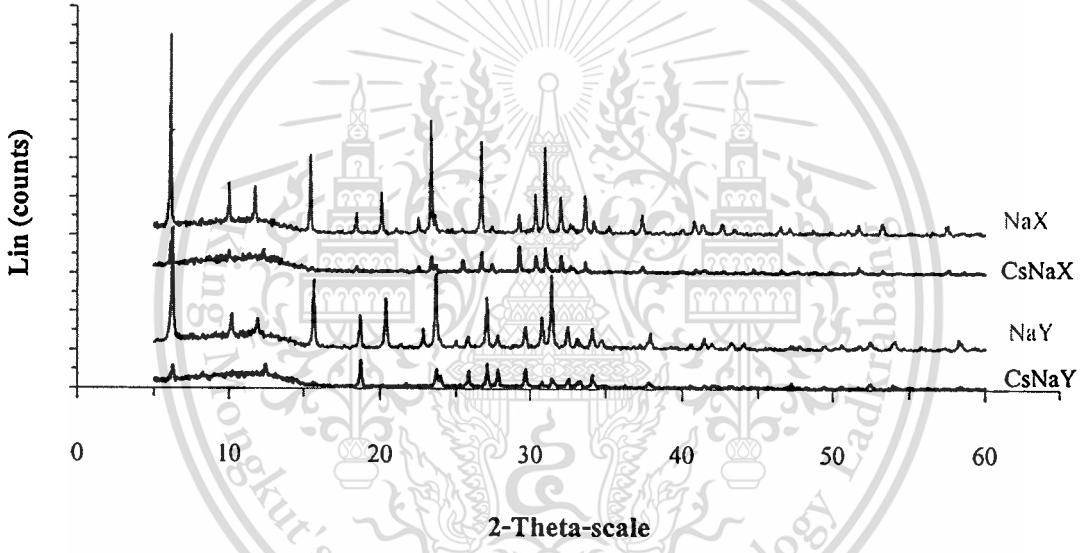

Figure 4.1 X-ray diffraction patterns of CsNaX, CsNaY, NaX and NaY.

The XRD patterns showed a decrease in peak intensity of the cesium incorporated in NaX and NaY zeolite. This lowering of peak intensity might be contributed from the difference of X-ray adsorption coefficient of the parent catalyst when the larger exchangeable cations (Cs^+) are incorporated [44]. Large cation can adsorb and scatter X-ray radiation, resulting in a reduction of the peak intensity. However, this shall not affect crystallinity of the sample. This is because when the cesium containing catalysts were back-ion exchanged with sodium cations, the peak intensity is recovered [45].Therefore, it was confirmed that the crystallinity and framework structure were retained after ion exchange or incorporation of the cesium cations.

4.1.2 Crystal morphology

Figure 4.2 and 4.3 show scanning electron micrograph of NaX (Molecular sieve 13X) and CsNaX, respectively. The crystal size of all samples is approximately 2.75 μm diameter and appears to be the same. It is expected that ion exchange shall not affect on the crystal size.

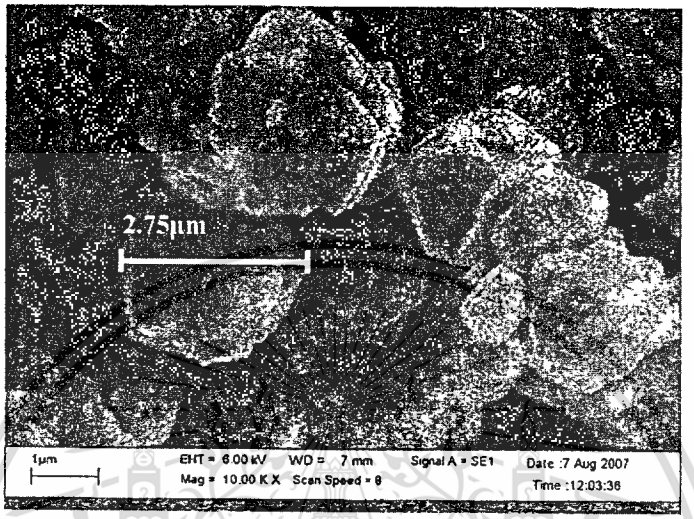

Figure 4.2 Morphology of calcined zeolite NaX.

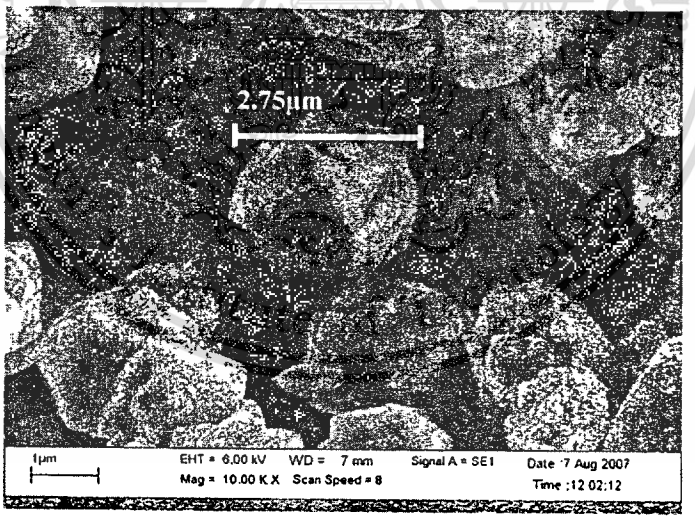

Figure 4.3 Morphology of calcined zeolite CsNaX.

Moreover, Figure 4.2 and 4.3 also show that no particle deposit on the zeolite surface. This suggests that all exchanged cations (Cs^{+}) are corporate into the zeolite cavity and do not form bulk oxide/carbonate on the external surface.

4.1.3 Elementals analysis and surface area

The silicon/aluminium molar ratio, degree of ion exchange and amount of excess cations per unit cell of zeolite catalysts were determined by X-ray fluorescence spectroscopy as shown in Table 4.1.

Table 4.1 Elemental analysis data of NaX, CsNaX, NaY and CsNaY catalysts.

Catalysts	Surface area	Total composition	
	(m^2/g)	Si/Al	Cs/Al
NaX	693	1.3	-
CsNaX	536	1.3	0.58
NaY	728	2.7	-
CsNaY	589	2.7	0.63

These values are calculated from elemental analysis as shown in Appendix A. The analysis indicates that a significant fraction of the initial sodium ions has been exchanged by cesium. This significant amount of ion exchange with some excess cesiums occluded in the zeolite, resulted in a noticeable drop in BET surface area and pore volume, as compared to those of the original NaX and NaY. This is because the cesium cation is much larger than the sodium cation and the exchanged cations preferentially occupy most available pore. However, it must be noted that, as the CsNaX and CsNaY samples were dried without washing during the preparation. Hence, excess Cs cations may be left on the sample as bulk particles of cesium oxide (Cs_2O), cesium peroxide (Cs_2O_2) or cesium superoxide (CsO_2) [46]. Therefore, a fraction of the observed drop in BET may also be due to pore occlusion by these species.

4.1.4 Carbon dioxide adsorption

The basicity of ion-exchanged zeolites arises from the framework negative charge, thus, the relatively high aluminum content of faujasite zeolite (zeolite X and Y) lead to electronegative framework, which makes faujasite zeolite one of the most basic zeolites when in the alkali-exchanged form. In addition to the reports in literature [47, 48], the excess cesium "cluster" can provide additional basicity in zeolites.

In order to verify the basicity contributed from the excess cesium "cluster" species in these catalysts, adsorption of carbon dioxide was tested for NaX, CsNaX, NaY and CsNaY. Isotherms for carbon dioxide adsorption on cesium exchanged faujasite zeolites are presented in Figure 4.4. The adsorbed amount is expressed by volume of carbon dioxide adsorption per gram of catalysts. The result has shown that the adsorption capacity of carbon dioxide on CsNaX and CsNaY are higher than that on NaX and NaY. This can be attributed to the fact that of cesium exchanged fuajasite zeolites are more basicity.

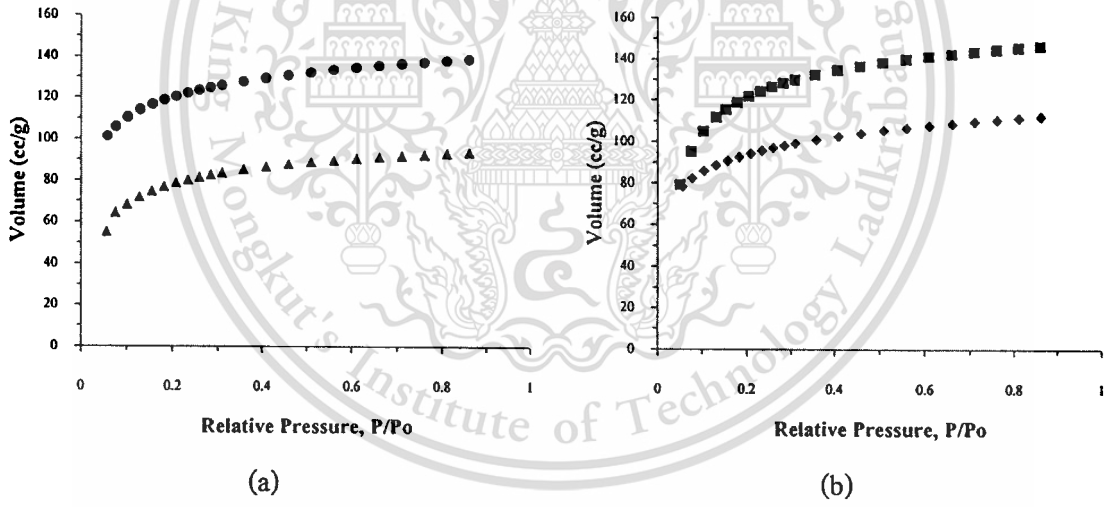

Figure 4.4 Isotherms concerning the adsorption of carbon dioxide measured on (a) CsNaX (●), compared to that on NaX (▲) and (b) CsNaY (■), compared to that on NaY (♦).

It is known that carbon dioxide is a good probe for basicity determination. An interaction of carbon dioxide with zeolite takes places at the framework oxygen adjacent to the charge balancing cations forming a bent configuration species where negative charge from the surface would be distributed in part over the two oxygens of the carbon dioxide. This carbonate like species can be stabilized by an interaction with the charge balancing cations and such interaction is facilitated by both the basicity of the framework oxygen and the polarizing capacity of the

exchangeable cation. Since cesium is a highly polarizable cation, carbon dioxide chemically adsorb on the basic framework of cesium exchanged zeolite X as demonstrated below;

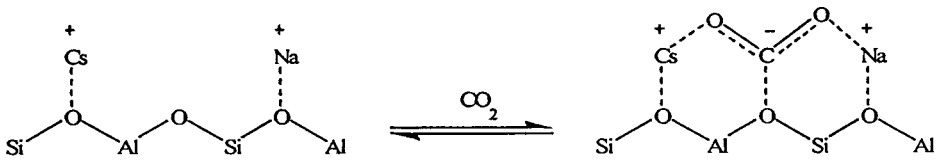

In addition, excess cesium cation "cluster" species may also facilitate the formation of carbonate-like structures. Over CsNaX, interaction of carbon dioxide with the excess cesium cation "cluster" can be postulated as follows:

In consistent with above hypothesis, the adsorption isotherm of carbon dioxide is well fitted with Langmuir adsorption isotherm as shown in Appendix B suggesting a chemisorbed monolayer of carbon dioxide on NaX, CsNaX, NaY and CsNaY surface. The adsorption equilibrium constants determined by Langmuir plot are summarized in Table 4.2.

Table 4.2 Langmuir adsorption equilibrium constant.

Catalysts	Langmuir constant (K)
NaX	23.93
CsNaX	42.69
NaY	28.15
CsNaY	48.43

It is clearly seen that Langmuir adsorption equilibrium constant (K) of both CsNaX and CsNaY are higher than that of NaX and NaY. This shows that the adsorption strength of carbon dioxide on CsNaX and CsNaY are stronger than that on NaX and NaY. From the results, it can be concluded that the basicity and basic strength of the zeolite catalyst increases with the size of the charge balancing cation.

4.2 Deoxygenation of palmitic acid over cesium faujasite catalyst

The deoxygenation of palmitic acid via *in-situ* esterification with methanol over CsNaX catalyst was studied in a fixed bed flow reactor. The liquid products were analyzed by GC-FID and identified by GC-MS.

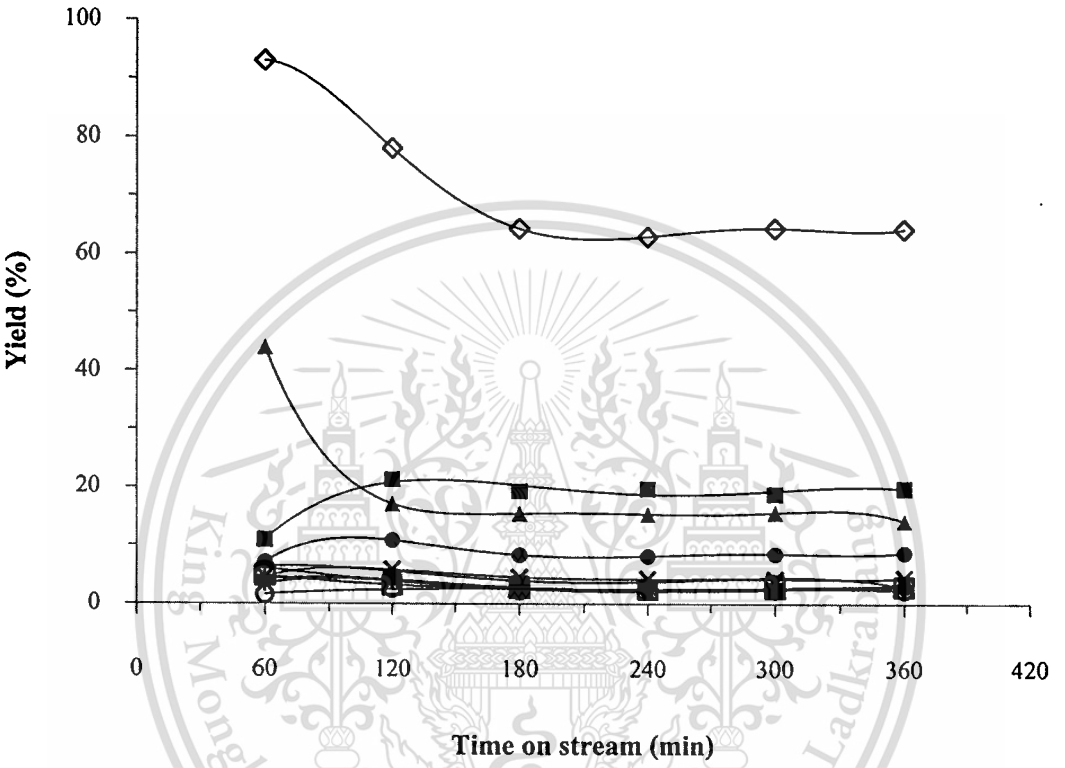

Figure 4.5 Conversion and yield of products from the reaction of 10 wt% palmitic acid, 45wt% methanol in THF over CsNaX.

Reaction conditions: W/F 450g·h/mol, 425 °C, 1 atm, 30 ml/min of Helium, C_{16} (○), C_{15} (■), C_{14} (●), C_{13} (x), C_{12} (*), C_{11} (♦), C_{10} (+), C_9 (□), Oxygenate (-), Gas product (▲), Conversion (◊).

From Figure 4.5, no palmitic acid was detected for all time on streams. It was believed that when the reactant included both palmitic acid and methanol were fed to reactor at 425 °C, the palmitic acid was all converted to methyl palmitate via *in-situ* esterification with methanol as shown [6];

$$CH_3OH + C_{15}H_{31}COOH \xrightarrow[\text{Heat.}]{\text{CsNaX}} C_{15}H_{31}COOCH_3$$

Methanol **Palmitic acid** ***in situ* Methyl palmitate**

The methyl palmitate conversion was defined as the summation of hydrocarbon product yields. From Figure 4.5, at the initiation of the reaction, the catalyst offers high conversion of methyl palmitate and gas hydrocarbons are the dominant products. These gas products may be formed by the cracking in the pore of the zeolite catalyst. However, a rapid decrease in conversion is observed at 1-3 hours on stream. This is probably due to coke accumulated in the pore of zeolite, partially inhibiting access to some active sites. Thereafter, the conversion remained constant and gas products were declined, the C_{15} and C_{14} hydrocarbons become main products. This suggests that there are available active sites, presumably at the pore mount which are not affected from the coke formation in the zeolite pore.

The formation of C_{15} and C_{14} hydrocarbons were presumably explained that the methoxyl group of methyl palmitate which formed *in-situ* by esterification. The proposed chemisorption of methyl palmitate over CsNaX forming "palmitate-like species" is consistent with the previous study on the deoxygenation of methyl octanoate over CsNaX [6]. It is suggested that the methyl palmitate can strongly adsorbed on basic sites of CsNaX. Due to the highly polarizable nature of methyl palmitate, the interaction between carbonyl ester and the basic framework oxygen will readily weaken the carboxylate C–O bond, leading to the decomposition of the ester into two surface-aldehydes, as generally observed over typical basic catalysts. The decomposed methoxyl group will form the "formate-like species" (surface-formaldehyde) while the other fragment will form a "palmitate-like species" (surface-palmitaldehyde). This "formate-like species" will then decompose into carbon monoxide and hydrogen leading to the formation of the long chain hydrocarbon [6]. Further, disperse species ("palmitate-like species") decompose in parallel to two major hydrocarbon products, C_{15} alkene and C_{14} alkene.

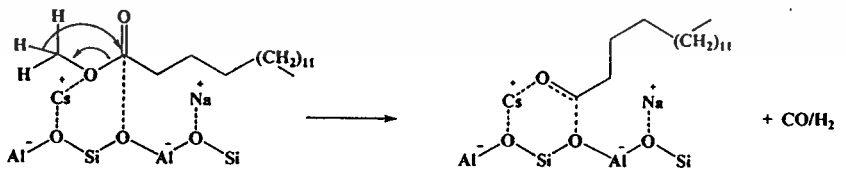

"palmitate-like species"

The β-hydrogen elimination [49] and subsequent decomposition of "palmitate-like species" would result in C_{15} alkene together with evolution of carbonmonoxide and hydrogen. This reaction may well be referred to as a reversible reaction of the typical hydroformylation [50]. Moreover, the C_{15} alkene could partially undergo hydrogen-transfer to form C_{15} alkane as shown;

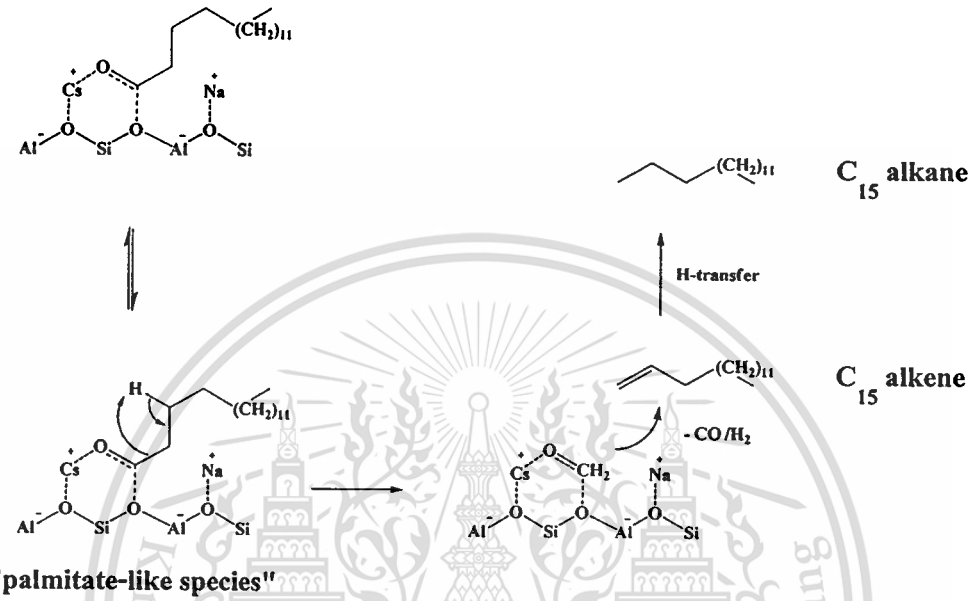

Alternatively, the cyclic-like intermediate can be formed and decomposed to more electrophilic acetaldehyde (enol-form) and C_{14} alkene, as shown below;

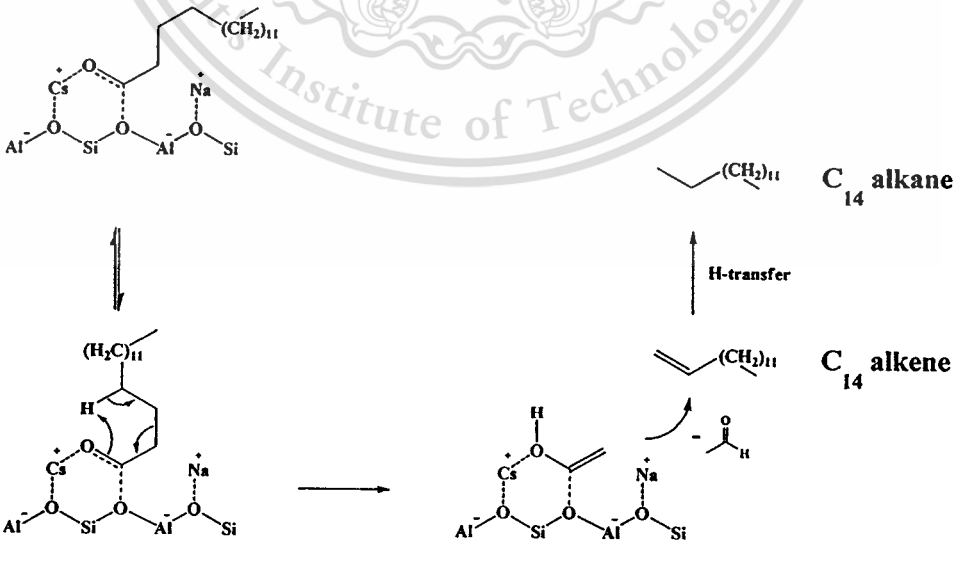

The acetaldehyde may be evolved as by-product or may undergo further aldol condensation/alkylation to form higher molecular weight oxygenates, as observed in small amounts. Again, hydrogen-transfer to C_{14} alkene could partially take place and C_{14} alkane could be obtained.

It is noted that small amount of C_{16} alkene is also obtained from the reaction. The formation of C_{16} alkene can be derived from hydrogen transfer over the cesium-exchanged zeolites [6]. As discussed above, due to the highly polarizable cesium cations, the basic sites can readily decompose methoxyl group, bearing virtual hydrogen pressure on the surface. Hence, the adsorbed "palmitate-like species" would act as hydrogen acceptor forming primarily C_{16} alcohol, which then rapidly undergo dehydration to form C_{16} alkene as shown;

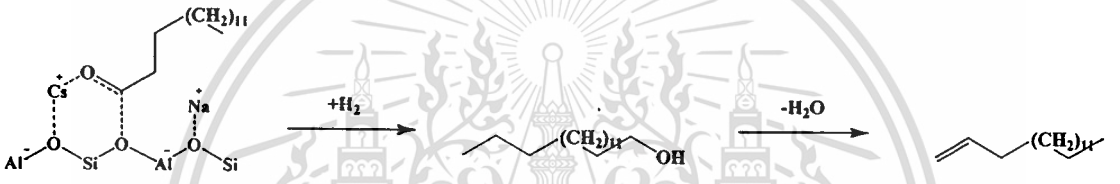

"palmitate-like species" **C_{16} Alkene**

From Figure 4.5, the C_9-C_{13} hydrocarbons are also observed. Such products are expected to be the secondary products from the cracking of C_{14}-C_{16} hydrocarbons. At high temperature, these products would be obtained from hydrogen-transfer from the hydrocarbon pools, presumably via radical intermediate that would further crack to smaller hydrocarbons. Generally, these cracked products can readily abstract hydrogen leading to the more saturated hydrocarbons. Hence, the unsaturated/saturated ratios of C_9-C_{13} hydrocarbons (the secondary products) are proportionally less than that of C_{14}-C_{16} primary products.

4.2.1 Study of space time over CsNaX

The product distribution obtained from the reaction over CsNaX at various space times (*W/F*) are shown in Figure 4.6.

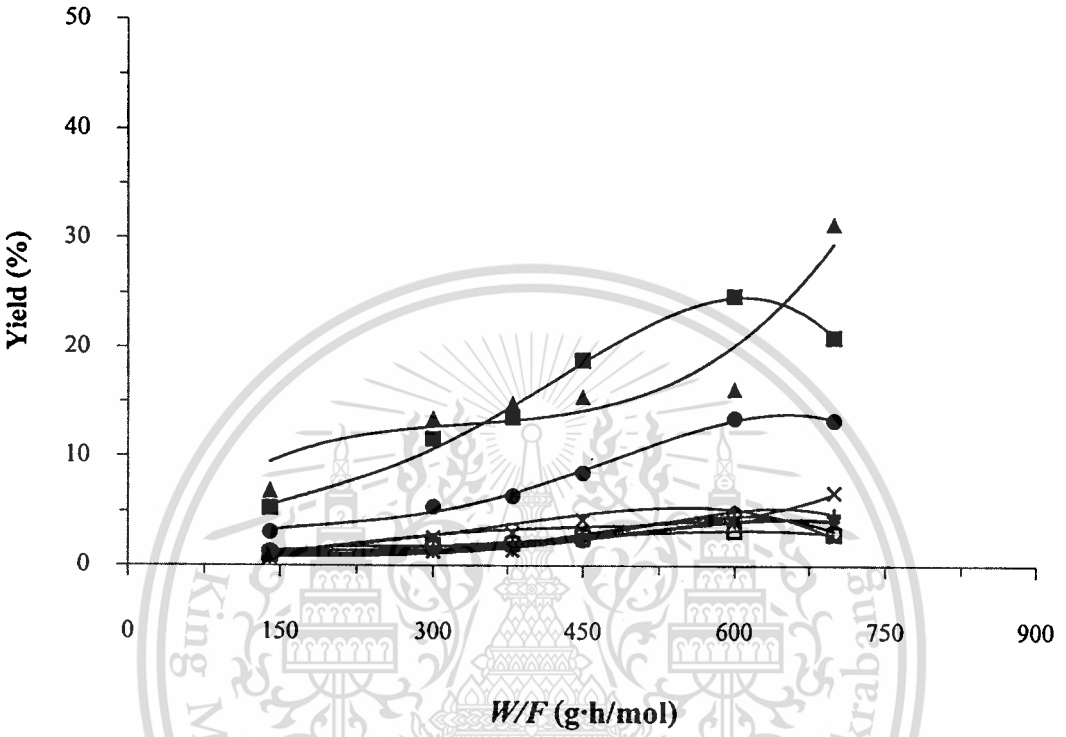

Figure 4.6 Yield of products from the reaction of 10 wt% palmitic acid, 45wt% methanol in THF over CsNaX as a function of space time (*W/F*).

Reaction conditions: 425 °C, 1 atm, 30 ml/min of Helium, C_{16} (○), C_{15} (■), C_{14} (●), C_{13} (x), C_{12} (*), C_{11} (♦), C_{10} (+), C_9 (□), Oxygenate (-), Gas product (▲).

From Figure 4.6, the conversion of methyl palmitate was increased with space time (*W/F*), as shown in Table 4.3. It is suggested that the activity toward the formation of products were functioned by the number of basic sites. Moreover, it was observed that C_{15} (>11.6% yield) and C_{14} (>5.4% yield) hydrocarbons were main product for all space times.

Table 4.3 Product distribution from reaction of palmitic acid with methanol in THF over CsNaX at various space times.

	W/F (g·h/mol)						
	140	300	380	450	600	700	
Conversion of methyl palmitate	19.9	44.1	50.9	64.5	88.0	93.5	
Liquid product yield (%)	15.2	30.7	36.1	49.0	71.8	62.2	
Product distribution							*Sat. : Unsat.*
C_{16}	1.4	1.7	2.2	2.4	4.8	3.1	*0 : 2.8*
C_{15}	6.1	11.6	13.6	18.8	24.7	20.9	*1 : 11.3*
C_{14}	2.4	5.4	6.4	8.5	13.5	13.3	*1 : 7.1*
C_{13}	1.2	2.6	3.0	4.2	4.1	6.7	*1 : 4.1*
C_{12}	0.7	1.3	1.4	2.4	4.0	4.0	*1 : 3.4*
C_{11}	0.7	1.5	1.6	2.6	4.1	4.1	*1 : 2.4*
C_{10}	0.6	1.8	2.0	2.7	5.0	4.7	*1 : 2.0*
C_9	0.7	1.9	2.0	2.7	3.2	2.9	*1 : 1.1*
Oxygenate	1.4	2.9	3.8	4.6	5.2	2.6	*0 : 3.8*
Gas product yield (%)	4.7	13.5	14.9	15.5	16.2	31.3	

Reaction conditions: 425 °C, 1 atm, 30 ml/min of Helium.

The increase in yield of liquid and gas products can be observed when increase in space time (*W/F* 140-600 g·h/mol). However, at very high space time (700 g·h/mol), the yield of liquid product was decreased, while the gas product was dramatically increased. It is clearly because the pool hydrocarbon can consecutively cracked to lighter hydrocarbons as the catalyst bed was increased. This leads to a lower yield of desirable liquid hydrocarbons (C_{14}-C_{15}).

4.2.2 Study on reaction temperature

It is known that the deoxygenation (decarbonylation/deacetalation) activity is thermodynamically favored at high reaction temperature. Accordingly, the increase in reaction temperature may highly affect the methyl palmitate conversion. The conversion of methyl palmitate at different reaction temperatures (400, 425, 450°C) were shown in Figure 4.7.

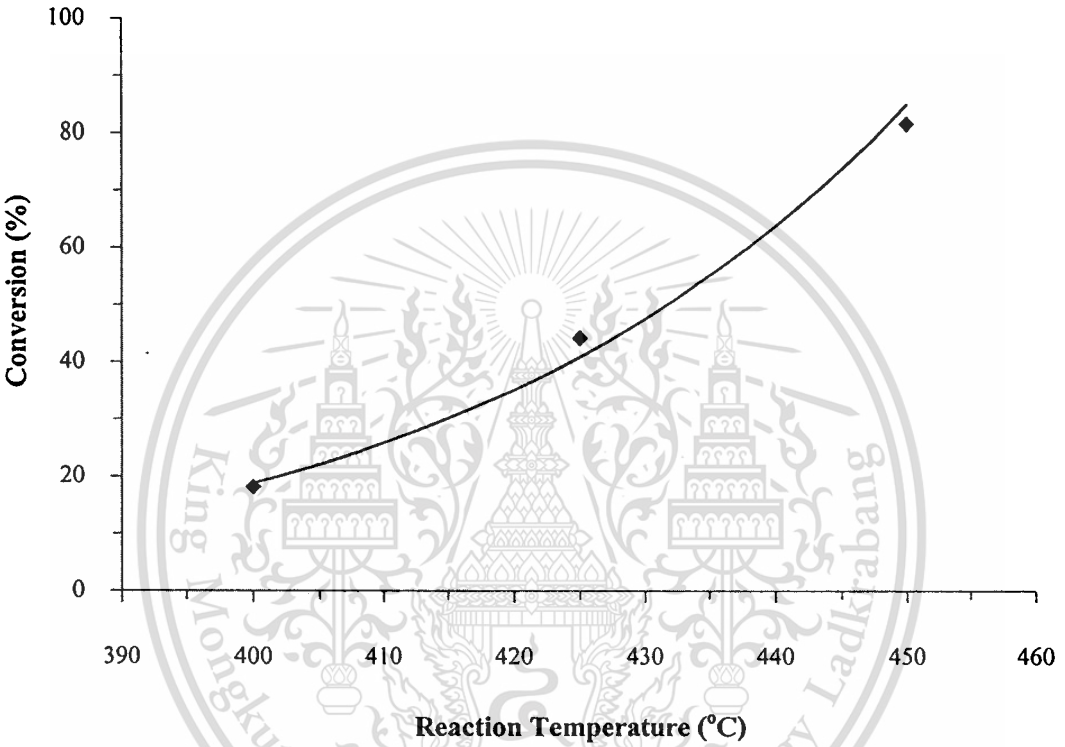

Figure 4.7 The effect of reaction temperature with conversion of methyl palmitate over CsNaX.

Reaction conditions: W/F 300 g·h/mol, 400-450 °C, 1 atm, 30 ml/min of Helium.

The result shows that the conversion of methyl palmitate increased with an increase in the reaction temperature. It is because the reactant molecules at a higher temperature have more thermal energy to react [51]. For this reason the reaction rate increases. The marked role of temperature suggests an endothermic nature of the decarbonylation and deacetalation reaction. Moreover, the result also shows that the yield of both main hydrocarbon products (C_{14} and C_{15} alkenes) and cracked products (C_9-C_{13} hydrocarbons) were increased with increasing the reaction temperature. This suggests that not only decarbonylation/deacetalation is promoted but also cracking activity is enhanced by increasing temperature.

Table 4.4 Product distribution from reaction of palmitic acid with methanol in THF over CsNaX at various reaction temperatures.

	Reaction temperature (°C)					
	400		425		450	
W/F (g·h/mol)	300		300		300	
Conversion of methyl palmitate	17.4		44.1		84.3	
Liquid products yield (%)	5.6		30.7		78.5	
Product distribution		*Sat. : Unsat.*		*Sat. : Unsat.*		*Sat. : Unsat.*
C16	0.2	*0 : 0.2*	1.7	*0 : 1.7*	4.1	*0 : 4.1*
C15	2.4	*1 : 10.2*	11.6	*1 : 11.0*	28.1	*1 : 13.2*
C14	0.9	*1 : 4.3*	5.4	*1 : 7.1*	13.1	*1 : 11.1*
C13	0.5	*1 : 3.4*	2.6	*1 : 4.1*	7.2	*1 : 4.4*
C12	0.2	*1 : 2.4*	1.3	*1 : 3.2*	4.6	*1 : 4.1*
C11	0.2	*1 : 1.4*	1.5	*1 : 2.1*	5.2	*1 : 2.4*
C10	0.2	*1 : 1.3*	1.8	*1 : 1.5*	5.5	*1 : 2.1*
C9	0.3	*1 : 1.1*	1.9	*1 : 1.2*	5.7	*1 : 2.0*
Oxygenate	0.7	*0 : 0.7*	2.9	*0 : 2.9*	5.0	*0 : 5.5*
Gas products yield (%)	11.8		13.5		5.8	

Reaction conditions: 400-450 °C, 1 atm, 30 ml/min of Helium.

In addition, the result shows that all ratios of saturated/unsaturated products are increase with reaction temperature. This also supports the hypothesis that both decarbonylation and deacetalation are endothermic reaction.

4.2.3 Study of feed ratio, methanol: palmitic acid

It is known that concentration plays a very important role in reactions, increasing the amount of one or more of the reactant concentrations may increase the reaction rate [51]. This work studies the conversion of methyl palmitate with different methanol concentration in the feed as shown in Figure 4.8

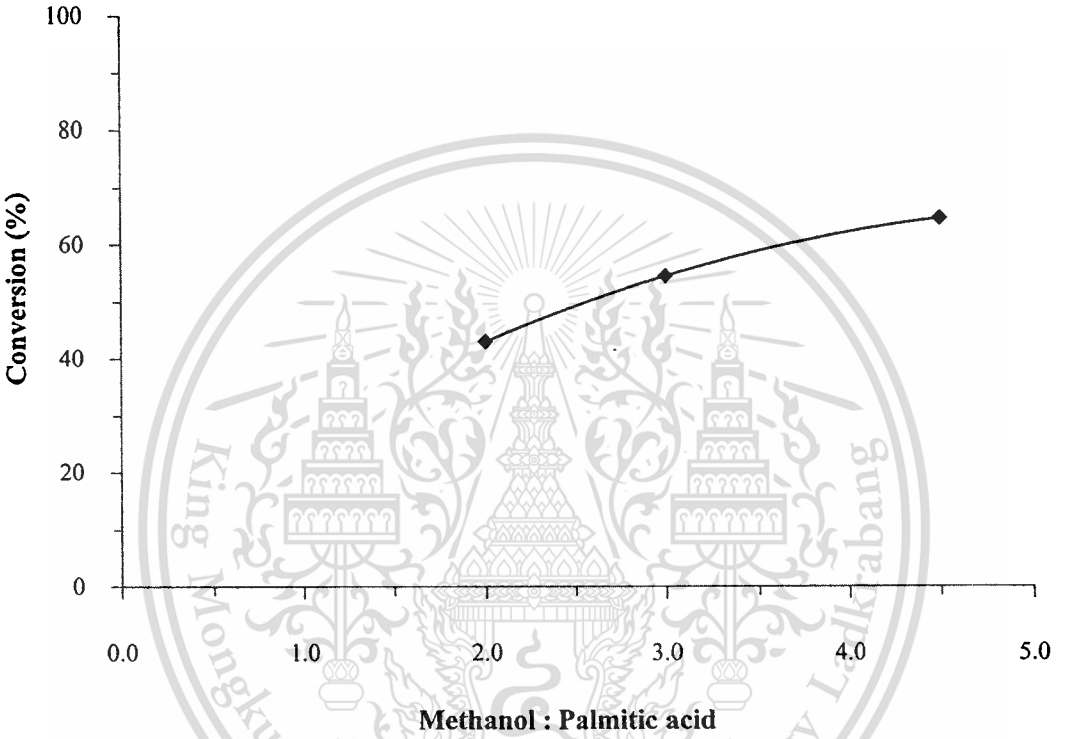

Figure 4.8 The effect of different feed weight ratios (methanol: palmitic acid) with methyl palmitate conversion over CsNaX.

Reaction conditions: W/F 450 g·h/mol, 425 °C, 1 atm, 30 ml/min of Helium.

The result shows that conversions of methyl palmitate were increased with increasing methanol concentration. It is because according to the collision theory of chemical reactions, molecules must collide in order to react together. Therefore, increasing the reactant concentrations it causes the collision of reactant molecules to happen more often, increasing the reaction rate. From Figure 4.9, it can be seen that a high activity was observed at the beginning of all reactions. However, for lower methanol concentration activity was rapidly decreased with time on stream. This is probably due to the catalyst deactivation from coke on surface. It is known that methanol is a high polar molecule; it can decompose to a surface CH_2O and hydrogen [43]. As a

result, adsorption of CH_2O and hydrogen inhibit the formation of high-molecular weight hydrocarbons (coke) on catalyst surfaces, resulting in better catalytic stability when higher methanol concentrations were used. This was confirmed by the DTG/TGA results of the used catalysts as shown in Figure 4.10. It can be seen that coke formation in used catalysts is decreased with increasing methanol concentration.

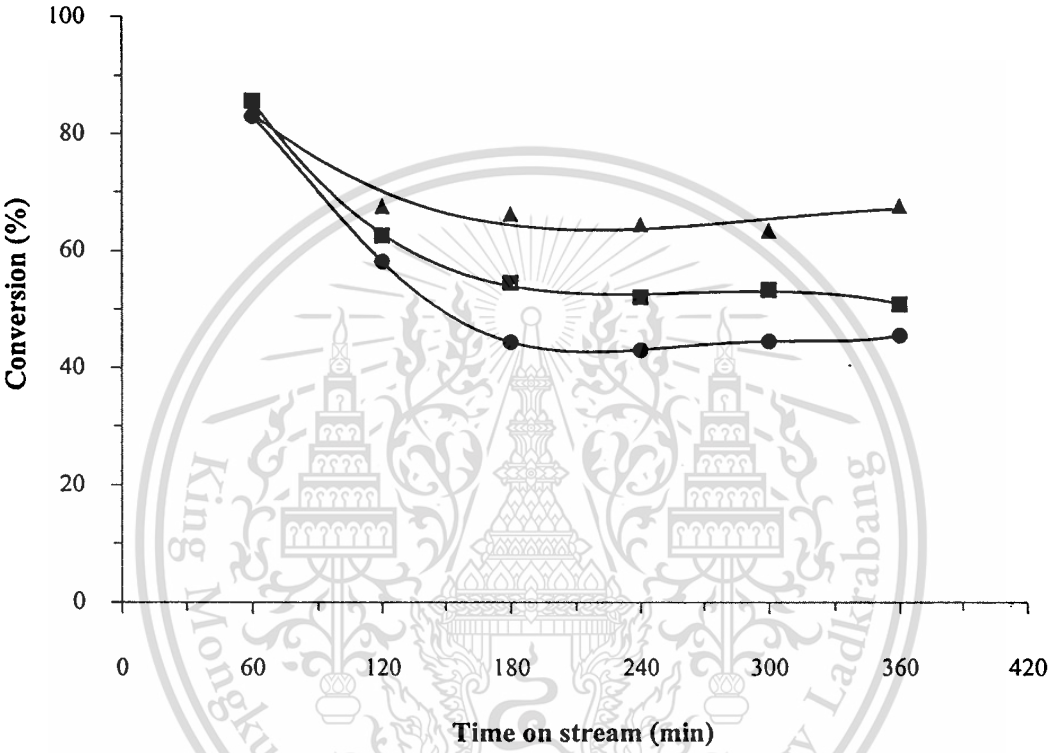

Figure 4.9 Conversion of methyl palmitate over CsNaX at various methanol: palmitic acid weight ratios.

Reaction conditions: W/F 450 g·h/mol, 425 °C, 1 atm, 30 ml/min of Helium, methanol: palmitic acid 4.5:1.0(▲), 3.0:1.0 (■), 2.0:1.0 (●).

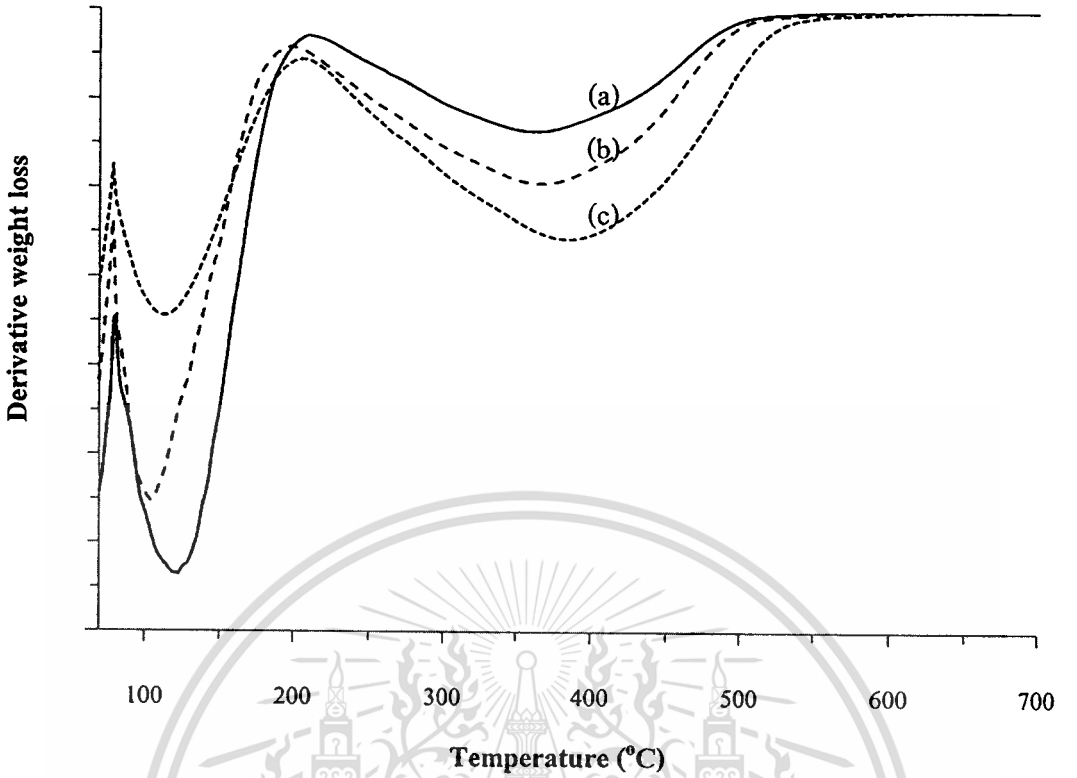

Figure 4.10 DTG/TGA of the used catalysts at various methanol: palmitic acid weight ratios; (a) 4.5:1.0, (b) 3.0:1.0, (c) 2.0:1.0.

From DTG/TGA (Figure 4.10), the decomposition of moisture in used catalyst starts from 80-200 °C and decomposition of coke takes place temperature at higher than 200 °C.

Table 4.5 Coke weight % in used catalysts at various methanol: palmitic acid weight ratios.

Methanol: Palmitic acid weight ratio	Coke (weight %)
4.5:1.0	5.9
3.0:1.0	8.4
2.0:1.0	11.1

The product distributions at different methanol: palmitic acid weight ratios were shown in Table 4.6. The result shows that all hydrocarbon products selectivity was not changed with methanol ratio. This result suggests that when methanol was in excess, it was not affected to product distributions but only acts as surface cleaner and also suppress pore blockage by high-molecular weight species.

Table 4.6 Product distribution from reaction of palmitic acid with methanol in THF over CsNaX at various methanol: palmitic acid weight ratios.

	Methanol: Palmitic acid weight ratio		
	2.0:1.0	3.0:1.0	4.5:1.0
W/F (g·h/mol)	450	450	450
Conversion of methyl palmitate	43.1	54.6	64.5
Selectivity (%)			
C16	3.3	4.0	3.7
C15	30.4	29.7	29.1
C14	12.1	12.5	13.2
C13	6.7	6.2	6.5
C12	3.3	4.2	3.7
C11	3.5	3.7	4.0
C10	3.9	3.8	4.2
C9	3.9	4.3	4.2
Oxygenate	7.2	6.8	7.1
Gas	25.7	24.7	24.2

Reaction conditions: 425 °C, 1 atm, 30 ml/min of Helium.

4.2.4 Study of effect of hydrogen as carrier gas

A major consideration in the production of hydrocarbon fuel from biomass is the consumption of hydrogen [52], which is typically needed in reactions involving deoxygenation steps. This study also investigated the impact of the presence of hydrogen on the overall activity and product distribution observed in the conversion of methyl palmitate over the CsNaX catalyst. Methyl palmitate conversion in the different atmospheres (helium vs hydrogen) are shown in Figure 4.11.

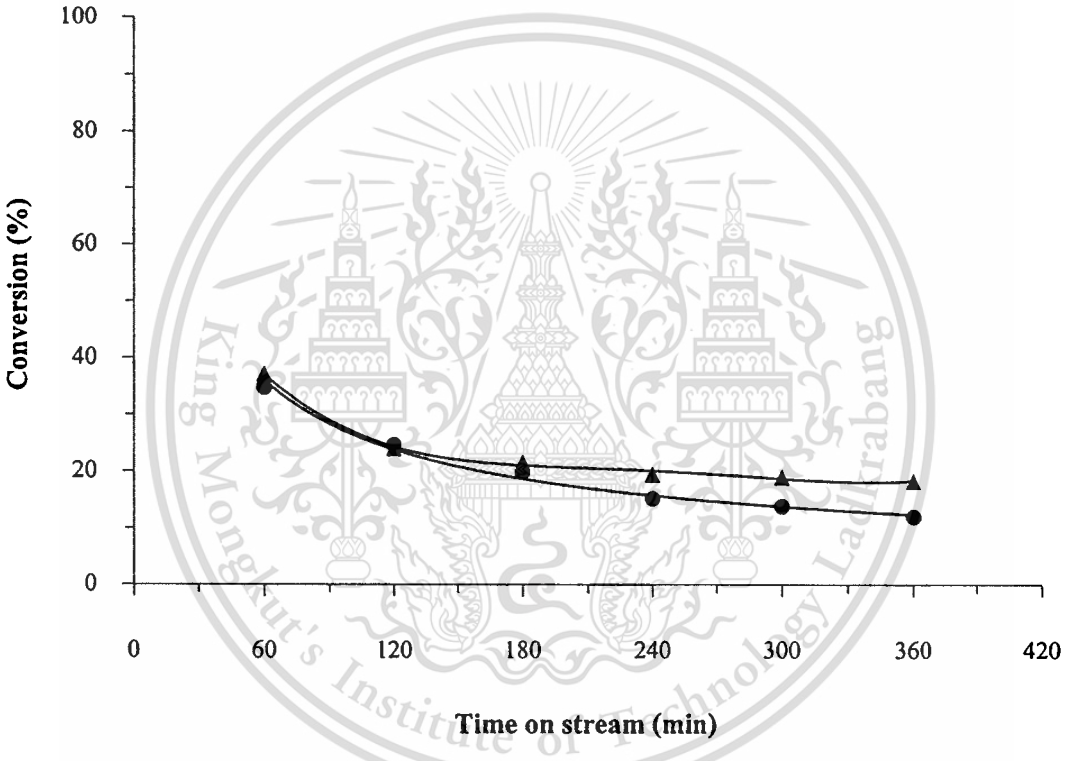

Figure 4.11 Conversion of methyl palmitate over CsNaX at the different carrier gas.

Reaction conditions: W/F 140 g·h/mol, 425 °C, 1 atm, 30 ml/min of Helium (●), Hydrogen (▲).

The result shows that the similar activity and product selectivity (Table 4.7) were observed at 425°C when comparing the reaction under hydrogen and under helium. A better stability was seen at reaction in hydrogen atmosphere. It is suggested that the presence of hydrogen can prevent catalyst deactivation from coking. The main deoxygenation products, C_{14} and C_{15} olefins, were dominant under both gases (He/H_2) indicating little effect of gas phase hydrogen in this reaction. It is also interesting to note that the C_{16} olefins (hydrogenolysis product) selectivity obtained under helium was higher than that under hydrogen. This is because hydrogenolysis reaction needs

hydrogen on the surface, not on the gas phase. Since, methanol can be decomposed to give *in-situ* hydrogen over catalyst active sites as previously discussed; the methanol decomposition activity will be favorable under helium atmosphere and result in an increase in surface hydrogen. While hydrogen in gas phase cannot dissociate over the catalyst surface or contribute hydrogenation activity. This result demonstrates that the deoxygenation over CsNaX does not require gas phase hydrogen when methanol is used as a co-reactant.

Table 4.7 Product distribution from reaction of palmitic acid with methanol in THF over CsNaX at various conditions.

	Carrier gas	
	Helium	Hydrogen
W/F (g·h/mol)	140	140
Conversion of methyl palmitate	19.9	21.6
Unsat./Sat. ratio	4.3	3.9
Selectivity (%)		
C16	6.9	3.7
C15	30.7	31.1
C14	12.2	14.3
C13	5.9	6.5
C12	3.5	3.4
C11	3.3	3.1
C10	3.1	3.6
C9	3.6	3.3
Oxygenate	7.1	6.8
Gas	23.7	24.2

Reaction conditions: 425 °C, 1 atm, 30 ml/min of carrier gas.

4.2.5 Study of effect Si/Al ratio over faujasite catalyst

It is well known that X and Y zeolites have the same framework type that is derived from "Faujasite" (FAU) zeolite structure but they have a different Si/Al ratio. The Y zeolite has Si/Al ratio higher than that of X zeolite. The effect of Si/Al ratio in theses catalysts were investigated for its activity. The result (Figure 4.12) shows that the conversion of methyl palmitate over CsNaX catalyst (Si/Al ~ 1) is similar to CsNaY (Si/Al ~ 2). Moreover, they have a same product distribution (Table 4.8). Although Si/Al ratio of the zeolites is different, the cesium contents in both catalysts are similar. It suggests that the number of cesium loading in catalysts plays more significant role on the conversion as compare to the Si/Al ratio.

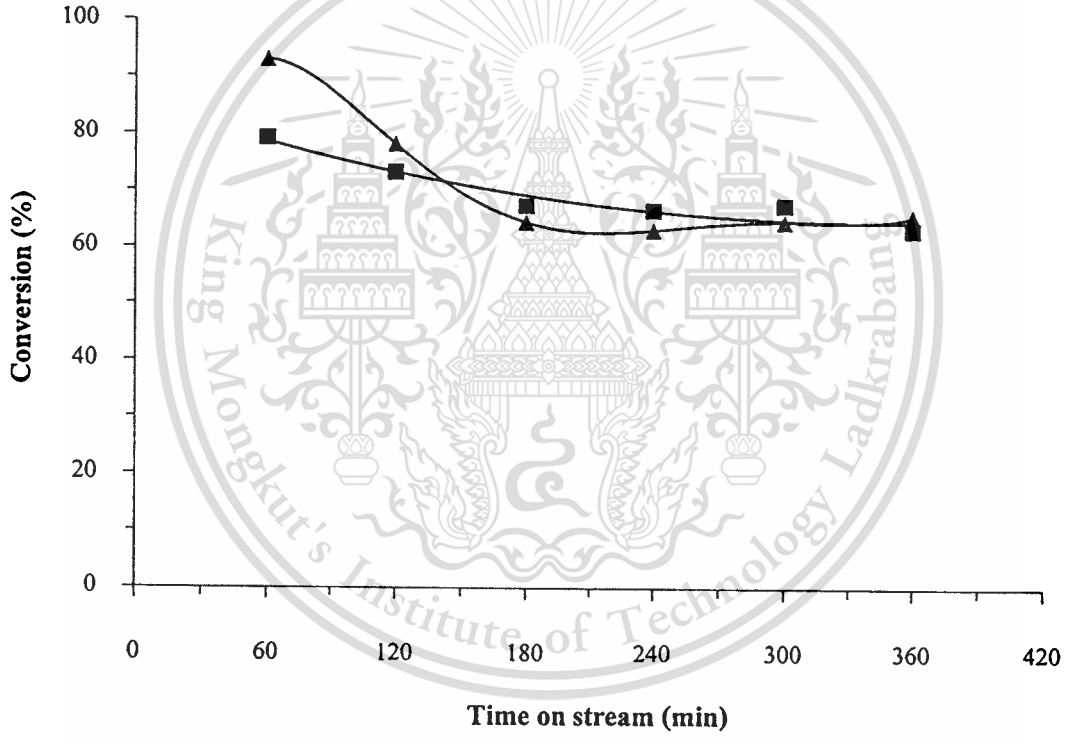

Figure 4.12 Conversion of methyl palmitate at the different catalyst.

Reaction conditions: W/F 450 g·h/mol, 425 °C, 1 atm, 30 ml/min of Helium, CsNaX (▲), CsNaY (■).

Table 4.8 Product distribution from reaction of palmitic acid with methanol in THF over CsNaX and CsNaY catalysts.

	Catalyst	
	CsNaX	CsNaY
Si/Al	1.3	2.7
Cs weight %	23.4	24.1
W/F (g·h/mol)	450	450
Conversion of methyl palmitate	64.5	66.2
Selectivity (%)		
C16	3.7	3.2
C15	29.1	28.2
C14	13.2	14.3
C13	6.5	6.1
C12	3.7	4.3
C11	4.0	3.6
C10	4.2	4.5
C9	4.2	3.9
Oxygenate	7.1	6.8
Gas	24.2	25.1

Reaction conditions: 425 °C, 1 atm, 30 ml/min of Helium.

4.2.6 Study of exchangeable cation in faujasite catalyst

The deoxygenation activity of palmitic acid over the Na-faujasite (NaX and NaY) was studied and compared to that over the Cs-faujasite (CsNaX and CsNaY) catalyst.

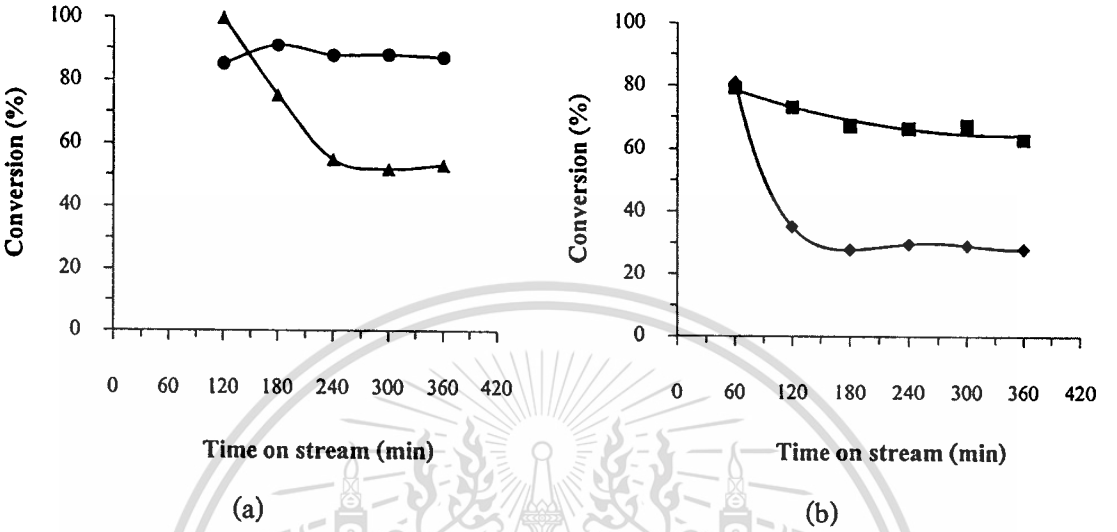

Figure 4.13 Conversion of methyl palmitate over (a) NaX compared to that on CsNaX, (b) NaY compared to that on CsNaY.

Reaction conditions: (a) W/F 600 g·h/mol, 425 °C, 1 atm, 30 ml/min of Helium. NaX (▲), CsNaX (●). (b) W/F 450 g·h/mol, 425 °C, 1 atm, 30 ml/min of Helium, NaY (♦), CsNaY (■).

At the beginning of the reaction (Figure 4.13), Na-faujasite (NaX and NaY) provides high conversion of palmitic acid and gas hydrocarbons are the dominant products. These gas products may be formed by typical acids catalysis (cracking). The results suggest that Na-faujasite zeolite contains some acidity [53]. This is because sodium cation is much harder than the cesium cation. It holds tightly the negative framework charge, providing weaker Lewis basicity for the oxygen bridges. Hence, the presence of sodium as exchangeable cation leads to an increase in weak Lewis acid sites in the catalyst. As this result, the reactions give a high initial conversion over this catalyst. However, a dramatic decrease in conversion of Na-faujasite is observed at 1-3 hours on stream, as compared to Cs-faujasite (CsNaX and CsNaY). This is probably due to coke formation catalyzed by such acid sites in both NaX and NaY. Conversion of palmitic acid over Na-faujasite is remained the same after 4 hours on stream. This suggests that there are available basic site in NaX and NaY. As the acid sites become deactivated, deoxygenation activity over basic site can still proceed and deactivates at a relatively lower rate (4-6 hours on stream). In this period, the

small hydrocarbons were declined, while C_{15} was obtained as main product in a manner similar to Cs-faujasite as shown in Table 4.9;

Table 4.9 Product distribution from reaction of palmitic acid with methanol in THF over NaX, NaY, CsNaX and CsNaY.

	Catalyst			
	NaX	CsNaX	NaY	CsNaY
W/F (g·h/mol)	600	600	450	450
Conversion of methyl palmitate	53.3	88.0	26.6	66.2
Liquid products yield (%)	21.5	66.6	14.3	49.6
Product distribution				
C16	0.8	4.8	0.5	2.2
C15	5.0	24.7	6.8	18.7
C14	2.1	13.5	2.1	9.4
C13	1.4	4.1	1.3	4.1
C12	1.4	4.0	0.8	2.8
C11	1.7	4.1	0.8	2.4
C10	2.3	5.0	0.8	2.9
C9	3.5	3.2	0.5	2.6
Oxygenate	3.3	5.2	0.7	4.5
Gas products yield (%)	32.6	16.2	12.3	16.6

Reaction conditions: 425 °C, 1 atm, 30 ml/min of Helium.

Table 4.9 shows the product distribution obtained over Na-faujasite, operating in the same conditions as Cs-faujasite after 4 hours on stream. It shows that the higher yield of gas products obtained from Na-faujasite was observed, as compared to Cs-faujasite, while the yield of liquid products were decrease, especially the products from decarbonylation (C_{15}). Gas products are believed to derive mainly from cracking of liquid products from palmitic acid over available acid sites as discussed above. The suggestion that the alkali-exchanged zeolites contain both acid and basic functions is in agreement with earlier studies [53].

CHAPTER 5

CONCLUSION AND SUGGESTION

5.1 Conclusion

The cesium faujasite catalysts have shown high activity towards reactions involving deoxygenates, as well as decarbonylation and deacetalation of palmitic acid to produce the long chain hydrocarbons in inert atmosphere. This can be achieved by converting palmitic acid to methyl palmitate via *in-situ* esterification with methanol over basic site and subsequent removal of carboxyl group via carbon monoxide and hydrogen evolution.

The products distribution from reaction show that linear long chain α-olefins C_{15} (>11.6% yield) and C_{14} (>5.4% yield) were major products and small amount of linear hydrocarbons C_9 – C_{16} were also obtained. The increase in yield of products were observed when space time was increased (300-600 g·h/mol). Except at very high space time 700 g·h/mol, the yield of liquid product was decreased because they tend to crack to lighter hydrocarbons.

The catalytic stability is a direct effect of the zeolite basicity that derived mainly from the cesium content in the zeolites. Hence, when the cesium is not present in catalyst (Na-Faujasite), rapid deactivation is obtained. Furthermore, the cesium content in the zeolite has affected to the product distribution as well as the zeolite Si/Al ratio. Moreover, the increase in catalyst basicity has also enhanced major product selectivity.

The study on reaction temperature shows an endothermic nature of both decarbonylation and deacetalation reactions which can be promoted at high temperature. The effect of methanol concentration in reactant shows that when methanol was in excess, it not affected to product distributions but only acts as surface cleaner and also suppress pore blockage by high-molecular weight species. This is because methanol can decompose to give *in-situ* hydrogen over catalyst active sites. For this reason, the deoxygenation over a cesium faujasite catalyst does not require gas phase hydrogen when methanol is used as a co-reactant. The presence of hydrogen only helps to prevent catalyst deactivation.

5.2 Suggestion for future studies

5.2.1 The linear long chain α-olefins products from deoxygenation of palmitic acid with methanol over cesium faujasite are economically valuable and widely used chemical intermediates in the production of other chemicals (including, but not limited to, polymers, plasticizer alcohols, surfactants, wax applications, and additives.). Moreover, they are low in acute toxicity and environmental effects. Thus, in future study, these products should be separated from reactant, solvent and oxygenated products.

5.2.2 It was found from the present study that cesium faujasite catalyst shows high activity to deoxygenation of *in-situ* methyl palmitate which converted from palmitic acid. Thus, in future study, this catalyst should be also tested for others fatty acid or applied to use FAME (Biodiesel) as direct reactant.

5.2.3 The basicity of catalysts is varied with the size of alkali exchangeable cations and also with degree of ion exchange. Thus, the further study should investigate the effect of both other alkali cation sizes (such as potassium) and degrees of ion exchange.

5.2.4 The coke formation has more effect to catalyst stability. Thus, the reused or regenerated catalysts are interesting to study in the next work.

REFERENCES

[1] George W.H., Iborra S. and Corma A. "Synthesis of Transportation Fuels from Biomass: Chemistry, Catalysts, and Engineering." **Chemical Reviews.**, vol. 106, no. 9, 2006. pp. 4044-4098.

[2] Goyal H.B., Seal D. and Saxena R.C. "Bio-fuels from thermochemical conversion of renewable resources: A review." **Renewable and Sustainable Energy Reviews.**, vol. 12, Issue 2, Feb. 2008. pp. 504-517.

[3] Ooi Y.S., Zakaria R., Mohamed A.R. and Bhatia S. "Catalytic Conversion of Fatty Acids Mixture to Liquid Fuel and Chemicals over Composite Microporous/Mesoporous Catalysts." **Energy & Fuels.**, vol 19, no. 3, 2005. pp. 736-743.

[4] Maki-Arvela P., Kubickova I., Snare M., Eranen K. and Murzin D.Y. "Catalytic Deoxygenation of Fatty Acids and Their Derivatives." **Energy & Fuels.**, vol. 21, no. 1, 2007. pp. 30-41.

[5] Maki-Arvela P., Kubickova I., Snare M., Eranen K. and Murzin D.Y. "Catalytic deoxygenation of unsaturated renewable feedstocks for production of diesel fuel hydrocarbons." **Fuel.**, vol. 87, Issue 6, May 2008. pp. 933-945.

[6] Sooknoi T., Danuthai T., Lobban L.L., Mallinson R.G. and Resasco D.E. "Deoxygenation of methylesters over CsNaX." **Journal of Catalysis.**, vol. 258, Issue 1, Aug. 2008. pp. 199-209.

[7] Maria A. P., Sooknoi T., Danuthai T. and Resasco D. E. "Deoxygenation of benzaldehyde over CsNaX zeolites." **Journal of Molecular Catalysis A: Chemical.**, vol. 312, Issues 1-2, Oct. 2009. pp. 78-86.

[8] Rohm and Haas Company. **"Esterification of fatty acids."** [Online]. Available : http://www.amberlyst.com/fatty_acids.htm. 2009.

[9] Jerry L. Sarquis. **"Fats and Fatty Acids."** [Online]. Available : http://www.chemistryexplained.com/Di-Fa/Fats-and-Fatty-Acids.html. 2010

[10] Beare-Rogers J., Dieffenbacher A. and Holm J. V. "Lexicon of lipid nutrition (IUPAC Technical Report)." **Pure Appl. Chem.**, vol. 73, no. 4, 2001. pp. 685-744.

[11] Frémy E. "Memoire sur les produits de la saponification de l'huile de palme." **Journal de Pharmacie et de Chimie XII.**, 1842. pp. 757.

[12] Ang, Catharina Y. W., KeShun Liu, and Yao-Wen Huang. **Asian Foods.** 1999.

[13] Liu Y., Lotero E. and Goodwin Jr. J.G. "Effect of carbon chain length on esterification of carboxylic acids with methanol using acid catalysis." **J. Catal.**, vol. 243, 2006. pp. 221-228.

[14] Yadav G.D. and Thathagar M.B. "Esterification of maleic acid with ethanol over cation exchange resin catalysts." **React. Funct. Polym., vol. 52,** 2002. pp. 99-110.

[15] Marchetti J.M., Miguel V.U. and Errazu A.F. "Heterogeneous esterification of oil with high amount of free fatty acids." **Fuel.**, vol. 86, 2007. pp. 906-910.

[16] Marchetti J.M. and Errazu A.F. "Esterification of free fatty acids using sulfuric acid as catalyst in the presence of triglycerides." **Biomass Bioenerg.**, vol. 32, 2008. pp. 892-895.

[17] Mbaraka I.K., Radu D.R., Lin V.S.-Y. and Shanks B.H. "Organosulfonic acid-functionalized mesoporous silicas for the esterification of fatty acid." **J. Catal.**, vol. 219, 2003. pp. 329-336.

[18] Maki-Arvela P., Kubickova I., Snare M., Eranen K. and Murzin D.Y. "Production of diesel fuel from renewable feeds: Kinetics of ethyl stearate decarboxylation." **Chemical Engineering Journal**, vol. 134, Issues 1-3, Nov. 2007. pp. 29-34.

[19] Dyer A. **An introduction to Zeolite Molecular Sieves.** UK : John Wiley & Sons. 1988

[20] Wolfwiki. 2009. **"Zeolites."** [Online]. Available : http://wikis.lib.ncsu.edu/index.php/Zeolites.

[21] Gates B.C. **Catalytic Chemistry.** Canada : John Wiley & Sons. 1992

[22] Tchobanoglous G. and Burton F. **Wastewater engineering : Treatment, Disposal and Resue.** New York : Mcgraw-Hill, Inc. 1991

[23] Wagner C., Riggs W., Davis L., Moulder J. and Muilenberg G. **Handbook of X-Ray Photoelectron Spectroscopy**. Minnesota : Perkin-Elmer Corporation. 1979

[24] Huang M., Kaliaguine S. and Auroux A. "Stud." **Surf. Sci. Catal.**, vol. 97, 1995. pp. 311-318.

[25] Sheldon R. A., Bekkum H. **Fine chemicals through Heterogeneous Catalysis.** Germany : Wiley-VCH. 2001

[26] George Lappin (ed.) (1989). **"Alpha Olefins Applications Handbook"** [Online]. Available : http://en.wikipedia.org/wiki/Linear_alpha_olefin

[27] Ineosoligomers "**Polyalpha Olefin (PAO)**" [Online].
Available : http://www.ineosoligomers.com/126-Products.htm

[28] Chevron Phillips Chemical Company. "**Normal Alpha Olefins**" [Online].
Available : http://www.cpchem.com/enu/nao_a_applications.asp

[29] Sadrameli S.M. and Alex E.S. Green. "Systematics of renewable olefins from thermal cracking of canola oil" **J. Anal. Appl. Pyrolysis.**, vol.78, 2007. pp. 445–451.

[30] Suppes G.J., Dasari M.A., Doskocil E.J., Mankidy P. J. and Goff M. J. "Transesterification of soybean oil with zeolite and metal catalysts." **Applied Catalysis A: General.**, vol. 257, 2004. pp. 213-223.

[31] Xie W., Huang X. and Li H. "Soybean oil methyl esters preparation using NaX zeolites loaded with KOH as a heterogeneous catalyst." **Bioresource Technology.**, vol. 98, 2007. pp. 936-939.

[32] Dora E. López, James G. Goodwin Jr., David A. Bruce and Edgar Lotero. "Transesterification of triacetin with methanol on solid acid and base catalysts." **Applied Catalysis A: General.**, vol. 295, 2005. pp. 97-105.

[33] Fangrui M., Milford A. Hanna. **Biodiesel production: a review Bioresource Technology**, vol. 70, 1999. pp. 1-15.

[34] Hak-Ju K., Bo-Seung K., Min-Ju K., Deog-Keun K., Jin-Suck L. and Kwan-Young L. "Development of heterogeneous catalyst system for esterification of free fatty acid contained in used vegetable oil." **Studies in Surface Science and Catalysis.**, vol. 153, 2004. pp. 201-204.

[35] Knothe G., Andrew C. Matheaus and Thomas W. Ryan III. "Cetane numbers of branched and straight-chain fatty esters determined in an ignition quality tester." **Fuel.**, vol. 82, 2003. pp. 971-975.

[36] Gerhard Knothe. "Dependence of biodiesel fuel properties on the structure of fatty acid alkyl esters." **Fuel Processing Technology.**, vol. 86, 2005. pp. 1059-1070.

[37] Gerhard Knothe. "Some aspects of biodiesel oxidative stability." **Fuel Processing Technology.**, vol. 88, 2007. pp. 669-677.

[38] Knothe G. and Kevin R. S. "Kinematic viscosity of biodiesel fuel components and related compounds. Influence of compound structure and comparison to petrodiesel fuel components." **Fuel.**, vol. 84, 2005. pp. 1059-1065.

[39] Knothe G. and Kevin R. S. "Kinematic viscosity of biodiesel components (fatty acid alkyl esters) and related compounds at low temperatures." **Fuel.**, vol. 86, 2007. pp. 2560-2567.

[40] Brands D.S., U-A-Sai G., Poels E.K. and Bliek A. "Sulfur Deactivation of Fatty Ester Hydrogenolysis Catalysts." **Journal of Catalysis.**, vol. 186, 1999. pp. 169-180.

[41] Brands D.S., U-A-Sai G., Poels E.K. and Bliek A. "Ester hydrogenolysis over promoted Cu/SiO2 catalysts." **Applied Catalysis A: General.**, vol. 184, 1999, pp. 279-289.

[42] Kubiková I., Mathias S., Kari E., Mäki-Arvela P. and Murzin D. Y. "Hydrocarbons for diesel fuel via decarboxylation of vegetable oils." **Catalysis Today.**, vol. 106, 2005. pp. 197-200.

[43] Sooknoi T. and Dwyer J. "Role of substrate's electrophilicity in base catalysis by zeolites: alkylation of acetonitrile with methanol." **Journal of Molecular Catalysis A: Chemical.**, vol. 211, 2004. pp. 155-164.

[44] Concepción-Heydorn P., Jia C., Herein D., Pfänder N., Karge H. G. and Jentoft F. C. "Structural and catalytic properties of sodium and cesium exchanged X and Y zeolites, and germanium-substituted X zeolite." **Journal of Molecular CatalysisA:Chemical.**, vol. 162, 2000. pp. 227-246.

[45] Occelli M. L. and Ritz P. "The effects of Na ions on the properties of calcined rare-earths Y (CREY) zeolites." **Applied Catalysis A: General.**, vol. 183, 1999. pp. 53-59.

[46] Xie J., Minming, Huang S. and Kaliaguine S. "Characterization of basicity in alkali cation exchanged Faujasite zeolites: an XPS study using chloroform as a probe molecule." **Applied Surface Science.**, vol. 115, 1997. pp. 157-165.

[47] Eric J., Doskocil A. and Davis R.J. "Spectroscopic Characterization and Catalytic Activity of Zeolite X Containing Occluded Alkali Species." **Journal of Catalysis.**, vol. 188, 1999. pp. 353-364.

[48] Laspéras M., Cambon H., Brunel D., Rodriguez I. and Geneste P. "Characterization of basicity in alkaline cesium-exchanged X zeolites post-synthetically modified by impregnation: A TPD study using carbon dioxide as a probe molecule." **Microporous Materials.**, vol. 1, 1993. pp. 343-351.

[49] Concepcio´n-Heydorn P., Jia C., Herein D., Pfa¨nder N., Karge H.G., Jentoft F.C. "Structural and catalytic properties of sodium and cesium exchanged X and Y zeolites, and germanium-substituted X zeolite." **Journal of Molecular Catalysis A: Chemical.**, vol. 162, 2000. pp. 227–246.

[50] Occellia M.L. and Ritzb P. "The effects of Na ions on the properties of calcined rare-earths Y (CREY) zeolites." **Applied Catalysis A: General.**, vol. 183, 1999. pp. 53-59.

[51] Wikipedia. **"Chemical kinetics"** [Online]. Available : http://en.wikipedia.org/wiki/Chemical_kinetics

[52] George W. H. and Corma A. "Synergies between Bio- and Oil Refineries for the Production of Fuels from Biomass." **Angew. Chem. Int. Ed.**, vol. 46, 2007. pp. 7184 – 7201.

[53] Forster H., Fuess H., Geidel E., Hunger B., Jobic H., Kirschhock C., Klepelc O. and Krausea K. "Adsorption of pyrrole derivatives in alkali metal cation-exchanged faujasites : comparative studies by surface vibrational techniques, X-ray diraction and temperature-programmed desorption augmented with theoretical studies." **Phys. Chem. Chem. Phys.**, vol. 1, 1999. pp. 593-603.

APPENDICES

APPENDIX A

CALCULATION

Example 1: Calculations of catalytic parameters

W/F, conversion, yield and selectivity

Example 2: Calculations of chemical composition

Si/Al ratio

Degree of ion exchange

Unit cell composition

Total cesium cations and excess cesium cation per unit cell

Calculations of catalytic parameters

W/F

$$W/F = \frac{\text{Weight of catalyst (g)}}{\text{Mole of reactant feed (mol/h)}}$$

In the reaction using 0.0003 mol/h of palmitic acid in feed and using 0.1805 grams of catalyst, the W/F is calculated as follow:

$$W/F = [0.1805\ (g)/0.0003(mol/h)]$$

$$= 600\ g \cdot h/mol$$

In a similar manner; W/F of catalysts with different catalyst weight and different feed rate are calculated.

Calculation of % yield from gas chromatography

From the chromatogram, the peaks of hydrocarbon samples were identified using of reference standard for comparison. The peak area of hydrocarbon (or oxygenated compounds) which possesses the equal number of carbon was summarized. The summation of the peak area obtained from chromatogram of a mixture hydrocarbon product is shown in Table A1.

Table A1 The summation of the peak area for hydrocarbon products.

Number of carbon	Peak area	Corrected peak area
C_9	2,453,160	272,573
C_{10}	1,640,424	164,042
C_{11}	1,237,542	112,504
C_{12}	1,053,018	87,752
C_{13}	1,548,791	119,138
C_{14}	2,903,115	207,365
C_{15}	5,797,196	386,480
C_{16}	1,235,026	77,189
Methyl palmitate	17,769,500	1,269,250
Total	35,637,772	2,696,293

$$\text{Corrected peak area in each product} = \frac{\text{Peak area of } C_n}{RF}$$

Where RF is the response factor of the analyzed sample (Carbon number).

For example;

$$\text{Corrected peak area of } C_9 = \frac{2,453,160}{9}$$

$$= 272,573$$

In the normalization method, the areas of all eluted peak were compute after correcting these areas for differences in the detector response to different compound types. After correcting areas, the concentration of the analyzed was found from the ratio of its area to the total area of all peaks.

Calculate the percent yield of each component in sample as follows:

$$\%\text{Yield in each product} = \frac{\text{Corrected peak area of } C_n \times 100}{\text{Total corrected area}}$$

For example;

$$\%\text{Yield of } C_9 = \frac{272,573 \times 100}{2,696,293}$$

$$= 10.1$$

The percent carbon yield of each sample which is obtained from above calculation is shown in Table A2.

Table A2 % Carbon yield derived by normalization method.

Number of carbon	%Yield of sample
C_9	10.1
C_{10}	6.1
C_{11}	4.2
C_{12}	3.3
C_{13}	4.4
C_{14}	7.7
C_{15}	14.3
C_{16}	2.9
Methyl palmitate	47.1
Total	100.0

Conversion

%Conversion can be calculated from the following equation.

$$\%\text{Conversion} = 100 - \%\text{Yield of methyl palmitate left in product}$$

For example;

$$\%\text{Conversion} = 100 - 47.1$$

$$= 52.9$$

Selectivity

%Selectivity can be obtained from the following equation.

$$\%\text{Selectivity in each product} = \frac{\%\text{ Yield in each product x 100}}{\%\text{ Conversion}}$$

For example;

$$\%\text{Selectivity of } C_9 = \frac{10.1 \times 100}{52.9}$$

$$= 19.1$$

Calculations of chemical composition

Table A3 Data from XRF, calculations of chemical composition of all catalysts.

	Weight % (%)				
	O	Na	Al	Si	Cs
CsNaX	58.82	1.83	5.05	6.95	24.77
NaX	71.46	12.74	6.80	8.81	-
CsNaY	58.47	2.93	3.91	11.27	23.39
NaY	72.09	9.41	4.65	13.74	-

For example; CsNaX

Molar Composition

Mole of silicon = W_{Si} / MW_{Si}

= 6.95 / 28

= 0.25

Mole of aluminium = W_{Al} / MW_{Al}

= 5.05 / 27

= 0.19

Mole of cesium = W_{Cs} / MW_{Cs}

= 24.77 / 133

= 0.19

Mole of sodium = W_{Na} / MW_{Na}

= 1.83 / 23

= 0.08

Si/Al ratio

Si/Al ratio = (mole of Si / mole of Al)

= 0.25/0.19

= 1.31

Degree of ion exchange

$$\text{Degree of ion exchange} = \frac{(\text{mole of Al} - \text{mole of Na}) \times 100}{\text{mole of Al}}$$

$$= \frac{(0.19 - 0.08) \times 100}{0.19}$$

$$= 57.89\%$$

Unit cell composition

$$\text{Unit cell composition} = T_{192}O_{384}$$

$$T = Al + Si$$

$$192 = Al + (Si/Al \times Al)$$

$$192 = Al + (1.31Al)$$

$$= 2.31Al$$

$$\therefore \textit{Aluminium atom per unit cell} = 192/2.31$$

$$= 83$$

$$\therefore \textit{Silicon atom per unit cell} = T - Al$$

$$= 192 - 83$$

$$= 109$$

$$\textit{Sodium atom per unit cell} = \frac{\text{Atom of Al} \times (100\text{-degree of ion exchange})}{100}$$

$$= \frac{83 \times (100-57.89)}{100}$$

$$\therefore \textit{Sodium atom per unit cell} = 35$$

$$\text{Exchangeable cesium atom/unit cell} = \text{Al atom per unit cell} - \text{Na atom per unit cell}$$

$$= 83 - 35$$

$$\therefore \textit{Cesium atom per unit cell} = 48$$

Unit cell composition of CsNaX can be expressed as; $Na_{35}Cs_{48}(Al_{83}Si_{109}O_{384})$

Total cesium cations and excess cesium cation per unit cell

$$\text{Total cesium per unit cell} = \frac{\text{Al per unit cell x mole of Cs}}{\text{mole of Al}}$$

$$= \frac{83 \times 0.19}{0.19}$$

$$= 83$$

$$\text{Excess cesium per unit cell} = \text{total Cs per unit cell} - \text{exchangeable Cs per unit cell}$$

$$= 83 - 48$$

$$= 35$$

APPENDIX B

LANGMUIR ADSORPTION ISOTHERM

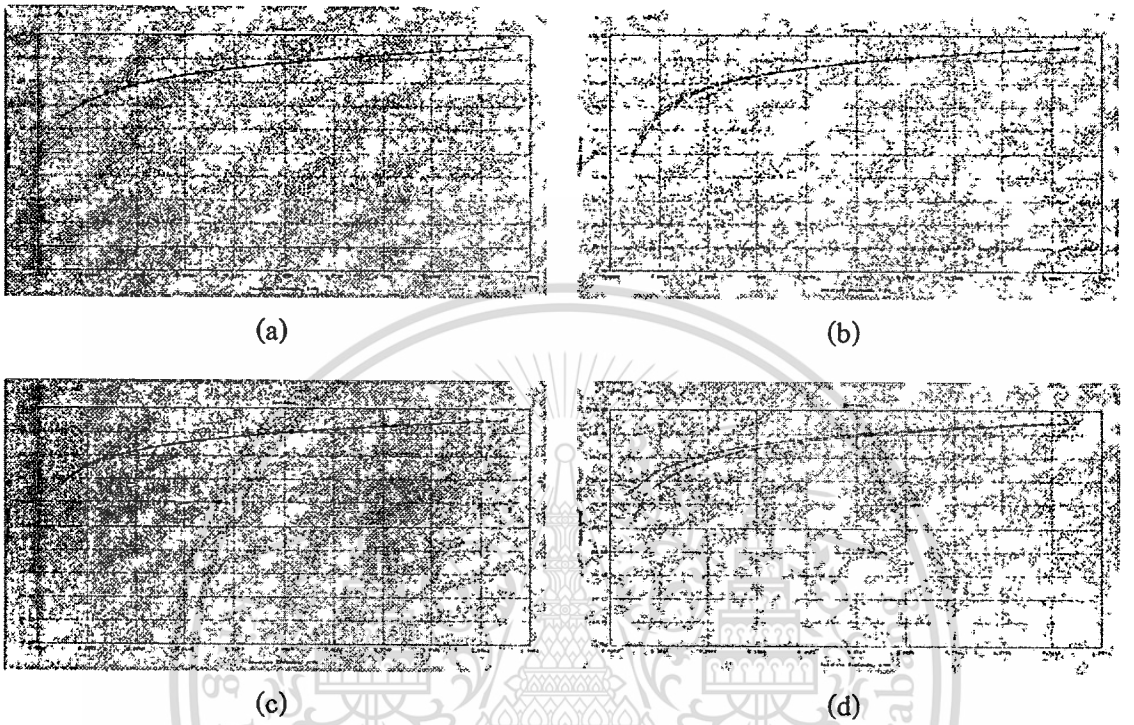

Figure B1 Adsorption-Desorption isotherm of (a) CsNaX, (b) NaX, (c) CsNaY, (d) NaY.

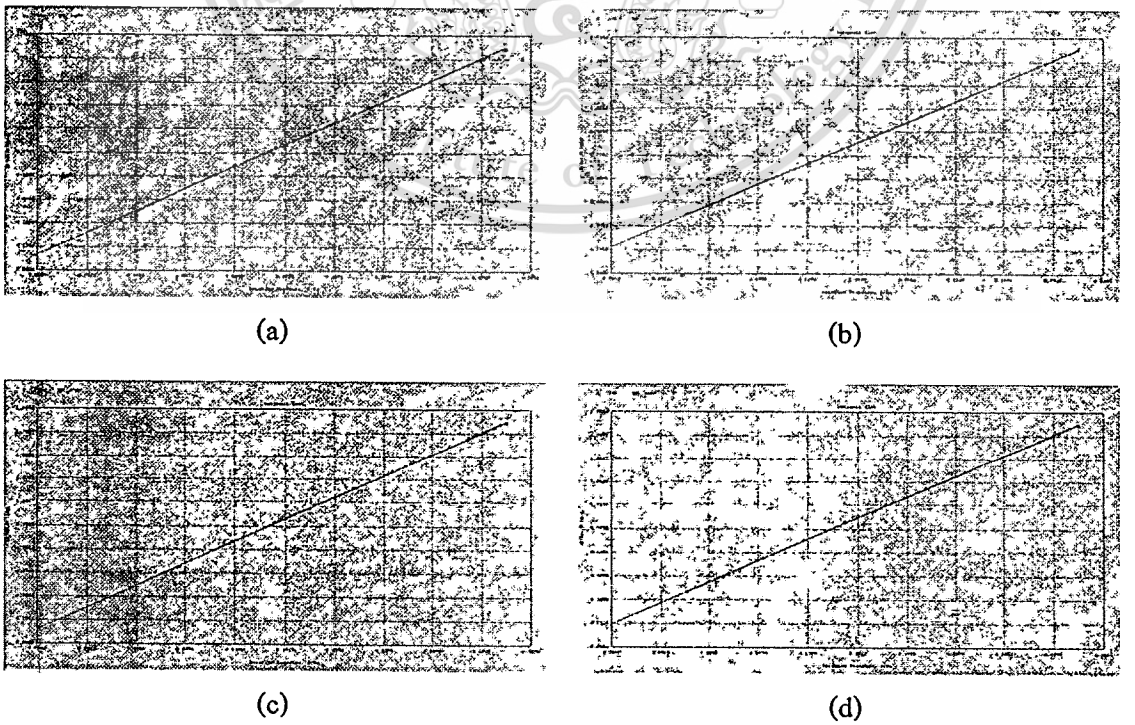

Figure B2 Langmuir isotherm of (a) CsNaX, (b) NaX, (c) CsNaY, (d) NaY.

Quantachrome Corporation
Quantachrome Autosorb Automated Gas Sorption System Report
Autosorb for Windows® Version 1.19

Sample ID	CsNaX				
Description	Ads-Des 20 pts,BET 11 pts				
Comments					
Sample Weight	0.0404 g				
Adsorbate	Carbon Dioxide	Outgas Temp	250 °C	Operator	BomB
Cross-Sec Area	21.0 Å²/molec	Outgas Time	12.0 hrs	Analysis Time	278.3 min
NonIdeality	9.100E-06	P/Po Toler	3	End of Run	10/01/2009 01:33
Molecular Wt	44.0100 g/mol	Equil Time	3	File Name	CSNAX.RAW
Station #	1	Bath Temp.	273.15		

Langmuir Data

P/Po	P/Po/W
5.4778e-02	2.857E-01
7.6627e-02	3.800E-01
1.0376e-01	4.934E-01
1.3058e-01	6.016E-01
1.5687e-01	7.051E-01
1.8257e-01	8.041E-01
2.0831e-01	9.017E-01
2.3374e-01	9.964E-01
2.5918e-01	1.090E+00
2.8456e-01	1.182E+00
3.0961e-01	1.272E+00

Langmuir surface area = 7.449E+02 m²/g

Slope = 3.858E+00

Y - Intercept = 9.037E-02

Correlation Coefficient = 0.999627

Langmuir constant K = 4.2688E+01

Figure B3 Langmuir plot data of CsNaX.

Quantachrome Corporation
Quantachrome Autosorb Automated Gas Sorption System Report
Autosorb for Windows® Version 1.19

Sample ID	NaX				
Description	Ads-Des 20 pts,BET 11 pts				
Comments					
Sample Weight	0.0623 g				
Adsorbate	Carbon Dioxide	Outgas Temp	250 °C	Operator	BomB
Cross-Sec Area	21.0 Å²/molec	Outgas Time	12.0 hrs	Analysis Time	320.7 min
NonIdeality	9.100E-06	P/Po Toler	3	End of Run	09/30/2009 04:17
Molecular Wt	44.0100 g/mol	Equil Time	3	File Name	NAX.RAW
Station #	1	Bath Temp.	273.15		

Langmuir Data

P/Po	P/Po/W
5.0123e-02	3.838E-01
7.4438e-02	4.738E-01
1.0233e-01	5.905E-01
1.3121e-01	7.117E-01
1.5228e-01	8.003E-01
1.7777e-01	9.075E-01
2.0406e-01	1.017E+00
2.3040e-01	1.124E+00
2.5651e-01	1.230E+00
2.8218e-01	1.334E+00
3.0859e-01	1.441E+00

Langmuir surface area = 6.971E+02 m²/g

Slope = 4.122E+00

Y - Intercept = 1.722E-01

Correlation Coefficient = 0.999960

Langmuir constant K = 2.3932E+01

Figure B4 Langmuir plot data of NaX.

Quantachrome Corporation
Quantachrome Autosorb Automated Gas Sorption System Report
Autosorb for Windows® Version 1.19

Sample ID	CsNaY				
Description	Ads-Des 20 pts,BET 11 pts				
Comments					
Sample Weight	0.0657 g				
Adsorbate	Carbon Dioxide	Outgas Temp	250 °C	Operator	BomB
Cross-Sec Area	21.0 Å²/molec	Outgas Time	12.0 hrs	Analysis Time	288.1 min
NonIdeality	9.100E-06	P/Po Toler	3	End of Run	09/27/2009 02:03
Molecular Wt	44.0100 g/mol	Equil Time	3	File Name	CSNAY.RAW
Station #	1	Bath Temp.	273.15		

Langmuir Data

P/Po	P/Po/W
5.6709e-02	4.098E-01
7.5524e-02	5.217E-01
1.0164e-01	6.730E-01
1.2887e-01	8.273E-01
1.5601e-01	9.787E-01
1.8203e-01	1.122E+00
2.0782e-01	1.262E+00
2.3340e-01	1.399E+00
2.5887e-01	1.534E+00
2.8409e-01	1.667E+00
3.0953e-01	1.800E+00

Langmuir surface area = 5.236E+02 m²/g
Slope = 5.488E+00
Y - Intercept = 1.133E-01
Correlation Coefficient = 0.999830
Langmuir constant K = 4.8427E+01

Figure B5 Langmuir plot data of CsNaY.

Quantachrome Corporation
Quantachrome Autosorb Automated Gas Sorption System Report
Autosorb for Windows® Version 1.19

Sample ID	NaY				
Description	Ads-Des 20 pts,BET 11 pts				
Comments					
Sample Weight	0.0331 g				
Adsorbate	Carbon Dioxide	Outgas Temp	250 °C	Operator	BomB
Cross-Sec Area	21.0 Å²/molec	Outgas Time	12.0 hrs	Analysis Time	333.0 min
NonIdeality	9.100E-06	P/Po Toler	3	End of Run	09/26/2009 20:13
Molecular Wt	44.0100 g/mol	Equil Time	3	File Name	NAY.RAW
Station #	1	Bath Temp.	273.15		

Langmuir Data

P/Po	P/Po/W
5.0499e-02	3.578E-01
7.4475e-02	4.518E-01
1.0054e-01	5.740E-01
1.2725e-01	6.911E-01
1.5448e-01	8.071E-01
1.8136e-01	9.201E-01
2.0769e-01	1.030E+00
2.3389e-01	1.139E+00
2.5900e-01	1.241E+00
2.8436e-01	1.343E+00
3.0960e-01	1.444E+00

Langmuir surface area = 6.822E+02 m²/g
Slope = 4.212E+00
Y - Intercept = 1.496E-01
Correlation Coefficient = 0.999838
Langmuir constant K = 2.8151E+01

Figure B6 Langmuir plot data of NaY.

APPENDIX C

GAS CHROMATOGRAM

Analysis liquid product from gas chromatography

The chromatogram of liquid products were identified using reference standard for comparison in Table C1.

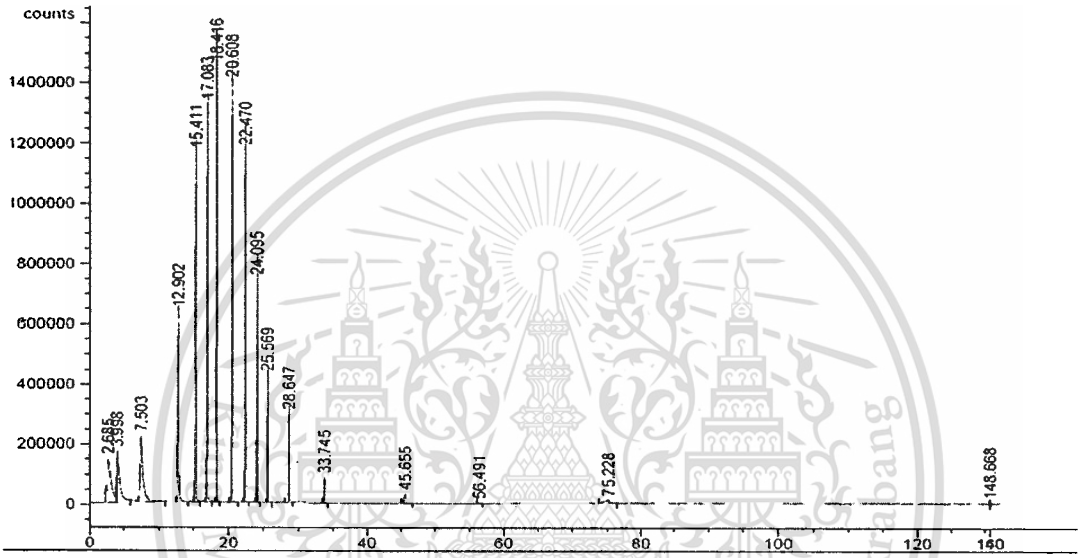

Figure C1 Chromatogram of saturated standard hydrocarbon.

Table C1 Chromatogram data of saturated standard hydrocarbon.

Hydrocarbon (Alkane)	Retention time of standard (min)	Hydrocarbon (Alkane)	Retention time of standard (min)
C6	2.685	C18	24.095
C7	3.998	C20	25.569
C8	7.503	C24	28.647
C9	12.902	C28	33.745
C10	15.411	C32	45.655
C11	17.083	C36	56.491
C12	18.416	C40	75.228
C14	20.608	C44	148.668
C16	22.470		

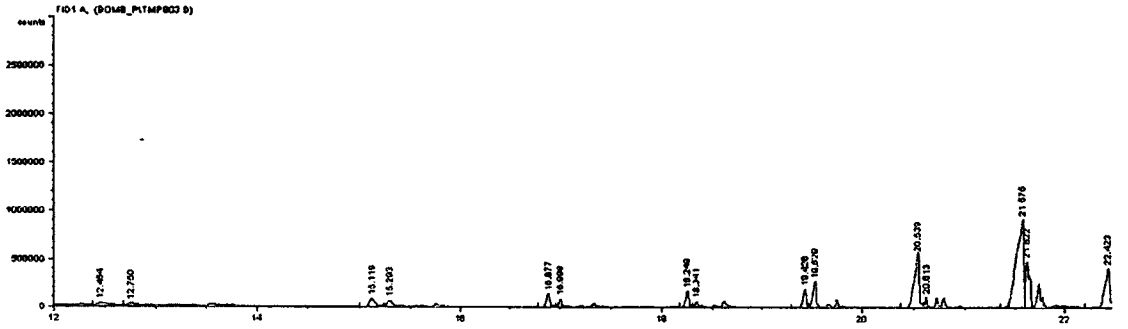

Figure C2 Chromatogram of hydrocarbon products at *W/F* = 140 g·h/mol (Helium).

Table C2 Product distribution from reaction of palmitic acid with methanol in THF over CsNaX at *W/F* = 140 g·h/mol (Helium).

	Time on stream (min)					
	60	120	180	240	300	360
Conversion of methyl palmitate	34.8	24.7	19.9	15.2	13.9	12.0
Liquid product yield (%)	26.6	18.9	15.2	11.6	10.6	9.2
Product distribution						
C_{16}	2.4	1.7	1.4	1.1	1.0	0.8
C_{15}	10.7	7.6	6.1	4.7	4.3	3.7
C_{14}	4.2	3.0	2.4	1.8	1.7	1.4
C_{13}	2.1	1.5	1.2	0.9	0.8	0.7
C_{12}	1.2	0.9	0.7	0.5	0.5	0.4
C_{11}	1.0	0.7	0.6	0.5	0.4	0.4
C_{10}	1.0	0.7	0.6	0.5	0.4	0.4
C_9	1.2	0.9	0.7	0.5	0.5	0.4
Oxygenate	2.4	1.7	1.4	1.1	1.0	0.8
Gas product yield (%)	8.2	5.8	4.7	3.6	3.3	2.8

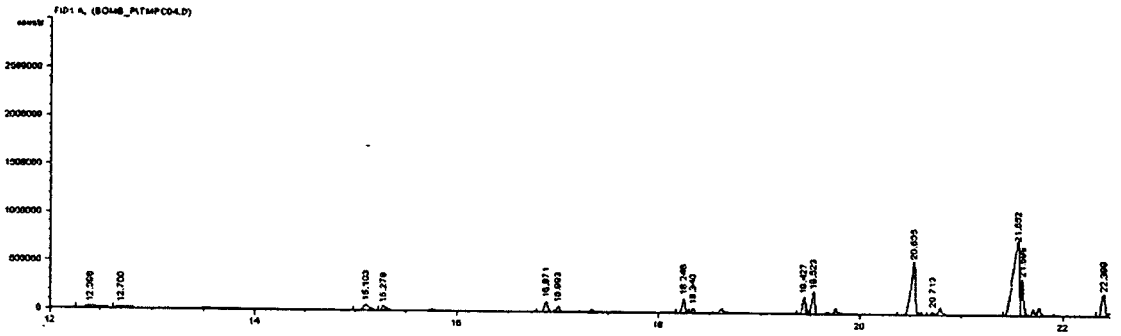

Figure C3 Chromatogram of hydrocarbon products at W/F = 140 g·h/mol (Hydrogen).

Table C3 Product distribution from reaction of palmitic acid with methanol in THF over CsNaX at W/F = 140 g·h/mol (Hydrogen).

	Time on stream (min)					
	60	120	180	240	300	360
Conversion of methyl palmitate	37.1	24.1	21.6	19.5	19.0	18.3
Liquid product yield (%)	28.2	18.3	16.4	14.8	14.4	13.9
Product distribution						
C_{16}	1.4	0.9	0.8	0.7	0.7	0.7
C_{15}	11.5	7.5	6.7	6.0	5.9	5.7
C_{14}	5.3	3.5	3.1	2.8	2.7	2.6
C_{13}	2.4	1.6	1.4	1.3	1.2	1.2
C_{12}	1.2	0.8	0.7	0.6	0.6	0.6
C_{11}	1.2	0.8	0.7	0.6	0.6	0.6
C_{10}	1.4	0.9	0.8	0.7	0.7	0.7
C_9	1.2	0.8	0.7	0.6	0.6	0.6
Oxygenate	2.6	1.7	1.5	1.4	1.3	1.3
Gas product yield (%)	8.9	5.8	5.2	4.7	4.6	4.4

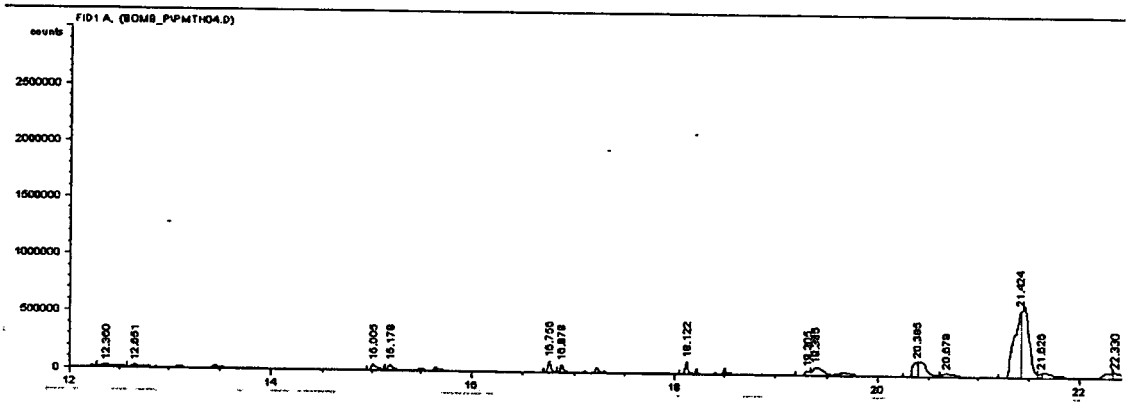

Figure C4 Chromatogram of hydrocarbon products at W/F = 300 g·h/mol (400 °C).

Table C4 Product distribution from reaction of palmitic acid with methanol in THF over CsNaX at W/F = 300 g·h/mol (400 °C).

	Time on stream (min)					
	60	120	180	240	300	360
Conversion of methyl palmitate	41.8	20.3	17.7	19.5	17.5	17.4
Liquid product yield (%)	32.7	10.3	4.7	4.8	4.6	5.6
Product distribution						
C_{16}	1.1	0.7	0.3	0.2	0.2	0.2
C_{15}	14.0	4.6	2.2	2.4	2.2	2.4
C_{14}	4.3	1.3	0.4	0.6	0.4	0.9
C_{13}	2.4	0.7	0.3	0.3	0.2	0.5
C_{12}	1.4	0.4	0.1	0.1	0.1	0.2
C_{11}	1.8	0.4	0.2	0.2	0.2	0.2
C_{10}	2.1	0.4	0.2	0.2	0.2	0.2
C_9	2.3	0.5	0.3	0.3	0.4	0.3
Oxygenate	3.3	1.4	0.7	0.5	0.6	0.7
Gas product yield (%)	9.1	10.0	13.0	14.7	13.0	11.8

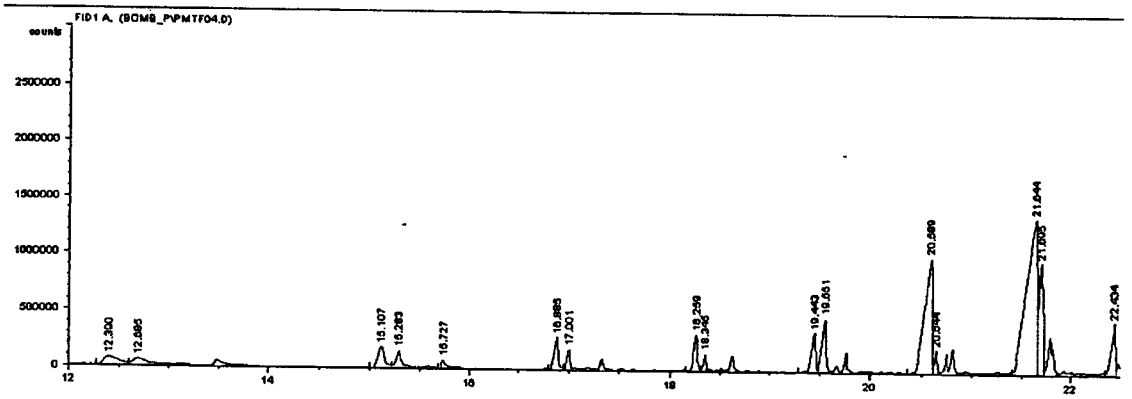

Figure C5 Chromatogram of hydrocarbon products at *W/F* = 300 g·h/mol (425 °C).

Table C5 Product distribution from reaction of palmitic acid with methanol in THF over CsNaX at *W/F* = 300 g·h/mol (425 °C).

	Time on stream (min)					
	60	120	180	240	300	360
Conversion of methyl palmitate	62.8	45.3	43.3	43.9	45.0	49.4
Liquid product yield (%)	30.4	38.4	31.6	29.5	30.8	36.3
Product distribution						
C_{16}	1.3	1.7	1.7	1.7	1.7	2.1
C_{15}	10.8	14.7	11.7	11.3	11.9	16.1
C_{14}	5.5	7.8	5.7	5.1	5.3	5.5
C_{13}	2.8	3.2	2.8	2.4	2.6	3.2
C_{12}	1.6	1.9	1.3	1.1	1.4	1.4
C_{11}	1.9	2.0	1.6	1.3	1.5	1.5
C_{10}	2.3	2.0	1.8	1.9	1.7	1.9
C_9	1.7	1.7	2.1	2.1	1.6	2.1
Oxygenate	2.5	3.4	2.9	2.6	3.1	2.5
Gas product yield (%)	32.4	6.9	11.7	14.4	14.2	13.1

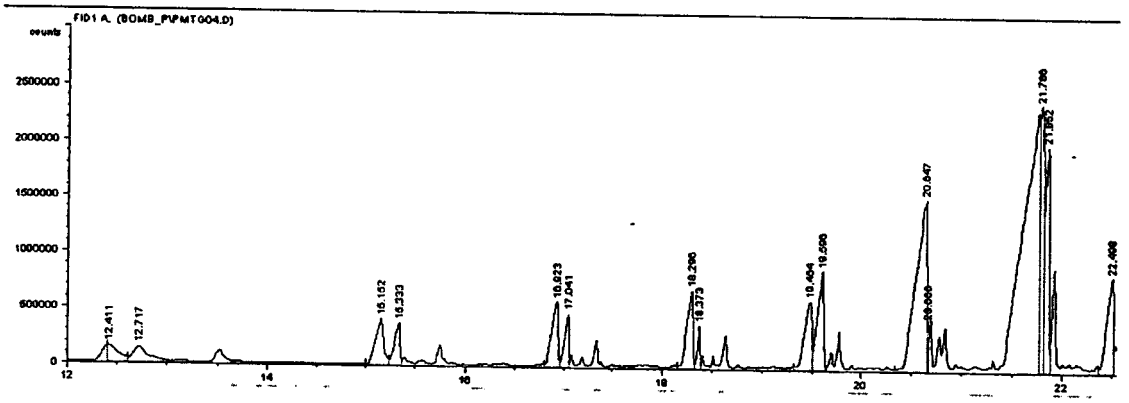

Figure C6 Chromatogram of hydrocarbon products at W/F = 300 g·h/mol (450 °C).

Table C6 Product distribution from reaction of palmitic acid with methanol in THF over CsNaX at W/F = 300 g·h/mol (450 °C).

	Time on stream (min)					
	60	120	180	240	300	360
Conversion of methyl palmitate	93.2	88.9	84.3	71.2	57.8	43.6
Liquid product yield (%)	59.2	81.2	78.5	61.0	49.5	35.3
Product distribution						
C_{16}	2.7	3.3	4.1	3.3	2.7	2.0
C_{15}	17.8	25.8	28.1	24.3	19.9	15.2
C_{14}	8.8	12.4	13.1	8.8	6.0	4.0
C_{13}	6.3	8.3	7.2	5.2	3.8	2.6
C_{12}	4.0	5.4	4.6	3.2	2.5	1.7
C_{11}	4.4	5.9	5.2	3.7	3.0	2.1
C_{10}	5.5	7.3	5.5	4.2	3.6	2.4
C_9	4.9	5.8	5.7	3.9	3.8	2.5
Oxygenate	4.9	7.1	5.0	4.4	4.2	3.0
Gas product yield (%)	33.9	7.7	5.8	10.2	8.4	8.4

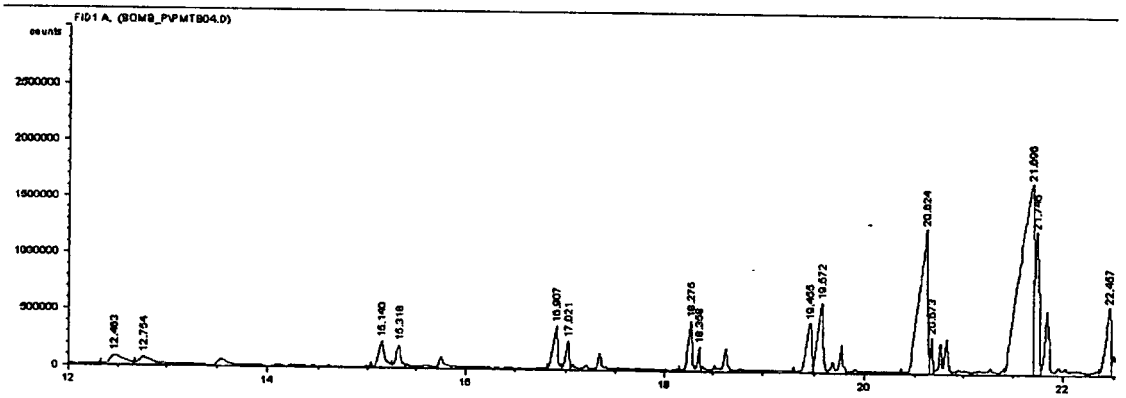

Figure C7 Chromatogram of hydrocarbon products at W/F = 380 g·h/mol.

Table C7 Product distribution from reaction of palmitic acid with methanol in THF over CsNaX at W/F = 380 g·h/mol.

	Time on stream (min)					
	60	120	180	240	300	360
Conversion of methyl palmitate	73.5	52.0	40.9	50.9	54.3	47.8
Liquid product yield (%)	36.3	36.7	31.3	36.1		33.9
Product distribution						
C_{16}	2.1	2.1	1.8	2.2	2.5	2.1
C_{15}	14.2	13.7	12.7	13.6	14.8	13.3
C_{14}	6.4	6.5	5.4	6.4	7.0	5.9
C_{13}	2.9	3.1	2.4	3.0	3.3	2.8
C_{12}	1.6	1.4	1.1	1.4	1.6	1.2
C_{11}	1.8	1.6	1.2	1.6	1.9	1.3
C_{10}	2.3	2.2	1.7	2.0	2.4	1.8
C_9	1.9	2.3	1.7	2.0	2.5	1.9
Oxygenate	3.1	3.8	3.3	3.8	3.4	3.6
Gas product yield (%)	37.2	15.3	9.6	14.9	14.9	13.9

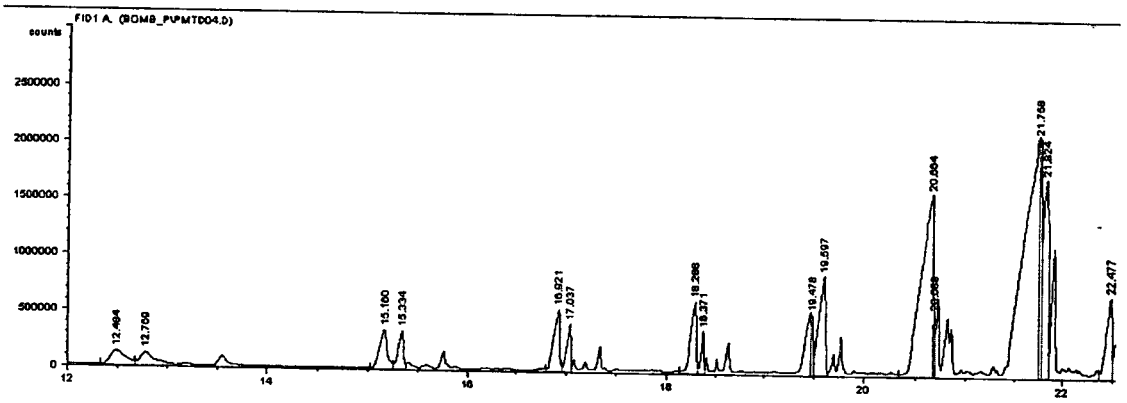

Figure C8 Chromatogram of hydrocarbon products at *W/F* = 450 g·h/mol (MeOH:Palmitic 4.5:1)

Table C8 Product distribution from reaction of palmitic acid with methanol in THF over CsNaX at *W/F* = 450 g·h/mol (MeOH:Palmitic 4.5:1).

	Time on stream (min)					
	60	120	180	240	300	360
Conversion of methyl palmitate	93.1	78.1	64.5	63.1	64.5	65.6
Liquid product yield (%)	47.3	66.3	60.1	57.3	47.9	50.1
Product distribution						
C_{16}	1.6	2.6	3.2	2.9	2.4	2.4
C_{15}	11.1	23.4	22.3	21.8	18.8	19.8
C_{14}	7.1	11.8	12.2	10.8	8.5	8.4
C_{13}	4.6	6.8	5.6	5.2	4.2	4.4
C_{12}	3.4	3.9	3.1	2.9	2.4	3.2
C_{11}	4.0	4.2	3.3	3.2	2.7	2.9
C_{10}	6.1	3.9	3.6	4.0	2.7	3.1
C_9	4.9	3.2	3.0	2.9	2.7	2.4
Oxygenate	4.5	6.4	3.8	3.5	3.5	3.4
Gas product yield (%)	45.8	11.8	4.3	5.7	16.6	15.5

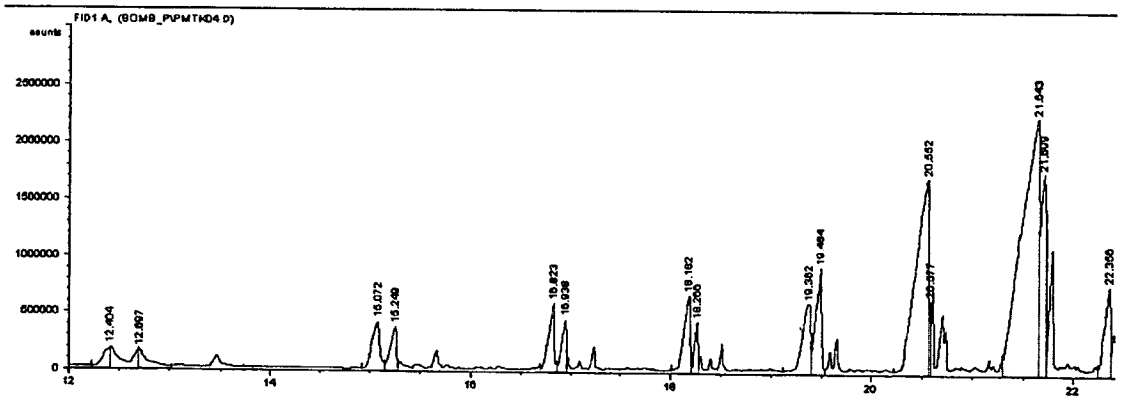

Figure C9 Chromatogram of hydrocarbon products at *W/F* = 450 g·h/mol (MeOH:Palmitic 3.0:1)

Table C9 Product distribution from reaction of palmitic acid with methanol in THF over CsNaX at *W/F* = 450 g·h/mol (MeOH:Palmitic 3.0:1).

	Time on stream (min)					
	60	120	180	240	300	360
Conversion of methyl palmitate	85.7	62.6	54.6	52.0	53.3	50.8
Liquid product yield (%)	64.4	47.0	41.1	39.1	40.0	38.2
Product distribution						
C_{16}	3.5	2.5	2.2	2.1	2.1	2.0
C_{15}	25.5	18.6	16.2	15.4	15.8	15.1
C_{14}	10.7	7.8	6.8	6.5	6.6	6.3
C_{13}	5.3	3.9	3.4	3.2	3.3	3.2
C_{12}	3.6	2.6	2.3	2.2	2.2	2.1
C_{11}	3.1	2.3	2.0	1.9	2.0	1.9
C_{10}	3.3	2.4	2.1	2.0	2.1	2.0
C_9	3.6	2.6	2.3	2.2	2.2	2.1
Oxygenate	5.8	4.2	3.7	3.5	3.6	3.4
Gas product yield (%)	21.3	15.6	13.5	12.9	13.2	12.6

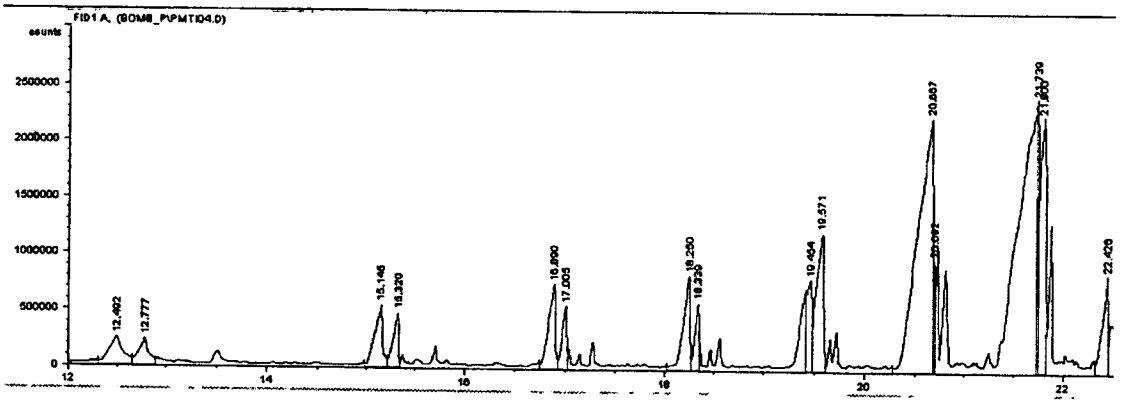

Figure C10 Chromatogram of hydrocarbon products at *W/F* = 450 g·h/mol (MeOH:Palmitic 2.0:1)

Table C10 Product distribution from reaction of palmitic acid with methanol in THF over CsNaX at *W/F* = 450 g·h/mol (MeOH:Palmitic 2.0:1).

	Time on stream (min)					
	60	120	180	240	300	360
Conversion of methyl palmitate	83.1	58.1	44.5	43.1	44.5	45.6
Liquid product yield (%)	61.7	43.2	33.0	32.0	33.0	33.8
Product distribution						
C_{16}	2.7	1.9	1.4	1.4	1.4	1.5
C_{15}	25.2	17.7	13.5	13.1	13.5	13.9
C_{14}	10.0	7.0	5.4	5.2	5.4	5.5
C_{13}	5.6	3.9	3.0	2.9	3.0	3.1
C_{12}	2.7	1.9	1.4	1.4	1.4	1.5
C_{11}	2.9	2.0	1.5	1.5	1.5	1.6
C_{10}	3.3	2.3	1.8	1.7	1.8	1.8
C_9	3.3	2.3	1.8	1.7	1.8	1.8
Oxygenate	6.0	4.2	3.2	3.1	3.2	3.3
Gas product yield (%)	21.4	15.0	11.5	11.1	11.5	11.7

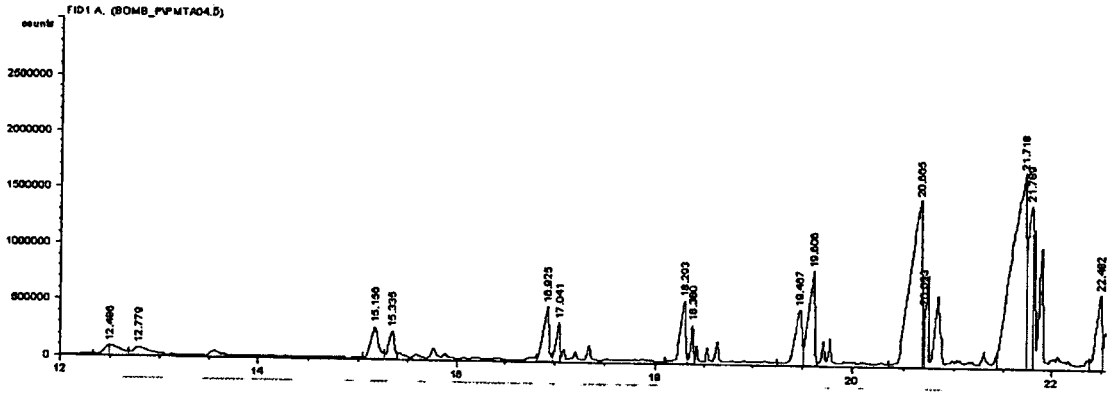

Figure C11 Chromatogram of hydrocarbon products at W/F = 600 g·h/mol.

Table C11 Product distribution from reaction of palmitic acid with methanol in THF over CsNaX at W/F = 600 g·h/mol.

	Time on stream (min)					
	60	120	180	240	300	360
Conversion of methyl palmitate	54.7	85.3	91.1	88.0	88.2	87.4
Liquid product yield (%)	51.0	78.6	44.7	71.8	75.5	80.7
Product distribution						
C_{16}	2.4	4.1	2.1	4.8	3.6	4.7
C_{15}	13.8	27.0	15.6	24.7	26.0	30.5
C_{14}	6.8	13.8	8.4	13.6	14.1	15.8
C_{13}	3.6	7.6	4.4	7.1	7.6	7.5
C_{12}	2.5	4.2	2.4	4.0	4.5	4.2
C_{11}	3.4	4.8	2.6	4.1	4.6	4.4
C_{10}	5.0	6.1	3.1	5.0	5.3	4.6
C_9	8.0	4.3	2.1	3.2	3.5	4.0
Oxygenate	5.4	6.7	4.0	5.2	6.4	5.0
Gas product yield (%)	3.7	6.8	46.4	16.2	12.6	6.7

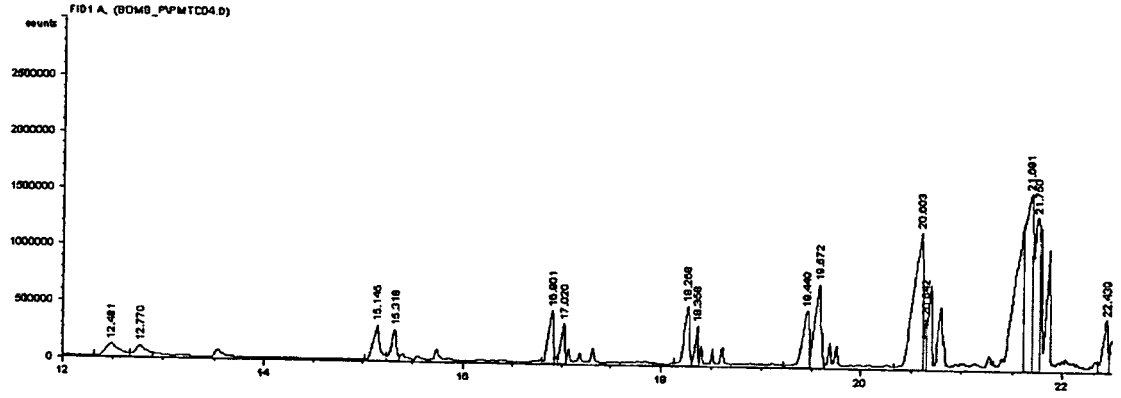

Figure C12 Chromatogram of hydrocarbon products at W/F = 700 g·h/mol.

Table C12 Product distribution from reaction of palmitic acid with methanol in THF over CsNaX at W/F = 700 g·h/mol.

	Time on stream (min)					
	60	120	180	240	300	360
Conversion of methyl palmitate	98.2	93.8	93.5	92.5	90.1	85.7
Liquid product yield (%)	22.4	56.7	62.2	54.1	56.0	47.2
Product distribution						
C_{16}	1.0	2.7	3.1	2.6	2.6	2.1
C_{15}	5.6	16.7	20.9	19.8	21.7	19.9
C_{14}	4.2	11.9	13.3	10.6	10.1	8.2
C_{13}	2.5	6.5	6.7	5.4	5.0	4.2
C_{12}	1.7	4.1	4.0	3.3	3.1	2.6
C_{11}	1.9	4.0	4.1	3.4	3.4	2.9
C_{10}	2.4	5.0	4.7	3.5	4.1	2.5
C_9	1.6	3.0	2.9	2.8	3.0	2.0
Oxygenate	1.5	2.9	2.6	2.8	2.9	2.7
Gas product yield (%)	75.8	37.1	31.3	38.5	34.1	38.5

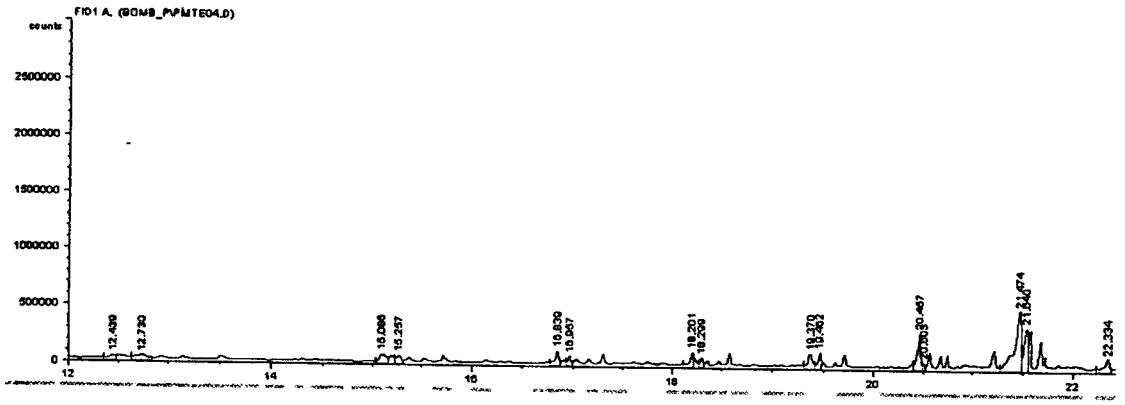

Figure C13 Chromatogram of hydrocarbon products over NaX at W/F = 600 g·h/mol.

Table C13 Product distribution from reaction of palmitic acid with methanol in THF over NaX at W/F = 600 g·h/mol.

	Time on stream (min)					
	60	120	180	240	300	360
Conversion of methyl palmitate	100	100	75.4	55.0	51.9	53.3
Liquid product yield (%)	0.0	0.0	52.5	35.6	24.1	21.6
Product distribution						
C_{16}	0.0	0.0	2.8	1.7	0.8	0.8
C_{15}	0.0	0.0	15.3	8.7	6.6	5.0
C_{14}	0.0	0.0	5.0	4.0	2.3	2.1
C_{13}	0.0	0.0	5.1	3.0	1.7	1.4
C_{12}	0.0	0.0	3.7	2.7	1.8	1.4
C_{11}	0.0	0.0	4.4	3.4	2.2	1.7
C_{10}	0.0	0.0	6.0	4.1	3.0	2.3
C_9	0.0	0.0	4.8	3.7	2.1	3.5
Oxygenate	0.0	0.0	5.4	4.4	3.6	3.3
Gas product yield (%)	100	100	22.9	19.4	27.7	32.6

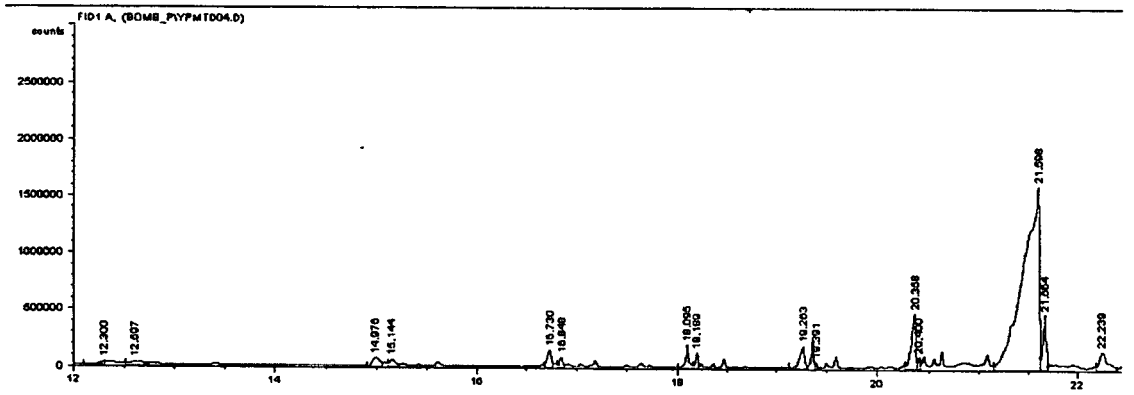

Figure C14 Chromatogram of hydrocarbon products over NaY at *W/F* = 450 g·h/mol.

Table C14 Product distribution from reaction of palmitic acid with methanol in THF over NaY at *W/F* = 450 g·h/mol.

	Time on stream (min)					
	60	120	180	240	300	360
Conversion of methyl palmitate	81.0	35.2	26.6	28.7	28.2	27.1
Liquid product yield (%)	43.5	19.1	14.3	15.4	15.2	14.6
Product distribution						
C_{16}	1.5	0.7	0.5	0.6	0.7	0.5
C_{15}	20.7	9.0	6.8	7.4	7.2	6.9
C_{14}	6.4	2.8	2.1	2.3	2.2	2.1
C_{13}	4.0	1.7	1.3	1.4	1.6	1.3
C_{12}	2.4	1.1	0.8	0.9	0.6	0.8
C_{11}	2.6	1.0	0.8	0.9	0.7	0.7
C_{10}	2.2	1.2	0.8	0.7	0.8	0.9
C_9	1.5	0.7	0.5	0.5	0.9	0.6
Oxygenate	2.2	0.9	0.7	0.7	0.5	0.8
Gas product yield (%)	37.5	16.1	12.3	13.3	13.0	12.5

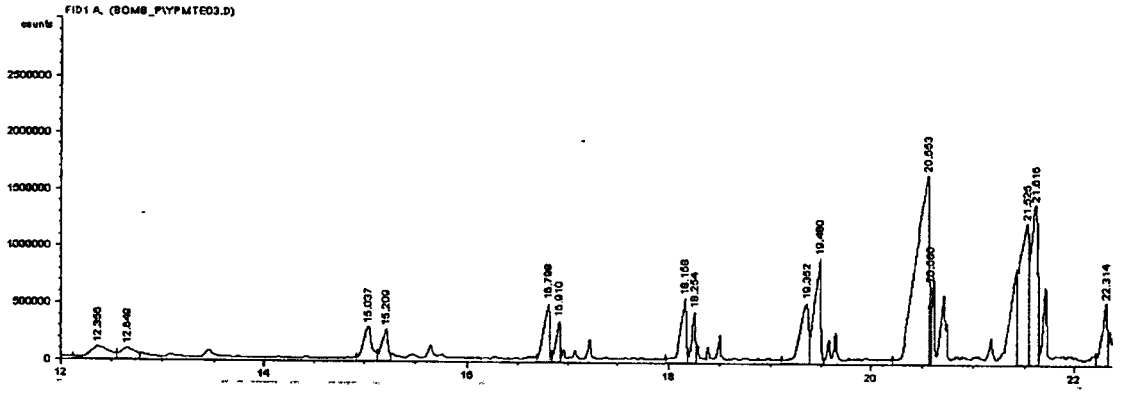

Figure C15 Chromatogram of hydrocarbon products over CsNaY at W/F = 450 g·h/mol.

Table C15 Product distribution from reaction of palmitic acid with methanol in THF over CsNaY at W/F = 450 g·h/mol.

	Time on stream (min)					
	60	120	180	240	300	360
Conversion of methyl palmitate	79.2	3.2	67.3	66.2	67.4	63.1
Liquid product yield (%)	61.9	59.2	50.6	49.6	55.1	53.8
Product distribution						
C_{16}	2.4	2.4	2.2	2.2	1.7	1.8
C_{15}	22.7	21.9	19.5	18.7	18.8	15.4
C_{14}	11.3	10.6	8.4	9.4	8.2	8.2
C_{13}	6.2	5.7	4.4	4.1	6.3	6.1
C_{12}	3.8	3.8	3.1	2.8	3.5	3.1
C_{11}	4.3	3.7	2.6	2.4	3.2	2.9
C_{10}	3.9	3.3	2.7	2.9	3.8	3.0
C_9	3.6	3.7	3.4	2.6	3.8	3.0
Oxygenate	3.7	4.1	4.3	4.5	3.9	4.1
Gas product yield (%)	17.3	14.0	16.7	16.6	14.2	15.3

APPENDIX D

THERMOGRAVIMETRIC ANALYSIS DATA

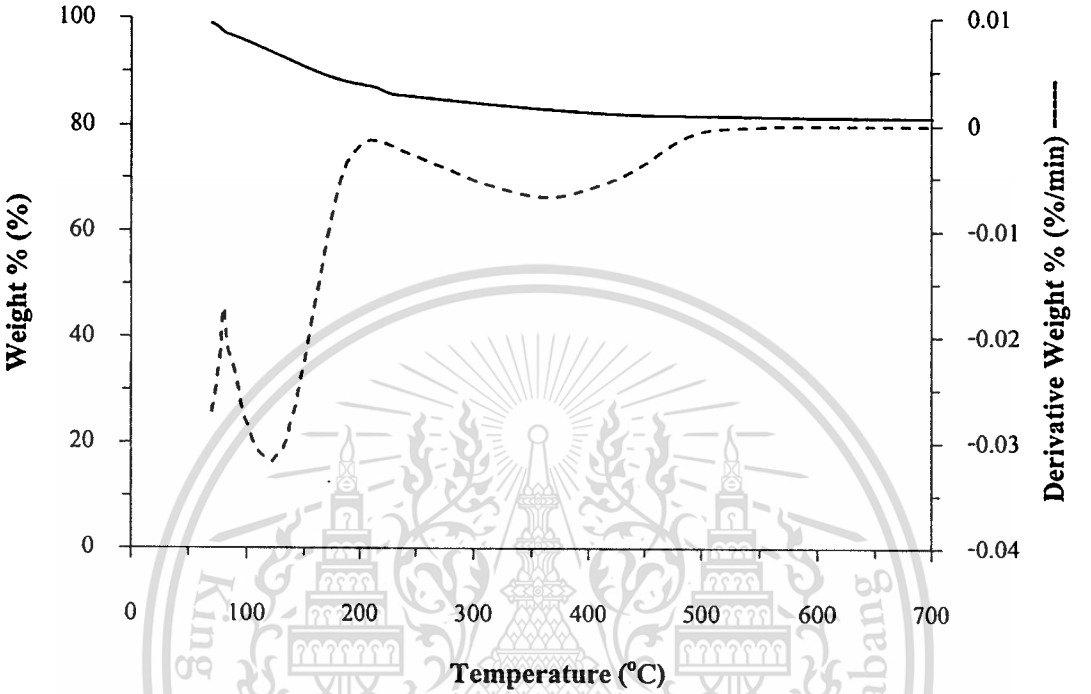

Figure D1 TGA/DTG of CsNaX at reactant composition MeOH:Palmitic = 4.5:1.0.

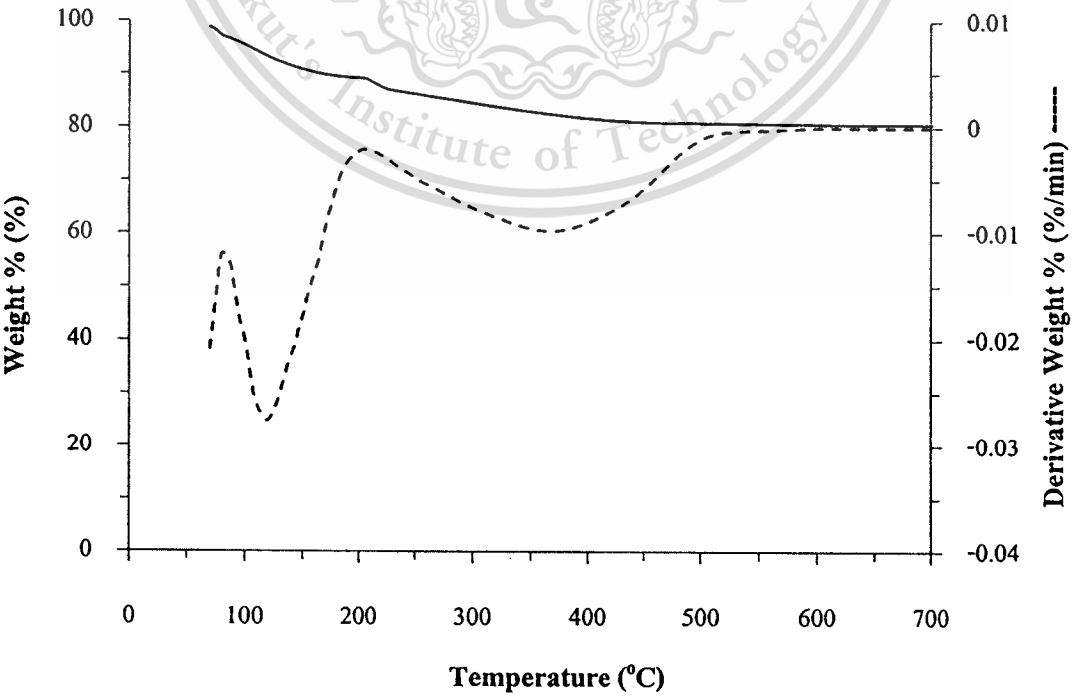

Figure D2 TGA/DTG of CsNaX at reactant composition MeOH:Palmitic = 3.0:1.0.

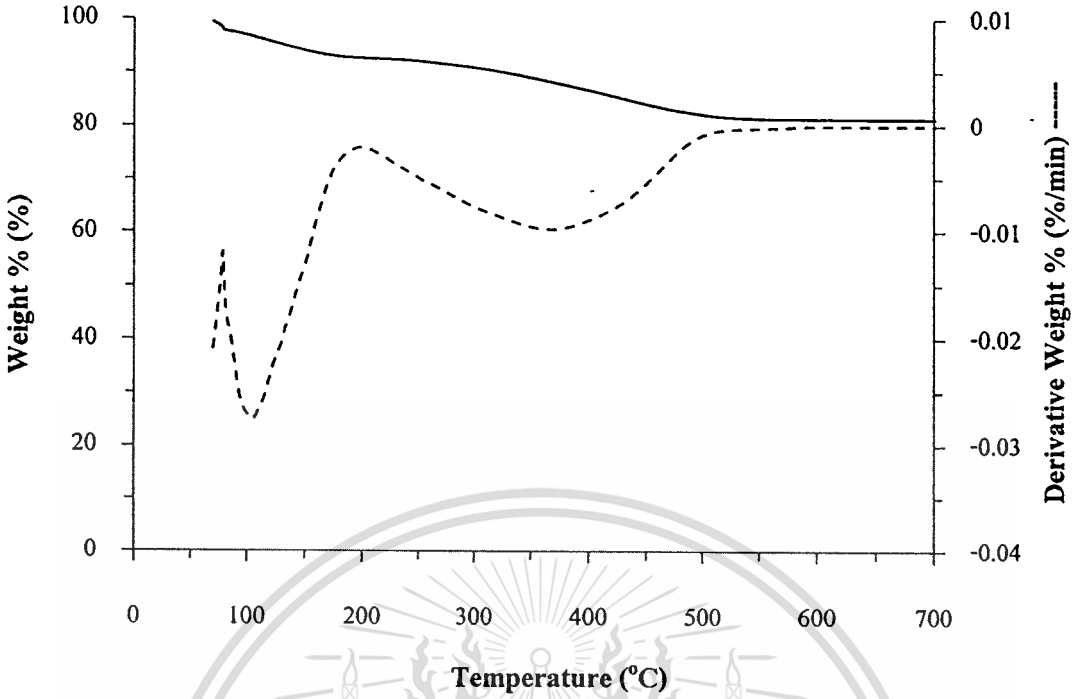

Figure D3 TGA/DTG of used CsNaX at reactant composition MeOH:Palmitic = 2.0:1.0.

AUTHOR BIOGRAPHY

Mr. Thanasak Solos was born on November 14, 1981 in Phattalung. He graduated a Bachelor degree in Chemical Engineering from the Department of Chemical Engineering, Faculty of Engineering, King Mongkut's Institute of Technology Ladkrabang in 2004. He has been a graduate student in Petrochemicals and Hydrocarbon Chemistry program of Faculty of Science, King Mongkut's Institute of Technology Ladkrabang, since 2006.

Work experiences:

2008 –2010 Ladkrabang.	Teacher Assistant, King Mongkut's Institute of Technology
2007 - 2008	Researcher Assistant (Part-time), Project: Renewable Diesel: Decarboxylation of Fatty Acids with Moderate Condition, PTT public company limited.

Conferences

2009	Thanasak Solos, and Tawan Sooknoi, Catalytic Decarbonylation of Palmitic Acid over CsNaX for the Production of Long Chain Hydrocarbons, Oral presentation, Pure and Applied Chemistry International Conference 2009 (PACCON 2009), January 14-16, 2009, Naresuan University, Phitsanulok, Thailand.
2011	Thanasak Solos, and Tawan Sooknoi, Catalytic Deoxygenation of Palmitic Acid over CsNaX for the Production of Long Chain Hydrocarbons, Poster presentation, Pure and Applied Chemistry International Conference 2011 (PACCON 2011), January 5-7, 2011, Miracle Grand Hotel, Bangkok, Thailand.